METABOLIC PROFILING OF COLORECTAL CANCER

MAINAK MAL

(M.Pharm, Jadavpur University, India)

A THESIS SUBMITTED

FOR THE DEGREE OF DOCTOR OF PHILOSOPHY

DEPARTMENT OF PHARMACY

NATIONAL UNIVERSITY OF SINGAPORE

2011

ACKNOWLEDGEMENTS

I would like to convey my sincere regards and gratitude to my supervisor Assoc. Prof. Eric Chun Yong Chan, (Dept. of Pharmacy, National University of Singapore) and co-supervisor Dr. Poh Koon Koh, (Deputy Director, Colorectal Cancer Research Laboratory, Dept. of Colorectal Surgery, Singapore General Hospital), for providing me an opportunity to work in this challenging project and for their continuous support, encouragement and invaluable guidance.

I would like to convey my appreciation to Assoc. Prof. Chan Sui Yung (Head of the Dept. of Pharmacy, National University of Singapore) as well as my PhD. thesis committee members, Assoc. Prof. Go Mei Lin (Deputy Head of the Dept. of Pharmacy, National University of Singapore) and Asst. Prof. Ho Han Kiat (Dept. of Pharmacy, National University of Singapore) for their help, support and encouragement.

I would also like to extend my sincere thanks to Dr. Peh Yean Cheah, Dr. Kong Weng Eu, Grace Wong and Elya at the Colorectal Cancer Research Laboratory, Dept. of Colorectal Surgery, Singapore General Hospital, for their help and support especially for collection of tissue samples and patient's metadata.

I would like to express my cordial thanks to Dr. Hector C Keun, Alexandra Backshall, Rachel Cavill, Prof. Jeremy K Nicholson and Dr. Toby Athersuch at the the Imperial College London, UK, for their help and support in HR-MAS NMR spectroscopy based metabolic profiling of colorectal cancer.

I would like to express my sincere gratitude and respect to my parents, grandparents and other family members who have always encouraged me to pursue higher studies, provided moral support and always stood by my side during this crucial phase of my life and career.

I would also like to thank my fellow research group members, New Lee Sun, Kishore K Pasikanti, Sudipta Saha, Tarang Nema, Chang Kai Lun, Thiru Selvi, Chng Hui Ting, Yip Lian Yee and Phua Lee Cheng for their valuable assistance and support.

Finally, I would like to express my sincere thanks to all my fellow research scholars and friends, especially Animesh, Goutam, Pradipto, Sandip and Tanay for providing the excellent camaraderie which was invaluable for successful completion of my PhD. project.

TABLE OF CONTENTS

SUMMARY

Colorectal cancer (CRC) is the second most common form of cancer in the world and the most common cancer in Singapore. The limitations of the currently available methods and biomarkers for CRC management highlight the necessity of finding novel markers. Alterations in different metabolic pathways in CRC as indicated by proteomic studies, are likely to result in changes in metabolic profile which if identified with the aid of metabolic profiling can help in the identification of marker metabolites and can provide molecular insight in CRC. Metabolic profiling is complementary to genomics and proteomics as it measures the perturbed metabolic end-points due to environmental, pharmacological or pathological influences while in genomics and proteomics, more upstream biological events are typically profiled and studied.

In this thesis, metabolic profiling of CRC was carried out with a non-targeted as well as a targeted approach to identify metabolite-based markers. For non-targeted metabolic profiling of CRC, three different analytical platforms namely GC/MS, HR-MAS NMR spectroscopy and GC×GC/TOFMS were explored. The data generated in conjunction with chemometric analysis led to the identification of marker metabolites belonging to diverse chemical classes. Although the orthogonal partial least squares discriminant analysis (OPLS-DA) models generated on the basis of profiled data using the three analytical platforms were capable of discriminating normal tissues from malignant ones, no valid OPLS-DA model was obtained using CRC stage as the classifier. This implied that the metabolic phenotype

associated with CRC although distinct from that of normal tissue, it is not sensitive enough to discriminate the different stages of CRC. Of the three analytical methods used, only HR-MAS NMR spectroscopy-based metabolic profiling was able to produce a valid OPLS-DA model capable of discriminating anatomical site of tumor. The identified marker metabolites when linked to metabolic pathways using KEGG database, revealed perturbations of various biochemical processes the majority of which could be attributed to the higher energy demand, tissue, hypoxia and altered synthetic rate of cellular components of rapidly proliferating tumor cells. In addition to this, altered eicosanoid biosynthetic pathway as indicated by reduced arachidonic acid (AA) levels in CRC tissues and presence of comparatively higher levels of picolinic acid in CRC tissues, implied an association of inflammatory environment with CRC development.

A strong evidence of association between inflammation and CRC exists. Moreover the significant role played by eicosanoids in inflammation, as well as the altered expression of key enzymes involved in eicosanoid biosynthesis in CRC, formed our objective to carry out targeted metabolic profiling of 8 biologically relevant eicosanoids and the major metabolic precursor AA. The main aim of this study was to record the fluctuations of these inflammatory metabolites and to better understand their implicated roles in inflammation mediated CRC carcinogenesis. An UPLC/MS/MS-based method was developed and validated successfully for this purpose. The results indicated deregulation of eicosanoid biosynthetic pathways and implied that a complex interaction between pro-tumorigenic and antitumorigenic eicosanoids is involved in inflammation-associated CRC carcinogenesis.

Metabolic profiling of CRC led to the identification of marker metabolites and revealed metabolic perturbations that may be exploited for future biomarker research or finding new therapeutic strategies.

LIST OF ABBREVIATIONS

1D	One-dimensional
2D	Two-dimensional
5-FU	5-fluorouracil
6-k-$PGF_{1\alpha}$	6-keto-$prostaglandin_{1\alpha}$
8-HETE	8-hydroxy-5Z,9E,11Z,14Z-eicosatetraenoic acid
12-HETE	12-hydroxy-5Z,8Z,10E,14Z-eicosatetraenoic acid
13S-HODE	13S-hydroxy-9Z,11E-octadecadienoic acid
15-HETE	15-hydroxy eicosatetraenoic acid
15-PGDH	15-hydroxyprostaglandin dehydrogenase
AA	Arachidonic acid
ACN	Acetonitrile
AJCC	American Joint Committee on cancer
Akt	Serine/threonine protein kinase
APC	Adenomatous polyposis coli
ASR	Age-standardized rate
AUC	Area under the ROC curve
BAX	B-cell lymphoma-2 associated X protein
bcl-2	B-cell lymphoma 2
BHT	Butylated hydroxyl toluene
BSA	Bovine serum albumin
BSTFA	N, O-bis (trimethylsilyl) trifluoroacetamide
CA 19-9	Carbohydrate antigen 19-9
CAD	Collision-activated dissociation
CD	Crohn's disease
CE	Capillary electrophoresis
CE/MS	Capillary electrophoresis mass spectrometry
ChoCC	Choline-containing compounds
CIN	Chromosomal instability
CIRB	Centralised Institutional Review Board
COSY	Correlation spectroscopy
COX	Cyclooxygenase

CPMG	Carr-Purcell-Meiboom-Gill
CRC	Colorectal cancer
CSI	Chemical shape indicator
CT	Computed tomographic
D_2O	Deuterium oxide
DCBE	Double contrast barium enema
DCC	Deleted in colorectal cancer
DModX	Distance to model plot
EGF	Epidermal growth factor
EI	Electron impact
EIA	Enzyme immunoassay
ESI	Electrospray ionization
FA	Formic acid
FAP	Familial adenomatous polyposis coli
FOBT	Faecal occult blood test
FTIR	Fourier transform infrared
GC×GC/TOFMS	Two dimensional gas chromatography time of flight mass spectrometry
GC/MS	Gas chromatography mass spectrometry
GC/MS/MS	Gas chromatography tandem mass spectrometry
GC/TOFMS	Gas chromatography time of flight mass spectrometry
HETEs	Hydroxy eicosatetraenoic acids
HMDB	Human Metabolome database
HMG-CoA	3-hydroxy-3-methyl-glutaryl-Coenzyme A
HNPCC	Hereditary nonpolyposis colorectal cancer
HPLC	High performance liquid chromatography
HR-MAS NMR	High resolution magic angle spinning NMR
Hz	Hertz
IBD	Inflammatory bowel disease
ICH	International Conference on Harmonization
i.d.	Internal diameter
IGFR2	Immunoglobulin G Fc Receptor II

IL-6	Interleukin-6
IRB	Institutional review board
IS	Internal standard
JRES	J-resolved
KEGG	Kyoto Encyclopedia of Genes and Genomes
KRAS	V-Ki-ras2 Kirsten rat sarcoma viral oncogene homolog
LC	Liquid chromatography
LC/MS	Liquid chromatography mass spectrometry
LC/MS/MS	Liquid chromatography tandem mass spectrometry
LOD	Limit of detection
LOQ	Limit of quantification
LOX	Lipoxygenase
LTB_4	Leukotriene B_4
LTs	Leukotrienes
LV	Leucovorin
LVs	Latent variables
MAC	Modified Astler Coller
min	Minute
MMR	Mismatch repair
MOX	Methoxyamine hydrochloride in pyridine
MRI	Magnetic resonance imaging
MRM	Multiple reaction monitoring
MS	Mass spectrometry
MSI	Microsatellite instability
MSTFA	N-methyl-N-trifluoroacetamide
m/z	Mass is to charge ratio
NF-κB	Nuclear factor kappa B
NIST	National Institute of Standards and Technology
NMR	Nuclear magnetic resonance
NOESY	Nuclear Overhauser effect spectroscopy
NSAIDs	Non-steroidal anti-inflammatory drugs
OPLS	Orthogonal partial least squares

OPLS-DA	Orthogonal partial least squares discriminant analysis
p53	Protein 53
PBS	Phosphate buffer saline
PC	Phosphocholine
PCA	Principal component analysis
PCs	Principal components
PE	Phosphoethanolamine
PGD_2	Prostaglandin D_2
PGE_2	Prostaglandin E_2
PGE_2-d_4	Deuterated prostaglandin E_2
$PGF_{2\alpha}$	Prostaglandin $F_{2\alpha}$
PGI_2	Prostacyclin
PGs	Prostaglandins
PHGDH	Phosphoglycerate dehydrogenase
PI3K	Phosphatidyl-inositol-3-kinase
PLS	Partial least squares
PLS-DA	Partial least squares discriminant analysis
PPARδ	Peroxisome proliferator activated receptor-δ
ppm	Parts per million
QC	Quality control
r^2	Correlation coefficient
RAS-MAPK	Rat sarcoma viral oncogene-mitogen activated protein kinase
RD	Recycle delay
RIA	Radioimmunoassay
ROC	Receiver operating characteristic
rpm	Revolutions per minute
RSD	Relative standard deviation
R_t	Retention time
s	Second
SD	Standard deviation
s/n	Signal-to-noise ratio

SGH	Singapore General Hospital
SI	Similarity index
TCA	Tricarboxylic acid
TGF-α	Tumor growth factor alpha
TGFBR2	Transforming growth factor-beta receptor II gene
TMCS	Trimethylchlorosilane
TNF-α	Tumor necrosis factor-alpha
TNM	Tumor, node, metastases
TOCSY	Total correlation spectroscopy
TS	Thymidylate synthase
TXA_2	Thromboxane A_2
TXB_2	Thromboxane B_2
TXs	Thromboxanes
UPLC/MS/MS	Ultra performance liquid chromatography tandem mass spectrometry
US-FDA	United States Food and Drug Administration
UV	Unit variance
V	Volt
VEGF	Vascular endothelial growth factor
WHO	World Health Organization
YSR	Year survival rate

LIST OF TABLES

LIST OF FIGURES

CHAPTER 1

INTRODUCTION

1.1. Overview of colorectal cancer

In this section an overview of different aspects of colorectal cancer (CRC) such as prevalence, etiology, pathways of CRC development, diagnosis, staging, prognosis, treatment, relation between inflammation and CRC and current challenges in CRC management is presented.

1.1.1. Prevalence of colorectal cancer

Worldwide statistics indicate that CRC is the third most common cancer in men (663000 cases, 10.0% of the total) and the second in women (571000 cases, 9.4% of the total) (Ferlay et al., 2008). Incidence rates are considerably prominent in men than in women [overall sex ratio of the age-standardized rate (ASR) is 1.4:1]. According to the World Health Organization (WHO), the ASR for incidence of CRC is greater than 49.4 per 100,000 per year, in regions such as North America, Europe, Japan, Israel, Singapore, Australia and New Zealand. In addition to this, CRC is relatively prevalent in some areas of Brazil, Argentina, Hong Kong, Southern China and Malaysia (ASR for incidence of CRC greater than 25.3 per 100,000 per year) (http://www.who.int, Rozen et al., 2006). In Singapore, CRC is the leading cancer in males and the second most common cancer in females, accounting for 17.9% of all cancers in males and 14.4% in females. When both genders

are combined, CRC is the most common cancer in Singapore. In the world, around 608000 deaths occur from CRC, constituting for 8% of all cancer deaths, making it the fourth most common cause of death from cancer. As observed for incidence, mortality rates are lower in women than in men, except in the Caribbean. There is less variability in mortality rates worldwide (6-fold in men, 5-fold in women), with the highest mortality rates in both sexes estimated in Central and Eastern Europe (20.1 per 100,000 for male, 12.2 per 100,000 for female), and the lowest in Middle Africa (3.5 and 2.7 respectively). Almost 60% of the cases occur in developed regions (Ferlay et al., 2008). The ASR for mortality from CRC in Singapore over the period from 2002 to 2006 was 18.1 per 100,000 per year in males and 12.5 in females (Tey et al., 2008). The ASR for CRC mortality rates in the United States and United Kingdom in 2002 according to the WHO were 14.8 and 17.3 per 100,000 per year, respectively (http://www.who.int). Certainly CRC has emerged as a serious threat to public health both in Singapore as well as overseas.

1.1.2. Etiology of colorectal cancer

On the basis of etiology, CRC can be inheritable, inflammatory or sporadic in nature. Lynch syndrome is the most common hereditary syndrome that predisposes patients to CRC, followed by familial adenomatous polyposis coli (FAP). Although the terms Lynch syndrome and hereditary nonpolyposis colorectal cancer (HNPCC) are often used synonymously, HNPCC specifically refers to those disorders that have similar phenotypes but lack the

specific mutations involved in Lynch syndrome. Lynch syndrome and HNPCC together account for 2-5% of all CRC. This form of heritable CRC is characterized by early onset and predominantly right-sided mucinous tumor. Germline mutations in the mismatch repair (MMR) genes namely MLH1 and MSH2 characterized by replication error and hence DNA or microsatellite instability (MSI), comprises the major genetic defect causing HNPCC or Lynch syndrome. Apart from CRC, HNPCC or Lynch syndrome also predisposes patients to other extra-colonic cancers such as small-intestine, renal pelvis and endometrial cancer (Lindor et al., 2005; Lynch et al., 2009). FAP which is responsible for less than 1% of all CRC cases occurs due to a mutation in the adenomatous polyposis coli (APC) gene. Development of hundreds to thousands of adenomatous polyps in the colon and rectum of individuals starting from early adolescence, which inevitably leads to CRC if untreated, is the main characteristic of FAP. FAP also leads to various extra-colonic manifestations like thyroid cancer, duodenal and fundic gland polyposis and desmoids (Jasperson et al., 2010). Inflammatory bowel disease (IBD) including Crohn's disease (CD) and ulcerative colitis may also lead to CRC. However patients with IBD represent only 1-2% of CRC cases. The risk of CRC is much higher in individuals having prolonged (more than 30 years) and extensive ulcerative colitis (Lakatos and Lakatos, 2008; Kraus and Arber, 2009). Majority of CRC (up to 80%) is sporadic in nature with no well defined etiology and occurs due to interaction between genetic and environmental factors (Cheah, 1990). Ageing is one of the major risk factors for sporadic CRC as 99% of cases occur in people more than 40 years of age and 85% in those more than 60 years of age. Higher incidence of CRC in affluent societies

is related to lifestyle related factors such as high intake of fat and red meat, insufficient intake of fiber rich food and vegetables, obesity and low physical activity. High alcohol consumption, diabetes mellitus and smoking also increase the risk of CRC (Ballinger and Anggiansah, 2007; Cunningham et al., 2010).

1.1.3. Pathways of colorectal cancer development

CRC develops because of genetic abnormalities most of which are caused by environmental and lifestyle related factors while some are inherited. The two major genetic pathways of CRC development are the chromosomal instability (CIN) pathway and the microsatellite instability (MSI) pathway. In most cases CRC develops by the CIN pathway which is characterized by aneuploidy. The most frequent genetic abnormality consists of mutations in the V-Ki-ras2 Kirsten rat sarcoma viral oncogene homolog (KRAS) and APC genes. Inherited mutations in the APC gene results in FAP whereas allelic loss of chromosome 5 (site of the APC gene) causes APC changes in sporadic CRC. Loss of function of the protein 53 (p53) is a crucial event related to the transformation of adenoma to carcinoma (Powell et al., 1992; Stoler et al., 1999; Vogelstein et al., 1988). The MSI pathway is characterized by the dysfunction of MMR gene. Such mutations may be inherited resulting in HNPCC or Lynch syndrome or may result from acquired epigenetic events. Genes which are more susceptible to mutations in this pathway include transforming growth factor-beta receptor II (TGFBR2) gene, B-cell lymphoma-2 (bcl-2) associated X protein (BAX) gene (essential for apoptosis)

and Immunoglobulin G Fc Receptor II (IGFR2) gene (essential for differentiation) (Grady, 2004). Apart from the CIN and the MSI pathways, CRC can also develop through the serrated adenoma pathway. This pathway is characterized by the absence of MSI and widespread methylation of genes SLC5A8, p16 and MGMT (Dong et al., 2005; Jass, 1999).

1.1.4. Diagnosis of colorectal cancer

CRC if diagnosed at an early stage improves the chances of survival of patients and reduces treatment-related morbidity. An individual may be diagnosed with CRC when he or she presents certain symptoms or as a result of any screening program. Usually the early stage CRC does not produce any detectable symptoms. Moreover, most of the symptoms of CRC such as change in bowel habits, blood in stool, general discomfort in the abdomen, weight loss and tiredness, lack specificity. Therefore it is essential to carry out regular screening programs to detect CRC. Endoscopy using either flexible sigmoidoscopy or colonoscopy with tumour biopsy is the most common diagnostic method for CRC. However, these techniques require extensive bowel preparation and lacks patient compliance due to their invasive nature. Double contrast barium enema (DCBE) is used as an adjunct diagnostic technique especially to detect tumours or polyps in tortuous anatomical sites where endoscopic study is difficult to carry out. Although faecal occult blood test (FOBT) for CRC diagnosis is simple and non invasive in nature, it lacks specificity. Faecal DNA based test is more sensitive than FOBT but it is tedious to administer and expensive. Computed tomographic (CT)

colonography, also termed as virtual colonoscopy, is a non- invasive diagnostic technique that produces two- and three-dimensional images of the colorectal tract. It is particularly useful for imaging the colonic lumen proximal to a stenosing or obstructed lesion which cannot be traversed by a flexible endoscope. It is also used to stage the extent of disease in patients with suspected distant metastasis from CRC. Magnetic resonance imaging (MRI) with its superior differentiation of tissue planes, is especially useful in assessing the local invasion of rectal tumors within the narrow confines of the pelvis. However, these imaging techniques do not allow for biopsies for histological proof and requires exposure to ionizing radiation or nephrotoxic contrast administration. Of the various serum-based markers for CRC that have been investigated, CEA has been found to be useful for preoperative staging and follow up. However, CEA is not recommended for diagnosis because of its low sensitivity and specificity. Genetic tests are required for screening of heritable forms of CRC (Cunningham et al., 2010; Labianca et al., 2010).

1.1.5. Staging of colorectal cancer

The Dukes classification (Dukes, 1932; Weiss, 2000) and the TNM (tumor, node, metastases) system (Fleming et al., 1997) are the two most common staging systems for CRC. The other less commonly used staging system is the modified Astler Coller (MAC) system (Astler and Coller, 1954; Gunderson and Sosin, 1974). The TNM system is mainly based on the size and degree of invasion of the primary tumour (T), extent of lymph node involvement (N)

and degree of metastasis (M). It was introduced by the AJCC and the most preferred system of staging of CRC. The TNM system and AJCC stage groupings with equivalent Dukes and MAC stages of CRC are summarized in Table 1.1. The TNM system encompasses both clinical and a pathological staging. The clinical classification is designated as cTNM and the histopathological classification is designated as pTNM. Usually the cTNM is used to select treatment regimen whereas the pTNM is used for prognosis of CRC. Preoperative staging involves assessment of patient's medical history, physical examination for hepatomegaly, ascites, lymphadenopathy, blood count, CEA, liver chemistries, examination of large intestine. Surgical staging of CRC involves an evaluation of extra-colonic metastases, nodal spread and degree of tumour invasion through the colonic wall and into surrounding structures (Labianca et al., 2010).

1.1.6. Prognosis of colorectal cancer

The extent of penetration of tumor through the colonic wall and the involvement of lymph nodes, are important prognostic factors of CRC. Other pertinent prognostic parameters include tumor grade, thymidine labelling index, vascular and perineural invasion and lymphoid inflammatory response. Grading of CRC tumors is carried out on the basis of histopathological parameters such as histologic type, quality of differentiation, polarity of nucleus, configuration of tubules, growth pattern, lymphocytic infiltration and extent of fibrosis. At present a three grade system is most widely used. Well differentiated tumors with well formed tubules and showing least nuclear

polymorphism and mitoses are termed as grade 1. Poorly differentiated tumors with rare glandular forms, multistructural cells and a high extent of mitoses are termed as grade 3. Tumors intermediate between grades 1 and 3 are considered as grade 2. Grade 1 CRC tumors are the least aggressive and the 5-year survival rate (YSR) is 59-93%. In case of grade 2 and 3 tumors the 5-YSR falls to 33-75% and 11-56% respectively (Jass et al., 1986; Qizilbash, 1982). The clinical utility of various other prognostic indicators like expression of p53, bcl-2, TGF-α, EGF, TGFBR2, deleted in colorectal cancer (DCC) gene, thymidylate synthase (TS), KRAS mutations, MSI status, allelic loss of chromosome 18q, has been investigated. Although 18q deletion and MSI status have shown promise, their practical utility remains to be confirmed by large scale studies (Deans et al., 1992; Steinberg et al., 1987; Sternberg et al., 1999). Location of CRC tumor is also a good indicator of prognosis. For instance, the left sided lesions favour patient survival whereas right sided tumors, especially those causing bowel obstruction, reduce the chances of survival (Wolmark et al., 1983). Presence of perforation in the colonic tract indicates negative prognosis (Steinberg et al., 1987). Increased pre-treatment levels of serological markers like carbohydrate antigen 19-9 (CA 19-9) and CEA are associated with poor prognosis (Filella et al., 1992). CRC patients who respond to chemotherapy with drugs like 5-fluorouracil (5-FU), irinotecan and oxaliplatin have longer median survival time than non-responders. Response to chemotherapy and chances of survival in cases of metastatic CRC are dependent on the extent of metastasis which can be evaluated by determining the number of sites to which metastasis has occurred, number of lesions in such sites and the extent to which the metastatic site is affected.

Table 1.1. TNM system and AJCC stage groupings with equivalent Dukes and MAC stages of CRC (adapted from Labianca et al., 2010).

TNM system			
Primary tumour (T) TX: Assessment of primary tumour cannot be done T0: Lack of evidence of primary tumour Tis: Carcinoma *in situ*: invasion of the lamina propria or intraepithelial T1: Submucosa invaded by tumour T2: Muscularis propria invaded by tumour T3: Invasion of tumour through the muscularis propria into the subserosa, or into the nonperitonealized pericolic or perirectal tissues T4: Tumour directly invades other organs or structures and/or perforates the visceral peritoneum			
Regional lymph nodes (N) NX: Assessment of regional nodes cannot be done N0: Regional lymph node metastasis absent N1: Metastasis in 1 to 3 regional lymph nodes N2: Metastasis in 4 or more regional lymph nodes			
Distant metastasis (M) MX: Presence of distant metastasis cannot be assessed M0: No distant metastasis M1: Distant metastasis			
AJCC stage grouping	**TNM value**	**Dukes Stage**	**MAC Stage**
Stage 0	Tis, N0, M0	-	-
Stage I	T1, N0, M0	A	A
	T2, N0, M0		B1
Stage IIA	T3, N0, M0	B	B2
Stage IIB	T4, N0, M0		B3
Stage IIIA	T1-2, N1, M0	C	C1
Stage IIIB	T3-4, N1,M0		C2
Stage IIIC	Any T, N2, M0		C3
Stage IV	Any T, any N, M1	D	D

Generally female patients have better survival time than male patients. Patients showing no symptoms of CRC exhibit better response to chemotherapy and survive longer than those showing symptoms. Prior chemotherapy results in resistance to second-line treatment (Buyse et al., 2000a, 2000b; Kohne et al., 2002).

1.1.7. Treatment of colorectal cancer

Surgery alone is the first line of treatment particularly for stage 0 and I CRC. Adjuvant chemotherapy is administered especially in high risk stage II and III CRC in order to reduce chances of recurrence and to increase survival time. 5-FU [with leucovorin (LV)] by infusion or capecitabine (oral prodrug of 5-FU) is usually used for adjuvant chemotherapy. In some cases, oxaliplatin in combination with 5-FU (with LV) is also used (Labianca et al., 2010). Unfortunately 25 to 30% of CRC patients reach stage IV at the time of diagnosis, implying that the optimal treatment window has already expired. In such cases, the standard treatment approach involves surgical removal of the primary tumor, treatment of extra-colonic metastases and palliative radiotherapy and chemotherapy. Liver is the commonest organ to be affected by distant metastasis from CRC followed by lung (Ridge and Daly, 1985). Treatment of metastases involves surgical resection if possible with or without additional chemotherapy. Radiotherapy and chemotherapeutic agents like 5-FU, irinotecan and oxaliplatin are used for palliative treatment in inoperable metastatic cases (Metrakos, 2009). In some cases, newer drugs such as bevacizumab [an inhibitor of vascular endothelial growth factor (VEGF)] and

cetuximab (an antibody against EGF) are used in combination with conventional drugs to enhance response and survival of metastatic CRC patients (Hurwitz et al., 2004; Kabbinavar et al., 2003; Saltz et al., 2004).

1.1.8. Inflammation and colorectal cancer

Past evidence suggest a strong association of inflammation with different forms of cancer including CRC. For instance, IBD is a considerable risk factor for CRC development. Inflammation is also linked to both hereditary and sporadic forms of CRC. Inflammation promotes tumor growth, partially through stimulation of proliferation and angiogenesis as well as by inhibiting apoptosis and immune surveillance. The underlying mechanisms involved in the interplay of inflammation and CRC are quite complicated. Although various inflammatory cytokines, such as tumor necrosis factor- alpha (TNF-α) and interleukin-6 (IL-6), have been found to be involved in CRC carcinogenesis, the two major bridging factors of inflammation and CRC are the cyclooxygenase-2 (COX-2) enzyme and nuclear factor kappa B (NF-κB) (Mantovani et al., 2008; Kraus and Arber, 2009; Terzic et al., 2010). NF-κB consists of a family of five closely related transcription factors which are involved in the modulation of inflammation and apoptosis (Dolcet et al., 2005). Activation of constitutive NF-κB promotes tumor growth in CRC. Of the different isoforms of COX, which catalyze the metabolism of arachidonic acid (AA) into eicosanoids, including prostaglandins (PGs) and thromboxanes (TXs), COX-2 is overexpressed in CRC (Kashfi and Rigas, 2005; Sano et al., 1995; Soslow et al., 2000). Some of the lipoxygenase (LOX) enzymes which

convert AA to eicosanoids like hydroxy eicosatetraenoic acids (HETEs) and leukotrienes (LTs) are also overexpressed in CRC (Shureiqi and Lippman, 2001; Soumaoro et al., 2006). As a consequence, perturbation of AA metabolic pathway, which plays a key role in inflammation mediated CRC carcinogenesis, occurs. Clinico-epidemiological studies have shown that chronic use of selective COX-2 inhibitors like coxibs and non selective non-steroidal anti-inflammatory drugs (NSAIDs) reduces the risk of CRC implying the importance of COX-2 in inflammation mediated development of CRC (Marnett, 1992; Smalley and DuBois, 1997).

1.1.9. Challenges in the management of colorectal cancer

Pre-symptomatic screening is carried out with the aim of detecting early stage CRC or precursor lesions in order to improve survival and reduce treatment-related morbidity. Unfortunately, only about 37% of CRC remain localized at the time of diagnosis. Present diagnostic and screening methods for CRC, such as colonoscopy, flexible sigmoidscopy, DCBE, CT, FOBT, faecal based DNA test, serological markers such as CEA, have certain limitations and shortfalls in their own ways. For instance, endoscopic diagnostic techniques are invasive and may cause iatrogenic injury resulting in poor patient compliance. Although the use of FOBT and colonoscopy in high risk individuals, has improved detection, CRC detected using these methods usually are not at early stages, meaning the chance of curing such patients has already passed. The limitations of these methods become more pronounced when it comes to prognosis of CRC. Although CEA measurement is minimally invasive, it

suffers from low specificity. Faecal DNA testing while more specific, is cumbersome to administer leading to poor patient compliance (Brenner et al., 2005). Although genomics and proteomics techniques have lead to the identification of many serum-based, tissue- based and faecal- based markers of CRC, the clinical utility of such markers is limited and in some cases controversial (de Noo et al., 2006; Locker et al., 2006).

Patients at high risk for CRC relapse following surgical resection may be given adjuvant chemotherapy to improve their survival time. Although the 5-year survival rate (YSR) for patients with stage II CRC is 75%, recurrence occurs in one fourth of these patients. Response of stage II or stage III CRC patients to 5-FU based adjuvant therapy is dependent on MSI status of patients. Responders usually have stable or low MSI whereas non-responders have high MSI. However, determination of MSI status is quite labour intensive and costly (Ribic et al., 2003). Therefore, some patients may not derive significant clinical benefits when given adjuvant chemotherapy and may in fact suffer from the toxic side effects of anticancer drugs. Therefore, there is a real need to identify new markers of CRC that demonstrate diagnostic and prognostic values as well as markers capable of patient stratification. This would enable oncologists to optimize the current clinical management of CRC (Crawford et al., 2003; Duffy et al., 2007).

1.2. Metabolic profiling

Since its inception in the late 1960's the field of metabolic profiling has grown remarkably in terms of its applications and contributions to system biology

research. Metabolic profiling which encompasses both metabonomics and metabolomics, provides a powerful tool for gaining valuable insight into functional biology, toxicology, pharmacology and diagnosis of diseases. Although the terms metabonomics and metabolomics are often used interchangeably there exists an important difference between the two. Metabonomics involves determination of changes in metabolic profiles of living organisms in response to any diseased condition or genetic modification or due to effect of environment or lifestyle related factors (Nicholson et al., 1999) whereas in metabolomics, metabolic profiling of living organisms under normal physiological conditions without any extraneous influence is carried out (Harrigan and Goodacre, 2003). Metabolic profiling is complementary to genomics and proteomics as it measures the perturbed metabolic end-points due to environmental, pharmacological or pathological influences while in genomics and proteomics, more upstream biological events are typically profiled and studied (Fiehn, 2001). It involves the analysis of various biological matrices such as plasma, urine and tissues using suitable analytical platforms. Metabolic profiling can be carried out with a global non-targeted approach as well as with a targeted approach. In targeted metabolic profiling, alterations in the levels of a specific class of metabolites or metabolites belonging to a specific metabolic pathway are ascertained using an appropriate analytical technique (Morris and Watkins, 2005; Urpi-Sarda et al., 2009). In global non-targeted metabolic profiling, metabolites belonging to diverse metabolic pathways are profiled. The metabolites that are determined in non-targeted approach belong to various chemical classes such as organic acids, amino acids, fatty acids, amines, sugars, sugar alcohols, steroids, nucleic acid

bases and other miscellaneous substances. So, multiple complementary analytical techniques are often utilized for non-targeted metabolic profiling of biological matrices, in order to cover as much of metabolic space as possible (Dunn and Ellis, 2005; Lindon et al., 2007a).

1.2.1. Biomatrices used for metabolic profiling

Plasma, urine, tissue specimens and tissue extracts are the commonly used biomatrices for metabolic profiling. As plasma and urine can be obtained in minimally invasive manner, metabolic profiling of these biomatrices, holds the potential for diagnosis of diseases. On the other hand tissue-based metabolic profiling furnishes spatial and site specific information about metabolites and provides molecular insight into disease conditions (Price et al., 2008). In addition to these, other biomatrices utilized for metabolic profiling include seminal fluid, saliva, cerebrospinal fluid, lung aspirates, gastrointestinal fluids, bile, tears, fluids obtained from cysts and blisters, amniotic fluid, synovial fluid and dialysis fluid (Lindon et al., 2007b). Metabolic profiling can also be carried out using *in vitro* cell culture systems such as cancer cells (Ippolito et al., 2005) and tissue spheroids (Bollard et al., 2002).

1.2.2. Analytical platforms used in metabolic profiling

In an ideal world, an analytical platform for metabolic profiling should allow analysis with minimal or no sample preparation, should be high throughput, highly sensitive and should exhibit high degree of robustness and

reproducibility. Moreover for non- targeted metabolic profiling, comprehensive coverage of metabolic space and ease of identification of profiled metabolites are additional desirable properties of an analytical platform. Analytical platforms that are commonly used for metabolic profiling include nuclear magnetic resonance (NMR) spectroscopy and mass spectrometry (MS) based techniques like direct infusion MS, gas chromatography mass spectrometry (GC/MS), liquid chromatography mass spectrometry (LC/MS) or capillary electrophoresis mass spectrometry (CE/MS). In addition to these techniques other methods like Fourier transform infrared (FTIR) spectroscopy, LC with ultraviolet or coulometric detection and CE with ultraviolet detection have also been used for metabolic profiling. In this section a brief overview of the different analytical methods used for metabolic profiling is provided.

1.2.2.1. Nuclear magnetic resonance (NMR) spectroscopy

NMR spectroscopy possesses many attributes of an ideal platform for metabolic profiling such as minimal sample pretreatment, high reproducibility, robustness, rapid analysis time, non-selectivity (in terms of metabolic space) and capability of providing detailed structural information about profiled metabolites. Although NMR spectroscopy is comparatively less sensitive than MS-based techniques, the availability of cryogenic NMR probes has improved the sensitivity and throughput of NMR spectroscopy (Keun et al., 2002). An estimate of NMR sensitivity in terms of number of metabolites measured can be obtained from a recent study in which NMR was able to measure 49

metabolites in human serum as compared to 96 by LC/MS and 99 by GC/MS (Psychogios et al., 2011). NMR spectroscopy has been utilized extensively for the metabolic profiling of liquid biomatrices like body fluids and tissue extracts. The introduction of high resolution magic angle spinning NMR (HR-MAS NMR) spectroscopy has extended the applicability of NMR spectroscopy for metabolic profiling of solid and semisolid biomatrices like intact tissue specimens. Proton (^{1}H) NMR spectroscopy is the dominant technique used for metabolic profiling. Spectral assignment and metabolite identification in ^{1}H NMR is quite complicated and dependent on chemical shifts, relative intensities, signal multiplicities of the ^{1}H resonances and coupling constants. Two dimensional ^{1}H NMR spectroscopic methods like correlation spectroscopy (COSY) and total correlation spectroscopy (TOCSY) are often utilized for spectral assignment and identification of metabolites. Apart from ^{1}H, other types of nuclei such as ^{15}N, ^{13}C or ^{31}P can also be exploited to aid spectral assignment in certain cases. Various NMR pulse sequences can be utilized to differentiate spectral contributions of macromolecules (such as proteins and lipoproteins) from those obtained from low molecular weight metabolites (Lenz and Wilson, 2007; Lindon et al., 2007b; Nicholson et al., 1995).

1.2.2.2. Mass spectrometry (MS) based techniques

MS can be used alone as direct infusion MS or in conjunction with separation techniques for metabolic profiling. Direct infusion of liquid biomatrices or tissue extracts into MS has been used for metabolic profiling in some cases.

Although it is a high throughput technique, it suffers from the disadvantage of high matrix effects, as proper sample preparation steps and chromatographic separation are not involved. Matrix effect can be defined as the indirect or direct changes or interference in response due to the presence of unintended analytes (for analysis) or other interfering substances in the sample (FDA, 2001). The limitations become more pronounced in the case of complex and variable biomatrices like urine and also in the case of isobaric analytes (Dunn et al., 2005).

High resolution, high sensitivity and availability of commercial libraries for metabolite identification render GC/MS an excellent and robust platform for the global non-targeted metabolic profiling of complex biomatrices. However, GC/MS analysis involves tedious sample preparation steps as it is necessary to derivatize analytes to reduce their polarity and increase volatility. This shortcoming is often tolerated in metabonomic research where the demand for chromatographic resolution takes priority over the need for the assay to be high throughput. The advent of two dimensional gas chromatography time of flight mass spectrometry (GC×GC/TOFMS) has comprehensively enhanced the metabolic space coverage of conventional GC/MS. Moreover, the development of softwares packages with deconvolution feature to differentiate co-eluting chromatographic peaks has facilitated shorter GC/MS analysis thus improving the throughput of the technique (Lenz and Wilson, 2007).

LC/MS has certain advantages over GC/MS in terms of ease of sample pretreatment and flexibility in throughput. The applicability of LC/MS in non-targeted metabolic profiling is comparatively restricted due to the constraint in

the number of metabolites amenable to analysis (Halket et al., 2005; Want et al., 2010). However, developments in diverse LC column chemistries and chemical derivatization strategies (Groger et al., 2003; Halket et al., 2005; Tolstikov and Fiehn, 2002) have enhanced the metabolic space coverage of LC/MS. Although LC/MS is considered as a suitable analytical platform for both targeted and non-targeted metabolic profiling, its applicability is more established in the case of targeted profiling of metabolites. This is due the fact that LC/MS can be operated in highly selective and sensitive mode if desired for targeted analysis. For non-targeted profiling, LC/MS is generally operated in both positive and negative electrospray ionization (ESI) modes for the comprehensive coverage of metabolic space. The emergence of microbore LC/MS and ultra performance LC (UPLC) systems has improved the resolving capacity, sensitivity and separation speed of conventional LC/MS (Lenz and Wilson, 2007; Lindon et al., 2007b; Wilson et al., 2005).

CE/MS has also been used as a platform for metabolic profiling especially for profiling low abundance metabolites. The separation mechanism of CE/MS makes it a suitable platform for analysis of polar, ionisable metabolites. Another advantage of CE/MS is the small sample volume needed. Moreover, liquid biomatrices like urine requires minimal sample preparation steps prior to analysis (Lee et al., 2007; Soga et al., 2003, 2007).

1.2.2.3. LC/NMR/MS hybrid techniques

For metabolic profiling, LC/NMR/MS hybrid platforms can also be utilized. In such systems the LC eluent is split into two parts and subjected to concomitant

analysis by both NMR and MS. The resulting NMR- and MS-based data provide in-depth molecular information and aids in metabolite identification (Lindon et al., 2000, 2004). Emergence of highly sophisticated data analysis techniques has further facilitated the analysis and interpretation of LC/NMR/MS hybrid platforms (Cloarec et al., 2007; Shen et al., 2002). LC/NMR/MS methods have shown promise in the discovery of metabolite based markers of xenobiotic induced renal toxicity (Foxall et al., 1996) and characterization of lipoproteins in human blood serum (Daykin et al., 2001). LC/NMR/MS has also been utilized for urinary metabolic profiling of pediatric metabolic disorders such as methylmalon aciduria (Zurek et al., 2005). It has also been used for the metabolic profiling of human amniotic fluid with an aim to diagnose disorders in the mother or developing fetus (Graca et al., 2008).

1.2.2.4. Other analytical techniques

Although LC with ultraviolet (Pham-Tuan et al., 2003) or coulometric detection (Gamache et al., 2004; Vigneau-Callahan et al., 2001) and CE with ultraviolet detection (Barbas et al., 1998; Zomer et al., 2004) have been explored for metabolic profiling, their usage is limited by their inability to identify metabolites directly. However, in the case of LC with coulometric detection, libraries of standard compounds can be created on the basis of LC retention times and redox properties for metabolite identification (Gamache et al., 2004). Although FTIR spectroscopy has been explored for metabolic profiling, its applicability is very limited as it does not provide sufficient

information to identify metabolites. However, the short analysis time required per sample (about 5 to 10 s) enables its usage as an optional tool for screening or group classification or as an adjunct method to other commonly used analytical platforms (Dunn et al., 2005; Harrigan et al., 2004; Kaderbhai et al., 2003; Leon et al., 2009). The advantages, disadvantages and applications of different analytical platforms used for metabolic profiling have been summarized in Table 1.2.

1.2.3. Chemometrics in metabolic profiling

Global non-targeted metabolic profiling results in the generation of huge and complex data sets containing a large number of variables. Multivariate statistical techniques or chemometric tools are indispensable for the analysis of such data sets. Of the different chemometric methods available such as hierarchical clustering, partitional clustering, artificial neural networks, support vector machine, evolutionary-based algorithms and regression trees, projection-based chemometric methods are extensively used (Goodacre et al., 2007). Projection-based methods include both unsupervised methods like principal component analysis (PCA) and supervised methods such as partial least squares discriminant analysis (PLS-DA) and orthogonal PLS-DA (OPLS-DA). Projection-based methods are based on the assumption that the system in question is controlled by a few latent variables (LVs) or principal components (PCs). In PCA, the variation in the data is approximated by a model plane of a low dimension on the basis of computed principal components. The largest variation in the data is defined by the first PC and the second largest variation

Table 1.2. Advantages, disadvantages and applications of different analytical platforms used for metabolic profiling

Analytical Technique	Advantages	Disadvantages	Applications
NMR spectroscopy	Involves minimal sample pretreatment Highly reproducible and robust High throughput Non-selective (in terms of metabolic space) Provides detailed structural information about profiled metabolites	Less sensitive than MS-based techniques Spectral assignment and metabolite identification is complicated	Metabolic profiling for xenobiotic toxicity assessment, different forms of cancer, neurological disorders, metabolic disorders, aging etc (Coen et al., 2008). Intact tissue based metabolic profiling using solid state MAS-NMR (Keun et al., 2002).
Direct infusion MS	High throughput	Suffers from high matrix effect and isobaric interference	Microbial metabolic profiling studies (Dunn et al., 2005)
GC/MS	High resolution and sensitivity Availability of EI spectra-based commercial libraries for metabolite identification Not susceptible to matrix effect	Involves tedious sample preparation Comparatively low throughput	Profiling of volatile metabolites in lung cancer (Chen et al., 2007) and skin emissions (Gallagher et al., 2008) using headspace GC/MS. Metabolic profiling for validating animal models of diseases (Chang et al., 2011), xenobiotic toxicity assessment (Boudonck et al., 2009), different forms of cancer (Denkert et al., 2008), metabolic disorders (Bao et al., 2009), neurological disorders (Underwood et al., 2006).

Table 1.2. Advantages, disadvantages and applications of different analytical platforms used for metabolic profiling (Continued).

Analytical Technique	Advantages	Disadvantages	Applications
LC/MS	Ease of sample pretreatment as compared to GC/MS Allows flexibility in throughput Highly suitable for targeted profiling	Susceptible to matrix effect Non-availability of EI spectra-based commercial libraries for easy metabolite identification	Metabolic profiling for xenobiotic metabolism and toxicity assessment (Chen et al., 2007), different forms of cancer (Ong et al., 2010), metabolic disorders (Wang et al., 2005), neurological disorders (Li et al., 2010).
CE/MS	Liquid biomatrices like urine requires minimal sample preparation Requires small sample volume	Metabolic space coverage restricted to polar, ionisable metabolites	Microbial metabolic profiling and as a complementary platform to GC/MS or LC/MS for metabolic profiling of diseases (Lenz and Wilson, 2007; Barbas et al., 2011)
LC/NMR/MS	Provides in-depth molecular information Combination of NMR and MS aids in metabolite identification	Highly expensive instrumentation	Metabolic profiling for metabolic disorders (Zurek et al., 2005) and human amniotic fluid (Graca et al., 2008).
FTIR spectroscopy	High throughput	Applicability is limited as it does not provide sufficient information to identify metabolites	Microbial metabolic profiling, metabolic profiling for cancer and other diseases (Dunn et al., 2005).
CE or LC with UV or coulometric detection	Comparatively inexpensive	Application limited due to inability to identify metabolites readily Less sensitive and less specific than MS-based techniques	Evaluation of food ingredient impact (Pham-Tuan et al., 2003; Vigneau-Callahan et al., 2001), animal model of diabetes (Barbas et al., 2011), profiling of exogenous metabolites (Gamache et al., 2004).

by the second PC and so on. These PCA model components are mutually orthogonal to each other. A score plot generated by plotting the first two components aids in the visualization of the relation between the observations or samples in the data set. The score plot is useful for identifying outliers and inherent clustering trends. Outliers can also be detected by using the distance to model plot (DModX) based on residual variance of the model. The contribution of the variables in the model plane and their interrelation are depicted by the loading plot (Lindon et al., 2001). PLS is a supervised method that is usually used to determine whether a quantitative relationship exist between two data matrices for instance X matrix and Y matrix. PLS when used to discriminate different classes, is termed as partial least squares discriminant analysis (PLS-DA). In PLS-DA, class information is used to enhance separation of observations belonging to different classes. The class information is provided by generating a Y data matrix composed of discrete dummy variables denoting specific class belonging. However the disadvantage of PLS models is that they are influenced by variation in the X matrix that is unrelated to the Y matrix. This results in difficulty of model interpretation and identification of variables contributing significantly to the model for instance identifying marker metabolites in the case of metabonomics (Wold et al., 1984). The orthogonal partial least squares (OPLS) method is a modified form of PLS where orthogonal signal correction is used to split the variation in X matrix into two parts, one that is unrelated or orthogonal to Y and the other that is related to Y. This eases model interpretation and identification of important variables contributing to the model. OPLS if used for class discrimination is termed as orthogonal partial least squares discriminant

analysis (OPLS-DA) (Bylesjö et al., 2006). In our global non-targeted metabolic profiling studies, we have used PCA to identify innate grouping trends and outliers (if any) and OPLS-DA to generate discriminating models and to identify marker metabolites. Chemometric softwares such as SIMCA-P and Unscrambler (CAMO software, Oslo, Norway), and mathematical environments such as MATLAB and R (open source GNU project) are typically employed for chemometric data analysis in metabonomics.

A typical chemometric model built in a metabonomic study is characterized by the use of a relatively small number of observations compared to the number of variables (Westerhuis et al., 2008). Therefore, in some cases, it is possible that optimistic performance characteristics observed in a PLS-DA or OPLS-DA model could be due to specimen artifacts, over fitting of data or chance correlation (Broadhurst and Kell, 2006; Smit et al., 2007; Trygg et al., 2007). Therefore, validation of each model should be performed before it can be leveraged to predict the unknown observations or identification of marker metabolites. Model validation can be performed in two stages starting with internal validation and followed by external validation. Internal validation of PLS-DA models can be performed using permutations test and receiver operating characteristic (ROC) analysis (Pasikanti et al., 2010). In permutation test, goodness of fit (R^2 and Q^2) of the original model is compared with the goodness of fit of several PLS-DA models built using the data matrix where the order of the Y-observations are randomly permuted, while the X-matrix is kept intact (Mahadevan et al., 2008; Wiklund et al., 2007). Subsequent to confirmation of validity of each model using internal validation strategies, model validity can be further confirmed

using external validation. To perform external validation, a subset of observations is randomly selected for building a training set and classification of the remaining samples are then predicted. The selection of training and tests sets should be defined prior to chemometric analysis to represent actual prediction of unknown samples and to avoid any bias related to data preprocessing and pretreatment. External validation can be performed iteratively by randomly selecting different combination of training and test sets to estimate the predictive ability of the model. Most software packages (SIMCA-P or MetaboAnalyst) offer in-built features to perform validation.

1.2.4. Role of metabolic profiling in colorectal cancer

The present challenges in the management of CRC imply that there is a dearth in the availability of clinically significant biomarkers of prognostic, diagnostic and patient stratification. Global non-targeted metabolic profiling has already shown potential in identifying metabolite-based markers in ovarian cancer (Denkert et al., 2006), prostate cancer (Cheng et al., 2005; Sreekumar et al., 2009), kidney cancer (Kind et al., 2007), bladder cancer (Pasikanti et al., 2009), liver cancer (Yang et al., 2004) and brain cancer (Petrik et al., 2006). Similar metabolic profiling of CRC may lead to the identification of marker metabolites which may provide greater insight into the carcinogenesis, diagnosis, prognosis and patient stratification. On the other hand, targeted metabolic profiling can help in recording the deregulation of a specific metabolic pathway and thereby elucidating the roles of the associated metabolites in CRC development.

1.3. Study hypotheses

1.3.1. Hypothesis for non-targeted metabolic profiling of CRC

Previous studies indicate that changes in gene expression and consequent up or down regulation of metabolic enzymes may result in perturbation of metabolic pathways in CRC (Bi et al., 2006; Longley et al., 2006). This led to our hypothesis that tissue-based non-targeted metabolic profiling of CRC if used to determine such changes in metabolic profiles would enable identification of marker metabolites differentially expressed in CRC and normal tissue and provide greater insight into disease progression, treatment response and carcinogenesis in CRC.

1.3.2. Hypothesis for targeted profiling of eicosanoids and arachidonic acid in CRC

Altered expression of COX-2 and LOX enzymes in CRC causes fluctuations in the levels of eicosanoids such as PGs, HETEs, TXs and LTs (Kashfi and Rigas, 2005; Sano et al., 1995; Shureiqi and Lippman, 2001; Soslow et al., 2000; Soumaoro et al., 2006). Therefore we hypothesized that targeted profiling of these eicosanoids and their major metabolic precursor AA would help to elucidate the deregulation of eicosanoid biosynthetic pathway as well as the implications of these profiled metabolites in inflammation-mediated CRC carcinogenesis.

1.4. Study objectives

The main objectives of this study are stated below.

- Tissue-based non-targeted metabolic profiling of CRC using three different analytical platforms viz. GC/MS, HR-MAS NMR spectroscopy and GC×GC/TOFMS followed by multivariate and univariate statistical analyses of generated data to identify marker metabolites and altered metabolic processes in CRC.

- Targeted metabolic profiling of eicosanoids and their major metabolic precursor AA using ultra performance liquid chromatography tandem mass spectrometry (UPLC/MS/MS) in order to identify significantly altered metabolites belonging to the eicosanoid biosynthetic pathway and their biological relevance in inflammation-mediated CRC development.

1.5. Significance of the study

Non-targeted metabolic profiling of CRC in conjunction with chemometric data analysis may help in the identification of marker metabolites and related metabolic pathways that are altered in CRC. This in turn would help to elucidate the metabolic phenotype of CRC and provide molecular insight in CRC development. Such information is valuable from the perspective of future biomarker research and identification of alternative therapeutic

strategies in CRC. Targeted metabolic profiling of relevant eicosanoids and AA in CRC would help to elucidate the role of these metabolites in associating inflammation with CRC. As NSAIDs exert their pharmacological effect primarily by inhibiting COX mediated synthesis of some of these eicosanoids, the targeted profiling of these metabolites would also help to postulate the mechanistic aspect of NSAID-based adjuvant chemotherapy in improving the prognosis of CRC.

CHAPTER 2

DEVELOPMENT AND VALIDATION OF A GC/MS METHOD FOR NON-TARGETED METABOLIC PROFILING OF HUMAN COLON TISSUE

2.1. Introduction

Tissue-based metabolic profiling differs from plasma- or urine-based metabolic profiling as it provides anatomical site-specific information of the endogenous metabolites. As these metabolites belong to diverse chemical classes and possess physicochemical heterogeneity, it is quite challenging to develop a robust and reproducible analytical method for their profiling. Among the various methods utilized conventionally for metabolic profiling, GC/MS has emerged as a potentially useful method because of its high sensitivity, reproducibility and peak resolution. Moreover identification of metabolites can be easily carried out using GC/MS electron impact (EI) spectral libraries. However chemical derivatization of the polar functional groups of analytes in order to decrease their polarity, increase their volatility and thermal stability, is usually required for GC/MS analysis. As a result of this tedious sample preparation process as well long elution time, GC/MS is considered as a low throughput technique when compared to other techniques like LC/MS or NMR spectroscopy (Pasikanti et al., 2008). Nonetheless, the ease of metabolite identification by GC/MS along with its high sensitivity and resolution makes it a feasible option in non targeted metabolic profiling. So far GC/MS has been used for tissue-based metabolic profiling of mice liver (Xin

et al., 2006), heart, muscle and adipose tissue (Atherton et al., 2006), human ovarian tissue (Denkert et al., 2006) and human colon tissue (Denkert et al., 2008).

This chapter deals with the development and validation of a GC/MS method for non-targeted metabolic profiling of human colon tissue. In this study, a suitable GC/MS method was developed, sample preparation steps were optimized and different validation parameters such as sensitivity, selectivity, linearity of response, precision, freeze-thaw cycle stability, auto-sampler stability and long term stability were investigated.

2.2. Experimental

2.2.1. Materials

Standard compounds such as standard alkane series (C-10 to C-40), L-alanine, L-valine, glycine, L-threonine, L-proline, L-phenylalanine, L-tyrosine, myo-inositol, uridine, uracil, D-glucose, D-mannose, D-galactose, L-(+)-lactic acid, fumaric acid, D-(+)-malic acid, arachidonic acid, phosphoric acid and cholesterol were obtained from Sigma-Aldrich Inc. (St. Louis, MO, USA). Spectroscopy grade methanol, chloroform and toluene were obtained from Tedia (Fairfield, OH, USA) and water used for the study was purified with a Milli-Q water purification system (Millipore, Billerica, MA, USA). N, O-bis (trimethylsilyl) trifluoroacetamide (BSTFA) with 1% trimethylchlorosilane (TMCS), N-methyl-N-trifluoroacetamide (MSTFA) with 1% trimethylchlorosilane (TMCS) and methoxyamine hydrochloride in pyridine

(MOX) were obtained from Thermo Fisher Scientific (Rockford, IL, USA) while sodium sulphate was obtained from Sigma-Aldrich (St. Louis, MO, USA).

2.2.2. Human colon tissue samples

Human colon tissues were provided by the Department of Colorectal Surgery, Singapore General Hospital (SGH), Singapore. The utilization of human tissue was approved by the institutional review board (IRB) at the SGH (IRB reference number 260/2007). For method development and validation, one representative normal colon tissue (3.00 g) was snap-frozen immediately following surgery and then stored at -80ºC until processing. The tissue was subsequently cut and divided into tissue masses of about 20 mg each for the GC/MS method development and validation.

2.2.3. Sample preparation

For the development of the sample preparation protocol, previously reported sample preparation strategies (James et al., 2004; Lin et al., 2007; Lisec et al., 2006; Pasikanti et al., 2008) were used as references. Various parameters such as different methods of extraction (homogenization alone, homogenization followed by ultra-sonication, ultra-sonication alone) and time periods of ultra-sonication (40, 60 and 100 min), weights of colonic tissue samples (5 to 40 mg) and derivatization strategies (incubation with BSTFA or MSTFA at 70ºC for 30 min and overnight methoximation using MOX followed by incubation

Figure 2.1. GC/MS chromatograms depicting results of development and optimization of sample preparation method. **A**: No appreciable difference observed between different extraction strategies. [Sonication for 100 min opted for ease of sample preparation].; **B**: Effect of different tissue weights on GC/MS profile [20 mg chosen as minimal weight for tissue]; C: Effect of different derivatization strategies [MOX effecting resolution as compared to MSTFA alone].

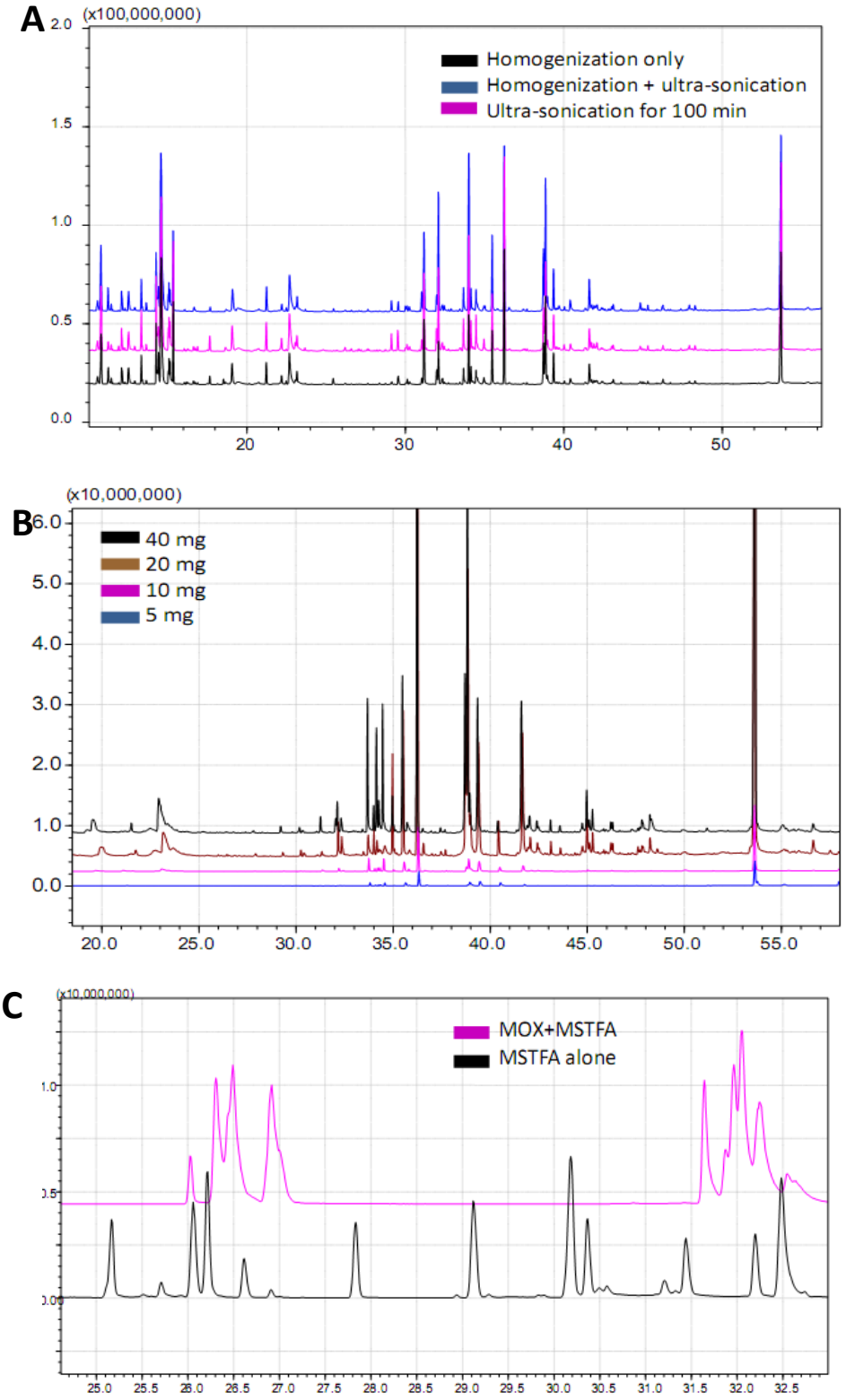

with MSTFA at 70ºC for 30 min) were explored to optimize the final sample preparation protocol. Some of the results obtained during development and optimization of sample preparation method are presented in Figure 2.1.

Using the optimized method, each colon tissue was weighed accurately and transferred to 15 mL glass centrifuge tubes. 1 mL of a mono-phasic mixture of chloroform-methanol-water in ratio of 20:50:20 (v/v) was added to each sample and the tissue sample along with the extraction solvent system was ultra-sonicated in a bath ultra-sonicator at ambient temperature (24ºC) for 100 min and then vortex-mixed for 2 min. The samples were subsequently centrifuged at 1800 g units for 3 min and 0.8 mL of the supernatant was collected separately from each sample in 15 mL glass tube. The collected supernatant was concentrated to complete dryness at 50ºC for 30 min using Turbovap LV nitrogen evaporator (Caliper Life Sciences, Hopkinton, MA, USA). 100 µL of toluene kept anhydrous with sodium sulphate was added to each of the dried tissue extracts, vortex-mixed for 1 min and again evaporated to complete dryness using Turbovap LV in order to eliminate any trace of water which might interfere with the GC/MS analysis. The dried samples were then derivatized by adding 100 µL of MSTFA with 1% TMCS to each sample. The samples were then vortex-mixed for 1 min and incubated at 70ºC for 30 min. After incubation, samples were again vortex-mixed for 1 min and then transferred to vials for GC/MS analysis.

2.2.4. GC/MS analysis

Analysis was performed on a Shimadzu QP2010 GC/MS system (Shimadzu, Kyoto, Japan). A HP-5MS 30 m × 250 µm (i.d.) fused silica capillary column (Agilent J&W Scientific, Folsom, CA, USA), chemically bonded with a 5% diphenyl 95% dimethylpolysiloxane cross-linked stationary phase (0.25 µm film thickness), was used with open split interface. Helium was used as the carrier gas at 1.2 mL/min and the injector split ratio was set to 1:5. An injection volume of 1 µL was used and the solvent cut-off time was 5 min. The injector and source temperatures were kept at 250 and 200ºC, respectively. Oven temperature was kept at 60ºC for 3 min, increased at 7ºC per min to 140ºC where it was held for 4 min and further increased at 5ºC per min to 310ºC where it remained for 6 min. The MS was operated in EI ionization mode at 70 eV. Data acquisition was performed in the full scan mode from *m/z* 50 to 650 with a scan time of 0.5 s. To detect and eliminate retention time (R_t) shift, standard alkane series mixture (C-10 to C-40) was injected periodically into the GC/MS system during analysis of each batch of samples. Chromatogram acquisition and preliminary compound identification by the National Institute of Standards and Technology (NIST) and Wiley EI mass spectral library search were performed using the Shimadzu GCsolution (Version 2.5) software. R_t correction of peaks based on R_t of standard alkane series mixture (C-10 to C-40) was performed using the automatic adjustment of R_t function of the Shimadzu GCsolution software. The chromatograms of all the samples analyzed were subjected to noise reduction and baseline correction using metAlign software (http://www.metalign.nl) prior to

integration of peak area. Integrated peak areas of multiple derivative peaks belonging to each of the same metabolites (D-mannose, D-galactose, D-glucose, myo-inositol) were summed and considered as single compound. All known artifact peaks, such as peaks due to column bleed and MSTFA artifact peaks were not considered in the final data analyses. Data normalization to a constant sum of the chromatographic peak area was carried out before statistical analyses.

2.2.5. Method validation

All the method validation studies, except for linearity validation, were carried out using unspiked human normal colon tissue samples (~20 mg each) according to the US-FDA guidelines for bio-analytical method validation with suitable modifications wherever necessary (FDA, 2001). A relative stability of 100 ± 15% and relative standard deviation (RSD) of 15% were considered as acceptable in our method validation. Calculations of method validation results were performed using Microsoft Excel 2007 software.

2.2.5.1. Freeze-thaw cycle and auto-sampler stability

For each stability study, 6 human colon tissues of ~20 mg each were used. In order to evaluate the freeze-thaw stability, the samples were stored at -80ºC for 24 h and then thawed unassisted at room temperature (24ºC). When completely thawed, the samples were refrozen for 24 h at -80ºC. The freeze-thaw cycle was repeated two more times and then the samples were processed

and analyzed in the third cycle. The results obtained were compared with that obtained from samples which were not subjected to freeze-thaw cycles in order to determine the freeze-thaw stability. Auto-sampler stability was evaluated by keeping the samples in the auto-sampler (24ºC) and re-injecting them after 50 h.

2.2.5.2. Long-term stability

Human colon tissue samples, stored at -80ºC, were processed and analyzed at intervals of 1 month and 3 months, respectively. At each sampling point, triplicate samples of ~20 mg each were analyzed. The results obtained were compared with that of samples analyzed on the first day of method validation.

2.2.5.3. Intra- and inter-day precision

6 human colon tissues of ~20 mg each were processed and analyzed for determination of both intra- and inter-day precision. The inter-day precision values were determined on three different days (first, second and third day of method validation).

2.2.5.4. Selectivity

The selectivity of the GC/MS method was investigated by comparing the chromatogram of blank sample (solvent blank) to that of processed sample (~20 mg of human colon tissue).

2.2.5.5. Linearity

19 of the identified endogenous metabolites were selected to investigate the linear response of the GC/MS method. These compounds cover a wide range of GC R_t (9.85-53.70 min), and belong to various classes of metabolites (amino acids, organic acids, fatty acids, inorganic acids, sugars, alcohols, pyrimidines and steroids) with diverse physicochemical properties. As all the 19 metabolites were endogenously present in colon tissue, it was practically not possible to obtain "blank" human colon tissue devoid of these metabolites. Therefore we validated the linearity of response by spiking the corresponding standard compounds before extraction by the solvent mixture composed of chloroform, methanol and water in the ratio of 20:50:20 (v/v). and then taken through the entire sample preparation process. The concentrations of standard compounds were calculated with respect to 20 mg of colon tissue. For instance, a spiked amount of 200 µg of any standard compound was considered equivalent to a concentration of 200 µg per 20 mg of colon tissue that is 10 µg/mg of colon tissue. The calibration curve of each of the 19 analytes was constructed by linear regression of the absolute integrated peak area data against its concentrations.

2.2.5.6. Sensitivity

The main objective of our study was to develop an optimal GC/MS method for the profiling of endogenous metabolites of colon tissue. Therefore, instead of determining limit of detection (LOD) and limit of quantification (LOQ) of

individual metabolites, it was considered comparatively more important to determine the minimal amount of colon tissue that was required to produce a reasonably sensitive profiling of the endogenous metabolites. In our method development, different weights of colon tissue (5, 10, 20 and 40 mg) were processed and analyzed to determine an optimal balance between tissue weight and generation of sufficient GC/MS data.

2.3. Results and discussion

While exploring various parameters during pre-validation development of sample preparation method, extraction of colon tissue samples by ultra-sonication for 100 min and derivatization using 100 µL of MSTFA at 70ºC for 30 min, were found to be optimal in terms of extraction of metabolites and metabolite extraction and coverage. Overnight methoximation of samples using MOX reagent prior to derivatization with MSTFA is considered a conventional step in sample preparation protocol for metabolic profiling (James et al., 2004). The methoximated derivatives of the monosaccharides were found to elute in quick succession in our GC/MS method as compared to the non-methoximated monosaccharides, thus affecting chromatographic resolution. Moreover overnight methoximation at 37ºC also meant comparatively longer sample processing time. Based on these factors, methoximation was eliminated from our colon tissue preparation protocol. As a result, multiple peaks were generated for the monosaccharides and their cumulative peak areas were used in the data analysis. A representative GC/MS chromatogram of normal human colon tissue is shown in Figure 2.2.

GC/MS analysis lead to the identification of 53 metabolites belonging to diverse chemical classes such as amino acids, organic acids, inorganic acids, monosaccharides, aldehydes, amines, amides, fatty acids, fatty acid esters, polyols and pyrimidines (Figure 2.2, Table 2.1). As our developed GC/MS method was the first method to be reported for metabolic profiling of human colorectal tissue samples, it was not feasible to compare it with other reported GC/MS method. However, in a concomitant study by another group a GC/TOFMS method for profiling of CRC tissue samples was used to obtain around 700 chromatographic peaks per sample (Denkert et al., 2008). However it should be noted that the MS used in their study was a TOFMS which allows spectral deconvolution of coeluting peaks and therefore it is not practical to compare it with our GC-single quadrupole MS platform. Later, when we used our developed sample preparation protocol and analyzed our samples using GCxGC/TOFMS (described in Chapter 5) we were able to obtain more than 800 chromatographic peaks per sample indicating that our developed method is quite comparable with that of Denkert et al.

Peaks with similarity index (SI) more than 70% were assigned compound names while those having less than 70% SI were considered as unknown compound. Identities of selected metabolites preliminarily identified by NIST mass spectral library were further confirmed by comparison of their mass spectra and R_t with those obtained using commercially available reference standards (L-alanine, L-valine, glycine, L-threonine, L-proline, L-phenylalanine, L-tyrosine, myo-inositol, uridine, uracil, D-glucose, D-mannose, D-galactose, L-(+)-lactic acid, fumaric acid, D-(+)-malic acid, arachidonic acid, phosphoric acid, boric acid, formaldehyde and cholesterol).

In actual clinical situations where colon tissues are collected from the hospital, stored and processed in the laboratory, the samples would ideally not be subjected to more than 2 freeze-thaw cycles. In this study, the stability of the colon tissue samples was validated over 3 freeze-thaw cycles. Since the stability studies were carried out using unspiked human colon tissue, all 53 identified metabolites (Table 2.1) were used in the validation studies. In clinical sample analysis, multiple samples may be submitted for batch analysis. As the analysis time for each sample is about 1 h, the time difference between the analyses of the first and final samples can be appreciable. In this study, a batch analysis of 50 samples was assumed and hence, the stability of processed samples was validated over 50 h while being kept in the auto-sampler. As colon tissue collected from the hospital may not be analyzed immediately, a long-term stability study was also performed (up to 3 months) where the samples were kept at -80ºC. As shown in Table 2.1., the relative stability of all the 53 metabolites was within the acceptable limits of 100 ± 15% for all three freeze-thaw, auto-sampler and long-term stability studies. Our results implied that human colon tissues are stable over 3 freeze-thaw cycles and when kept at -80ºC for up to 3 months. Our results also confirmed that batch analysis can be performed for up to 50 processed samples with minimum compromise in the integrity of the metabolites. These findings are important in guiding future GC/MS profiling of human colon tissue in terms of the collection, processing, storage and analysis of the samples.

All the 53 identified metabolites were taken into consideration to investigate the precision of the method. The RSD of all the 53 metabolites in terms of intra- and inter-day precision studies was found to be less than 15%

(Table 2.1.). The high precision of the developed GC/MS method observed in our study is pertinent to the success of a metabolic profiling study since the variations in the levels of the metabolites should be an outcome due to an environmental or pathological perturbation rather than a compromise in the precision of the analytical method. A comparison of GC/MS chromatogram of blank and processed colon tissue samples revealed interferences during the first 6 min of the chromatogram due to MSTFA artifacts which would not interfere with the peaks of relevant metabolites. Thus the developed GC/MS method was found to be sufficiently selective.

Each of the 19 metabolites selected for investigating the linearity study showed a satisfactory linear response as evident from their respective r^2 values (Table 2.2.). GC/MS analysis involves tissue metabolite extraction and derivatization. The latter process may affect the linearity of the method. As metabolic profiling of the colon tissue is a semi-quantitative experiment, it becomes important to validate the linearity of the detection.

Figure 2.2. Representative GC/MS metabolite profile of normal human colon tissue. The numbering of metabolite peaks corresponds to peak number of metabolites as shown in Table 2.1. Metabolites are also classified according to their chemical classes.

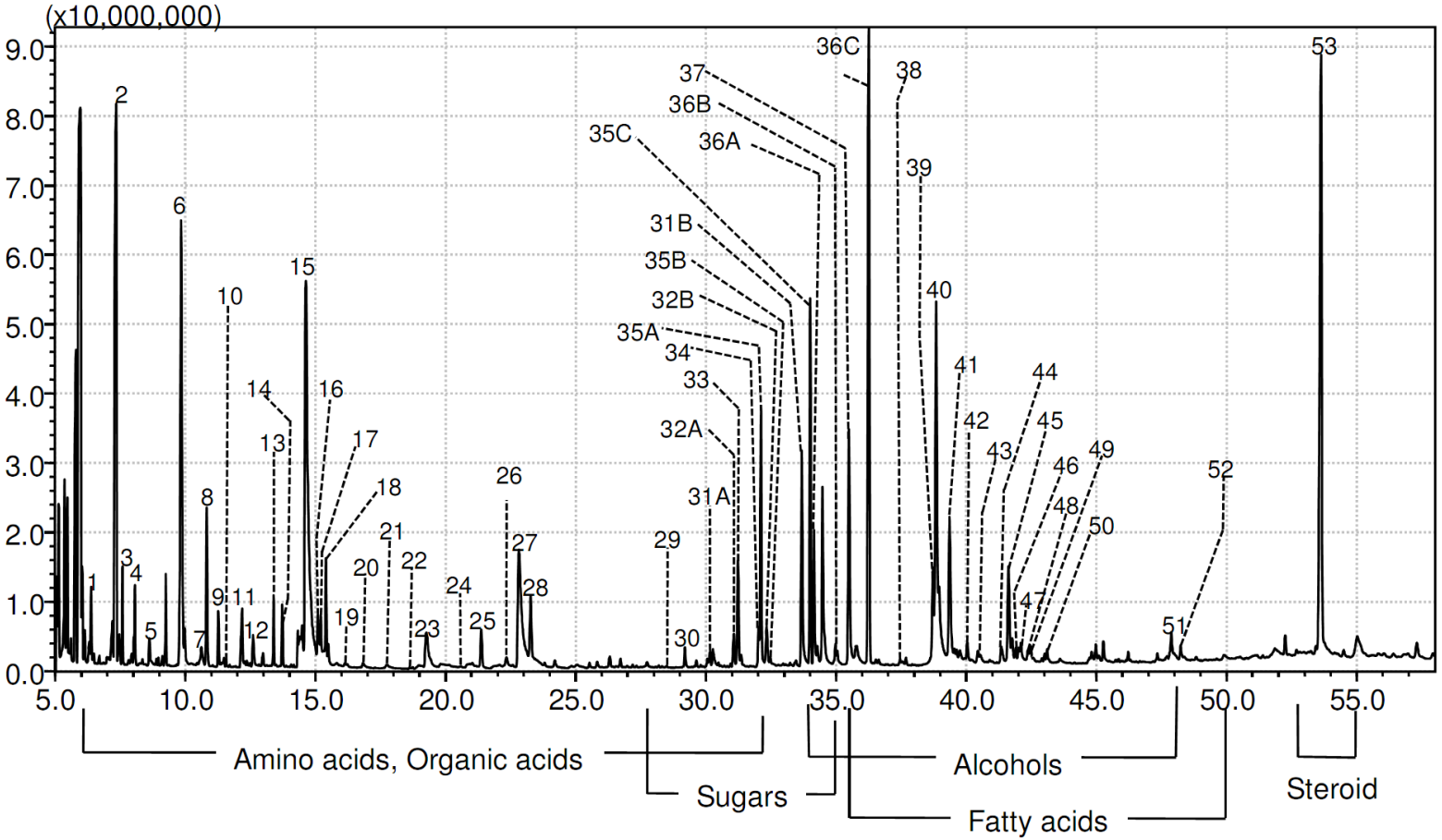

Table 2.1. Endogenous metabolites and results of stability and precision studies.

Peak No.[a]	Metabolites	% Freeze thaw stability	% Auto-sampler stability	% Long term stability		Intra-day Precision %RSD	Inter-day Precision %RSD
				1 month	3 months		
1	Formaldehyde	100.58	98.99	100.80	102.22	1.92	2.20
2	Ethylamine	101.78	97.62	100.72	99.61	1.85	2.15
3	L-Norvaline	101.33	100.18	103.35	103.96	1.50	1.47
4	Boric acid	100.50	100.70	101.50	102.44	1.36	1.43
5	Methyl cyclopent-3-ene	103.59	98.35	105.62	109.54	3.01	3.22
6	Lactate	100.45	99.25	100.39	101.78	1.79	1.73
7	L-Valine	101.84	100.24	100.50	101.92	1.67	2.09
8	L-Alanine	97.69	94.28	92.68	95.05	4.84	5.18
9	Glycine derivative	99.95	99.54	102.72	103.74	2.38	2.50
10	Pyruvate	101.03	101.21	103.75	102.97	2.00	2.06
11	(S)-2-amino-4-methyl-pentanamide	100.48	100.11	100.70	102.52	1.52	1.52
12	Ethanethioic acid	101.13	100.42	101.41	104.79	1.33	1.33
13	L-Valine derivative	100.44	100.58	102.15	102.12	2.40	2.31
14	L-Serine derivative	98.71	98.70	99.05	101.36	1.97	1.93
15	Phosphate	100.51	101.77	102.25	100.63	2.25	2.20
16	L-Threonine derivative	97.86	94.80	97.02	97.93	2.61	2.52
17	L-Proline derivative	100.69	100.67	99.46	102.20	2.22	2.55
18	Glycine	98.88	101.18	99.76	100.57	3.93	5.25

a. Similar numbers are used to mark the peaks in the GC/MS chromatogram as shown in Figure 2.1.

Table 2.1. Endogenous metabolites and results of stability and precision studies (continued).

Peak No.[a]	Metabolites	% Freeze thaw stability	% Auto-sampler stability	% Long term stability		Intra-day Precision %RSD	Inter-day Precision %RSD
				1 month	3 months		
19	Uracil	103.94	106.57	110.75	114.32	9.24	12.37
20	Fumarate	100.24	105.55	95.70	105.45	6.48	6.44
21	L-Threonine	100.51	103.88	97.50	104.47	4.61	4.59
22	L-Methionylglycine	87.32	103.02	89.79	85.13	12.51	13.53
23	2-Hydroxy-3-methylvalerate	102.09	102.76	101.93	102.85	1.72	1.86
24	Methylamine	100.74	99.86	100.77	102.03	1.50	1.49
25	Malate	101.44	102.18	101.40	102.83	1.69	1.74
26	L-Proline	101.65	99.84	102.92	104.01	2.59	4.25
27	Phenylalanine	98.46	99.10	99.36	103.39	2.89	3.59
28	Creatinine enol	114.30	113.07	111.67	108.71	6.78	11.23
29	D-γ-lactone-xylonic acid	92.01	96.06	94.53	104.46	8.87	10.95
30	L-α-glycerophosphate	102.32	101.23	101.27	102.30	3.43	3.66
31-A,B	D-Mannose	105.84	98.33	89.83	93.17	7.27	8.52
32-A,B	D-Galactose	100.58	101.83	99.55	98.72	1.76	1.80
33	Cadaverine	104.26	98.78	100.78	100.98	4.11	4.12
34	L-Tyrosine	100.82	100.65	101.23	101.97	3.23	3.77
35-A,B,C	D-Glucose	100.87	99.12	102.48	106.05	2.20	2.14
36-A,B,C	Myo-inositol	103.21	102.12	107.94	105.92	1.65	1.77

a. Similar numbers are used to mark the peaks in the GC/MS chromatogram as shown in Figure 2.1.

Table 2.1. Endogenous metabolites and results of stability and precision studies (continued).

Peak No.[a]	Metabolites	% Freeze thaw stability	% Auto-sampler stability	% Long term stability		Intra-day Precision %RSD	Inter-day Precision %RSD
				1 month	3 months		
37	Palmitic acid	100.78	99.69	97.45	98.77	4.42	4.79
38	Margaric acid	97.38	98.60	98.55	103.69	3.83	4.79
39	(Z,Z)-9,12-Octadecadienoic acid	93.35	99.35	97.17	98.27	4.96	5.83
40	Oleic acid	100.74	102.05	103.48	107.23	2.29	3.00
41	Stearic acid	100.03	101.28	104.84	102.61	5.65	5.60
42	Mannose-6-phosphate	101.03	100.51	100.84	103.78	1.17	1.19
43	1-Hexadecanol	85.04	106.99	85.57	86.40	11.76	11.83
44	D-Glucose-6-phosphate	99.37	99.24	100.69	101.09	2.47	2.47
45	Arachidonic acid	113.62	104.05	98.32	102.64	6.42	6.91
46	D-Glucopyranose-6-phosphate	90.63	98.25	103.84	101.36	11.73	11.67
47	Uridine	98.28	90.32	109.55	111.31	8.56	9.22
48	11,14-Eicosadienoic acid	98.40	95.83	90.00	94.59	5.36	5.23
49	11-Eicosenoic acid	108.76	103.27	99.94	110.71	9.34	8.86
50	1-O-Heptadecylglycerol	100.09	106.46	94.72	105.31	7.51	7.47
51	1-Monooleoylglycerol	94.49	102.74	86.48	87.42	11.14	11.38
52	Propyl octadecanoate	94.14	105.28	101.11	108.94	9.49	9.04
53	Cholesterol	85.26	101.85	85.54	85.86	10.14	10.10

a. Similar numbers are used to mark the peaks in the GC/MS chromatogram as shown in Figure 2.1.

Table 2.2. Results of linearity of response of 19 selected standard metabolites (spiked before extraction and then taken through the entire sample preparation process).

Compound	Concentration Range (µg/mg of tissue)	r^2
Lactate	0.025-10.0	0.9988
Fumarate	0.25-10.0	0.9963
Malate	0.5-10.0	0.9979
L-Alanine	0.05-10.0	0.9967
L-Valine	0.025-10.0	0.9962
L-Proline	0.5-10.0	0.9938
L-Threonine	0.5-10.0	0.9944
L-Phenylalanine	1.0-10.0	0.9954
D-Glucose	0.1-10.0	0.9994
D-Mannose	0.25-10.0	0.9929
D-Galactose	0.25-10.0	0.9998
Uridine	0.5-10.0	0.9972
Arachidonic acid	0.5-10.0	0.9985
Cholesterol	0.5-10.0	0.9956
Phosphate	0.5-10.0	0.9962
Myo-inositol	0.5-10.0	0.9908
L-Tyrosine	0.25-10.0	0.9950
Glycine	0.5-10.0	0.9953
Uracil	1.0-10.0	0.9974

During method development, it was determined that at least 20 mg of colon tissue sample was needed to generate a reasonably sensitive profiling of the endogenous metabolites. So far Denkert et al. had demonstrated that 5 mg of tissue is sufficient to produce satisfactory metabolic profile using gas chromatography coupled to time of flight mass spectrometry (GC/TOFMS) (Denkert et al., 2006, 2008). The relatively greater amount of tissue needed in our case was possibly related to the difference in the inherent sensitivity of our GC/MS (single quadrupole) system as compared to GC/TOFMS.

2.4. Conclusion

A suitable GC/MS method for the non-targeted metabolic profiling of human colon tissue was developed and successfully validated in terms of its sample stability, reproducibility, selectivity, linear response and sensitivity. Our developed GC/MS method could be used alone or in conjunction with other complementary analytical techniques like NMR, especially HR-MAS NMR spectroscopy for the comprehensive non-targeted metabolic profiling of human colon tissue.

CHAPTER 3

NON-TARGETED METABOLIC PROFILING OF COLORECTAL CANCER USING GC/MS

3.1. Introduction

In this chapter, tissue-based non-targeted metabolic profiling of CRC using GC/MS is described. The GC/MS method that we developed and validated, (described in Chapter 2) was utilized for the said purpose. The clinical samples consisted of CRC and normal colon tissues obtained from 31 CRC patients. The data obtained was subjected to multivariate as well as univariate statistical analyses to identify marker metabolites expressed differentially in CRC and normal tissue.

3.2. Experimental

3.2.1. Clinical population and tissue samples

Clinical data such as age, gender, ethnicity, location of primary tumor, histological staging and grade were obtained from a prospectively maintained computerized database at the Singapore Polyposis Registry & the Colorectal Cancer Research Laboratory, Department of Colorectal Surgery, SGH. The anatomical and clinicopathological characteristics related to the clinical tissue samples analyzed by GC/MS are summarized in Table 3.1. The study population comprised of 31 patients with a mean age of 67 ± 13 years at the

time of cancer diagnosis. 3 patients were younger than 50 years old (T11, T13 and T21). There were 18 males (58%) and 13 females (42%). The majority (87%) of the patients were Chinese (n = 27), while the remaining comprised 2 Indians (T5 and T27), 1 Malay (T7) and 1 of other ethnicity (T16, T23; n = 1). The CRC anatomical site, tissue histology, tumor grade, TNM and Dukes stages are presented in Table 3.1. There were 22 left-sided tumors (defined as those arising distal to the splenic flexure) of which 14 were in the rectosigmoid or rectum. The tumors were predominantly moderately differentiated (81%; n = 25), and the remaining 6 comprised 2 each of mucinous, well and poorly differentiated tumors. Although not presented in Table 3.1., tumor invasion of neighboring organs, lesion nature and dimension, and presence of angiolymphatic or perineural invasion were also noted. This study was approved by the IRB at the SGH (IRB reference number 260/2007). Matched CRC and normal tissue (n = 63) were obtained from the 31 CRC patients during surgery. Among these subjects, 1 patient provided two matched pairs of tissues (M23, T23, M16 and T16), while another only provided the normal mucosa (M19). None of the patients received neoadjuvant chemotherapy or radiotherapy prior to surgical excision. Resection of tissue samples were carried out by trained personnel at Singapore General Hospital. Fresh tumor tissue and matched normal mucosa were snap-frozen immediately following excision of the specimen at surgery, then stored at -80°C until processing. Tumor specimens were carefully micro-dissected to ensure that at least 90% of the analyzed tissue contained cancer cells. Matched normal tissues were taken at least 5-10 cm away from the edges of the tumor. All CRC tissues and matched normal tissue were cut and weighed accurately

Table 3.1. Summary of anatomical and clinicopathological characteristics of the clinical tissue samples analyzed by GC/MS.

Normal[a]	CRC[a]	CRC anatomical site	Histology	Grade[c]	TNM Stage	Dukes Stage
M23	T23[b]	Caecum	Adenocarcinoma	MD	T3N0M0	B
M16	T16[b]	Caecum	Adenocarcinoma	MD	T3N0M0	B
M7	T7	Caecum	Adenocarcinoma	MD	T3N2M0	C
M4	T4	Ascending colon	Adenocarcinoma	MD	T3N1M0	C
M2	T2	Hepatic flexure	Adenocarcinoma	MD	T2N0M1	D
M1	T1	Transverse colon	Adenocarcinoma	MD	T3N2M0	C
M8	T8	Transverse colon	Adenocarcinoma	MD	T3N2M0	C
M30	T30	Transverse colon	Adenocarcinoma	MD	T3N0M0	B
M31	T31	Descending colon	Adenocarcinoma	MD	T3N0M0	B
M19	-	Descending colon	Adenocarcinoma	PD	T4N1M0	C
M6	T6	Sigmoid colon	Adenocarcinoma	PD	T2N1M0	C
M33	T33	Sigmoid colon	Adenocarcinoma	MD	T3N1M0	C
M24	T24	Sigmoid colon	Adenocarcinoma	MD	T3N1M0	C
M28	T28	Sigmoid colon	Adenocarcinoma	MD	T3N0M0	B
M29	T29	Sigmoid colon	High-grade dysplasia	MD	T2N0M0	A
M32	T32	Sigmoid colon	Adenocarcinoma	WD	T4N0M0	B
M27	T27	Sigmoid colon	Mucinous	M	T3N1M0	C
M17	T17	Sigmoid colon	Adenocarcinoma	MD	T3N1M0	C
M3	T3	Rectosigmoid colon	Adenocarcinoma	MD	T2N0M1	D
M15	T15	Rectosigmoid colon	Adenocarcinoma	MD	T1N0M0	A
M11	T11	Rectosigmoid colon	Adenocarcinoma	WD	T3N1M0	C
M25	T25	Rectum	Adenocarcinoma	MD	T3N2M0	C
M10	T10	Rectum	Adenocarcinoma	MD	T3N1M1	D
M5	T5	Rectum	Adenocarcinoma	MD	T2N0M0	B
M12	T12	Rectum	Adenocarcinoma	MD	T2N0M0	A
M26	T26	Rectum	Adenocarcinoma	MD	T3N0M0	B
M22	T22	Rectum	Adenocarcinoma	MD	T3N0M0	A
M9	T9	Rectum	Adenocarcinoma	MD	T2N0M0	B
M13	T13	Rectum	Adenocarcinoma	MD	T4N0M1	D
M20	T20	Rectum	Mucinous	M	T3N1M0	C
M21	T21	Rectum	Adenocarcinoma	MD	T3N0M0	B
M18	T18	Rectum	Adenocarcinoma	MD	T3N0M1	D

[a] For each T (CRC) sample, matched M (normal) tissue was provided, with the exception of M19 (i.e. no matched T19).

[b] M16, T16, M23 and T23 were obtained from one patient.

[c] MD, WD, M and PD are moderately differentiated, well-differentiated, mucinous and poorly differentiated, respectively.

where approximately 20 mg of each tissue was reserved for GC/MS analysis. The samples were kept at -80°C until analysis. The remaining specimens were preserved in formalin and submitted for routine histological examination with hematoxylin and eosin staining by a gastrointestinal pathologist to determine the tumor stage and differentiation.

3.2.2. GC/MS analysis

Tissue samples for GC/MS analysis were prepared as per the procedure described in section 2.2.3 of Chapter 2. The same GC/MS conditions as described in section 2.2.4. of Chapter 2 were used for analysis. The total analysis time (including sample preparation and data acquisition) for each sample was approximately 200 min.

3.2.3. GC/MS data analysis

All known artifact peaks, such as peaks due to column bleed and MSTFA artifact peaks, were not considered in the final data analyses. The GC/MS data was pre-processed by normalization to a constant sum of the chromatographic peak area before chemometric and statistical analyses. The normalization step was used to account for variations of the overall concentrations of samples caused by subtle variations in wet weight of tissue samples, variations introduced during sample preparation and variations caused by instrument response. Metabonomic/metabolomic responses and fluxes mainly influence a certain number of metabolites in body fluids and consequently certain number

of peaks of the corresponding chromatogram/spectrum. These specific changes are visible as relative changes of concentrations of few metabolites related to the concentrations of all other metabolites, which represent the overall concentration of the sample. Usually these specific relative changes are of interest in metabolic profiling studies in contrast to the overall concentration of the sample. Therefore, a normalization step, which compensates for the differences of the overall concentration, is crucial, as variations of the overall concentrations obscure specific changes of metabolites. As internal standards are usually spiked into tissue matrix and then subjected through sample preparation procedure they can account for the variations caused by sample preparation, instrument response but they cannot account for variations introduced by subtle variations in tissue wet weight. Although normalization to total area may become suboptimal in case of huge metabolic changes but still it is a popular normalization method and has been successfully used in other tissue based metabolic profiling studies (Denkert et al., 2006, 2008; Wang et al., 2005; Yang et al., 2007). The normalized data was subjected to PCA to identify clustering trends and outliers followed by OPLS-DA (Bylesjö et al., 2006) using chemometric SIMCA-P software (Umetrics, Umeå, Sweden). The data were mean-centered and Pareto-scaled during chemometric data analysis. An independent 't' test with Welch's correction using SPSS software (Version 11.0, SPSS Inc., Chicago, IL, USA) was used for the comparison of the marker metabolite levels to determine their statistical significant differences between the CRC and normal mucosa groups ($p < 0.05$ was considered to be statistically significant). The Welch correction is designed to provide a valid t-test in the presence of unequal population

variances. Receiver operating characteristic (ROC) is a graphical plot of the sensitivity, or true positive rate, vs. false positive rate (1 − specificity or 1 − true negative rate), for a binary classifier system as its discrimination threshold is varied. Each point on the ROC curve represents a sensitivity/specificity pair corresponding to a particular decision threshold. The area under the ROC curve is a measure of how well a parameter can distinguish between two diagnostic groups (diseased/normal). ROC analysis was performed using the GraphPad Prism software (Version 5.02., GraphPad Software Inc., La Jolla, CA, USA) to validate the robustness of the OPLS-DA model using the cross-validated (7-fold) predicted Y values. Cross-validation is a procedure where multiple models are generated each excluding a different portion of the data (in our case every 7th sample), such that all samples are excluded once and once only. Predicted classifications (Y values) were then generated for each set of excluded samples using the appropriate model, in order to estimate the predictive performance of the classification algorithm. The area under the ROC curve denoted as AUC was calculated using the trapezoidal rule.

3.3. Results and discussion

In total, 31 tumor samples and 32 normal tissues from 31 CRC patients were analyzed by GC/MS (Table 3.1.). The representative chromatograms of CRC and normal tissue extracts are illustrated in Figure 3.1. From the chromatogram, it was clear that the GC/MS platform was highly reproducible in the elution time of the metabolites. The PCA plot using the GC/MS data has been presented in Figure 3.2. The scores plot of the OPLS-DA model

generated using the GC/MS data has been presented in Figure 3.3. [2 LV, $R^2(Y)$ = 0.849, $Q^2(cum)$ = 0.784]. LV, R^2Y and $Q^2(cum)$ are the latent variables, fraction of the sum of squares of all Y values explained by the current latent variable and cumulative Q^2 for the extracted latent variable, respectively. Q^2 is given by the expression $Q^2=1-\sum(Y_{predicted}-Y_{true})^2 \div \sum Y^2_{true}$. The overall explained variance, R^2Y, has the same expression as Q^2 but calculated for a model generated with all the training data (Keun et al., 2003). The model was subjected subsequently to ROC analysis using the cross-validated predicted Y values (Figure 3.4., AUC 0.9726). An AUC value of 1.0 corresponds to a prediction model with 100% sensitivity and 100% specificity, whereas an AUC value of 0.5 correspond to a poor predictive model. The high AUC values of the ROC analysis indicated that the OPLS-DA model was robust in this discrimination. The marker metabolites that were responsible for the separation of CRC specimens from their matched normal tissues in the OPLS-DA model are summarized in Table 3.2. Except for fumarate, malate, mannose, galactose, glucose and AA which were found to be present at higher levels in normal tissues, the remaining marker metabolites were found in greater amounts in the CRC specimens. All the metabolites were found to be statistically different between the two test groups ($p < 0.05$). The marker metabolites as presented in Table 3.2. are also labelled in Figure 3.1. to aid visualization of their R_t. OPLS-DA was also performed with different combinations of anatomical sites and Dukes stages of CRC specimens as test classifiers. However, no valid model was obtained. In addition to the existing literature, the Human Metabolome database (HMDB) (Wishart et al., 2009) and the Kyoto Encyclopedia of Genes and Genomes (KEGG) (Kanehisa and

Figure 3.1. GC/MS chromatogram overlay of CRC and normal tissues depicting the marker metabolite peaks.

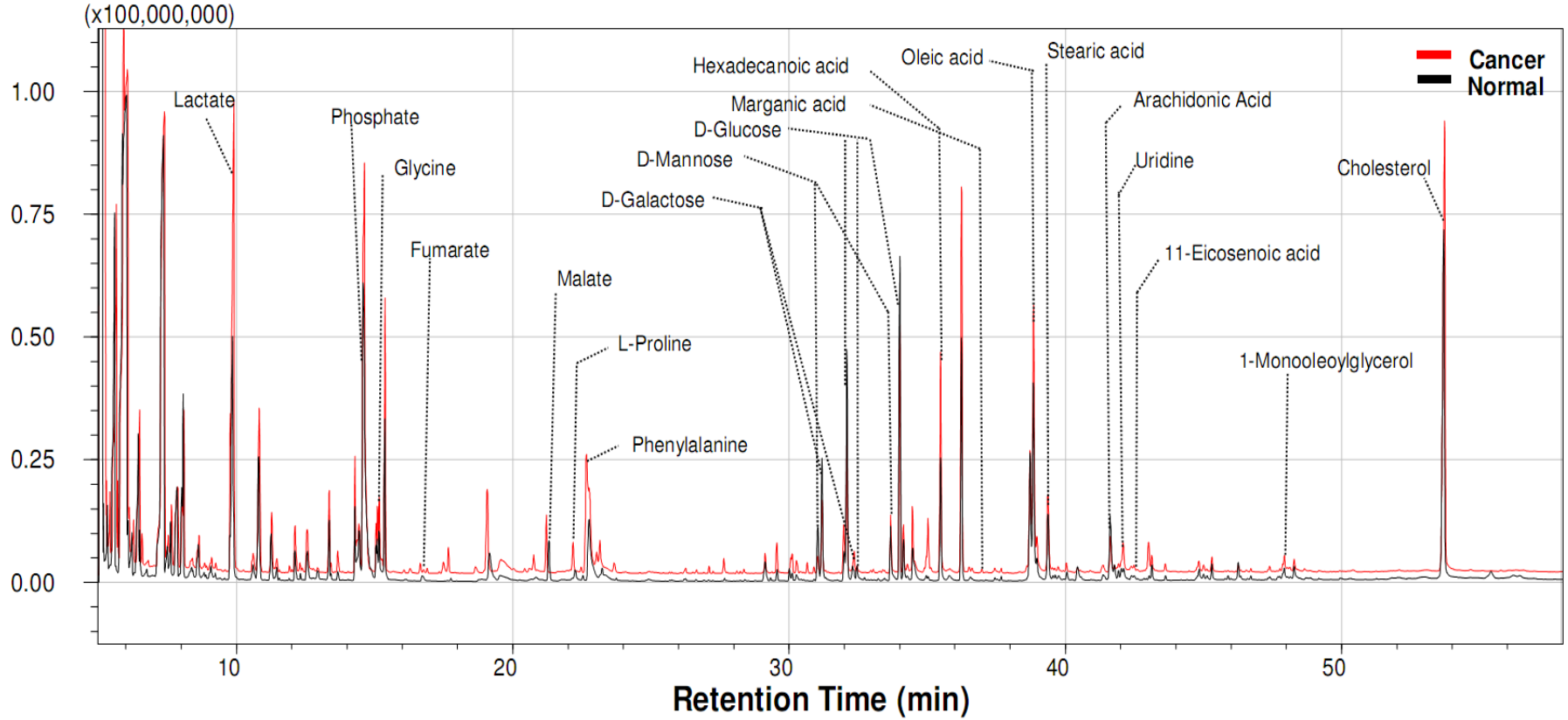

Table 3.2. Marker metabolites identified by GC/MS.

Metabolite	R_t (min)	Chemical class	Identified by[a]	% fold change of cancer from normal[b]	p value[c]
Lactate	9.85	Organic acid	Standard	40.1	<0.0001
Phosphate	14.65	Inorganic acid	Standard	6.1	<0.05
Glycine	15.40	Amino acid	Standard	38.5	<0.0001
Fumarate	16.76	Organic acid	Standard	-20.1	<0.05
Malate	21.41	Organic acid	Standard	-25.1	<0.0005
L-Proline	22.37	Amino acid	Standard	71.6	<0.05
L-Phenylalanine	23.06	Amino acid	Standard	72.5	<0.05
D-Mannose[d]	30.10, 33.72	Monosaccharide	Standard	-28.5	<0.0001
D-Galactose[d]	31.00, 32.38	Monosaccharide	Standard	-36.8	<0.0005
D-Glucose[d]	32.16, 32.41, 34.00	Monosaccharide	Standard	-67.0	<0.0001
Palmitic acid	35.53	Fatty acid	NIST	38.1	<0.0001
Margaric acid	37.44	Fatty acid	NIST	64.2	<0.01
Oleic acid	38.90	Fatty acid	NIST	13.1	<0.05
Stearic acid	39.44	Fatty acid	NIST	39.0	<0.0001
Arachidonic acid	41.71	Fatty acid	Standard	-16.7	<0.05
Uridine	42.18	Pyrimidine nucleoside	Standard	102.4	<0.0001
11-Eicosenoic acid	42.51	Fatty acid	NIST	59.6	<0.0005
1-Monooleoylglycerol	47.96	Polyol derivative	NIST	119.5	<0.0001
Cholesterol	53.70	Steroid	Standard	13.8	<0.005

[a] Metabolite identification using standard compound or NIST library search.
[b] Positive and negative percentages indicate higher levels of metabolites in cancer and normal tissues, respectively.
[c] Statistical p value calculated using the independent 't'-test with Welch's correction (significance at $p < 0.05$).
[d] Multiple peaks were observed for each compound in the GC/MS chromatogram.

Figure 3.2. PCA plot of CRC and normal tissues based on GC/MS metabolic profiles.

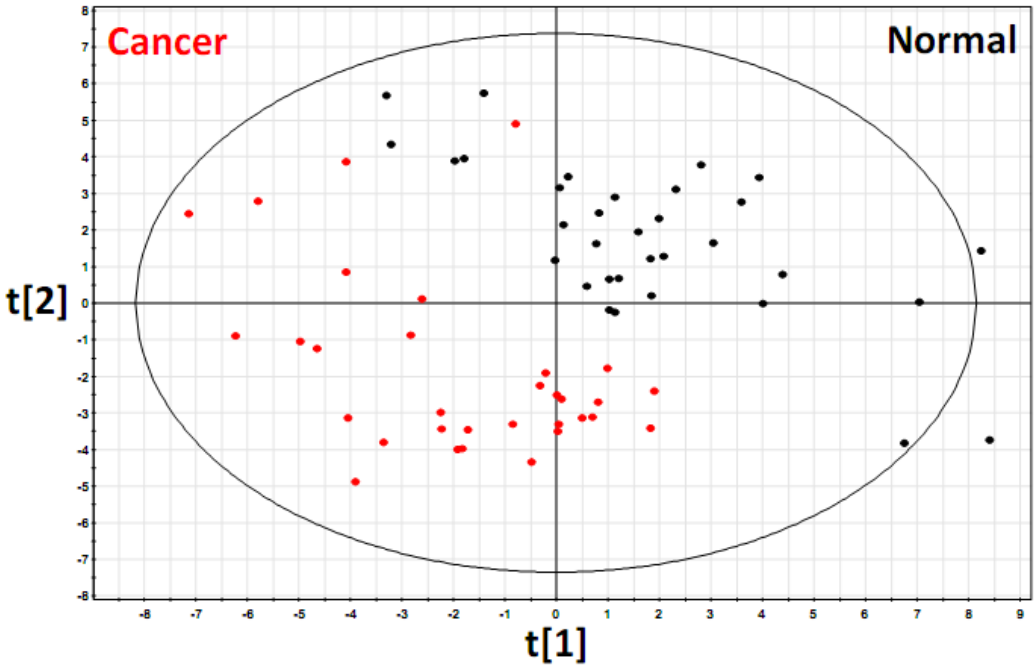

Figure 3.3. OPLS-DA scores plot discriminating CRC from normal tissues based on GC/MS metabolic profiles.

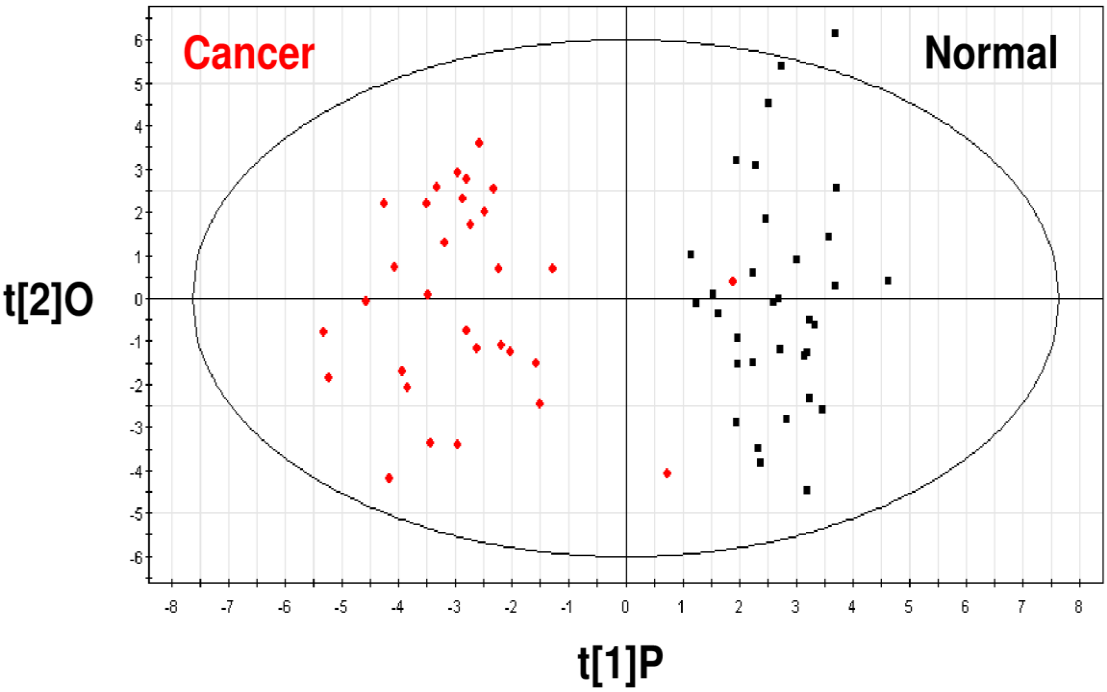

Figure 3.4. ROC curve determined using the cross-validated predicted Y values of the GC/MS OPLS-DA model.

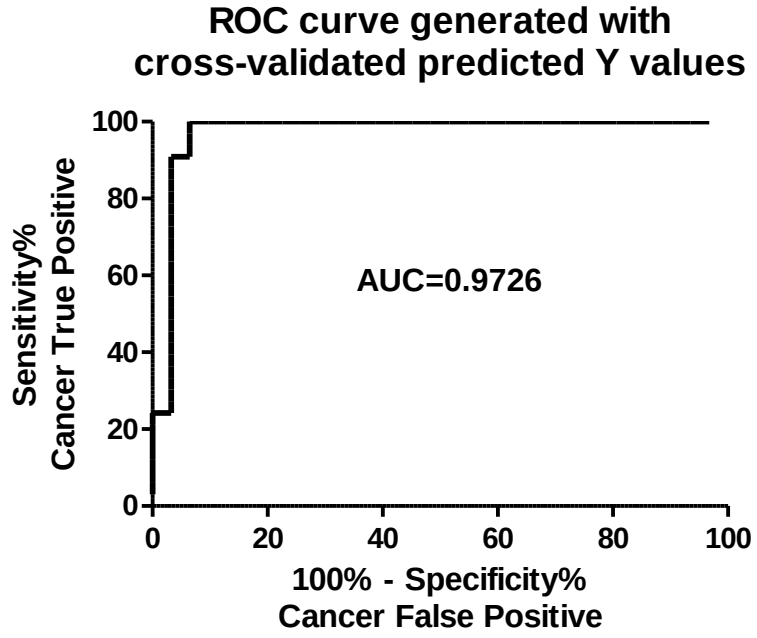

Goto, 2000) were also used to obtain information about the identified marker metabolites and their related metabolic pathways, respectively.

Using GC/MS, lactate and glycine were consistently found to be higher in CRC specimens while glucose was consistently lower (Table 3.2.). Lactate is an end product of glycolysis that increases rapidly during hypoxia and ischemia. Hypoxic regions of tumors develop when a tumor outgrows its vasculature. As increased lactate levels have been associated with a range of tumors (Griffin and Shockcor, 2004), our observation in this study was not unexpected. Higher levels of glucose uptake, consumption and conversion to lactate is a common observation in tumor cells even in high oxygen conditions, and was first observed by Otto Warburg (Warburg et al., 1956). Glycine can be formed from the glycolytic intermediate 3-phosphoglycerate, and its increased levels in CRC could relate to this glycolytic phenotype.

Alternatively, glycine is an important source of the one-carbon units for *de novo* purine synthesis, as shown by NMR experiments in the MCF7 breast tumor line (Fu et al., 2001). Hence the observed increase in glycine content could reflect enhanced nucleotide synthesis.

Based on the GC/MS non-targeted metabolic profiling approach, monounsaturated fatty acids (oleic acid and 11-eicosenoic acid) were found to be elevated in CRC specimens when compared to normal tissues (Table 3.2.). It is an established fact that 18-carbon chain length monounsaturated lipids were implicated in the apoptotic process (Griffin and Shockcor, 2004). Moreover such fatty acids have been shown to have tumor promoting effects in murine models of cancer and are often considered as a risk factor for CRC (Reddy, 1986, 1992).

Our GC/MS data indicated clearly that AA level was reduced in CRC specimens compared to normal tissues (Table 3.2.). The depletion of AA in CRC tissue substantiated the overexpression of COX-2 and LOX enzymes in CRC which catalyze the conversion of AA to eicosanoids viz. PGs. TXs, HETEs and LTs which act as inflammatory mediators. Alteration in the endogenous levels of AA emphasizes the role of these eicosanoids in bridging inflammation and CRC (Kashfi and Rigas, 2005; Sano et al., 1995; Shureiqi and Lippman, 2001; Smith, 1992; Soslow et al., 2000; Soumaoro et al., 2006).

The geographical incidence of CRC correlates well with high fat diets (Lipkin et al., 1999). Patients with CRC, have high levels of faecal bile acids and cholesterol. It is thought that faecal bile acids and cholesterol metabolites may act as promoters, co-carcinogens or carcinogens in large bowel tunmorigenesis. Cholesterol is an obligatory precursor of bile acids and 3-

hydroxy-3-methyl-glutaryl-Coenzyme A (HMG-CoA) reductase is involved in its synthesis. Higher levels of cholesterol were associated with the CRC specimens as demonstrated by GC/MS (Table 3.2.). This finding is consistent with earlier reports on the overexpression of HMG-CoA in colon cancer cell lines (Hentosh et al., 2001; Wachtershauser et al., 2001).

In line with other studies (Denkert et al., 2008; Ong et al., 2010), we also found lower levels of malate and fumarate in the CRC specimens (Table 3.2.) which are most likely related to deregulation of tricarboxylic acid (TCA) cycle and the higher energy demand in tumors. Uridine, a pyrimidine nucleoside, was also elevated in CRC specimens (Table 3.2.). These alterations are probably associated with the higher propagation rate of the tumor cells.

3.4. Conclusion

GC/MS was successfully utilized to profile metabolites in CRC and normal biopsied tissue specimens obtained from CRC patients. The data thus obtained was subjected to OPLS-DA which in turn generated a robust model capable of discriminating CRC from normal tissues. Moreover chemically diverse marker metabolites were identified which suggested perturbations of processes such as tissue hypoxia, glycolysis, TCA cycle, steroid metabolism, nucleotide biosynthesis, lipid metabolism and biosynthesis of eicosanoids. However the GC/MS data was unable to generate any OPLS-DA model capable of discriminating different stages of CRC or anatomical site of tumor.

CHAPTER 4

NON-TARGETED METABOLIC PROFILING OF COLORECTAL CANCER USING HR-MAS NMR SPECTROSCOPY

4.1. Introduction

HR-MAS NMR spectroscopy is a solid state NMR technique in which the sample is spun rapidly at an angle of 54.7° ("magic angle") with respect to the magnetic field resulting in attenuation of line broadening effects and generation of high resolution NMR spectra. HR-MAS NMR spectroscopy is a valuable analytical platform for metabolic profiling of intact tissue specimens. The probe heads used for HR-MAS NMR spectroscopy are capable of studying the samples in rapid rotation (4-6 kHz) around an axis of 54.7° tilted relative to that of the static magnetic field. As a result, chemical shift anisotropy, contributions from dipolar couplings and susceptibility distortions are largely reduced providing high-resolution spectra from semisolid and solid samples, such as tissues. HR-MAS NMR spectroscopy has been used in the analysis of gastrointestinal biopsies (Backshall, 2009; Seierstad et al., 2008; Tugnoli et al., 2006a; Wang et al, 2005, 2007, 2008), prostate tumors (Cheng et al., 2005; Swanson et al., 2003, 2006; Teichert et al., 2008), breast tumors (Sitter et al., 2006), brain tissue (Barton et al., 1999; Cheng et al., 1996, 1997, 2000; Tugnoli et al., 2006b; Tzika et al., 2007), renal cancer biopsies (Moka et al., 1998; Tate et al., 2000), heart tissue (Bollard et al., 2003) and liver tissue (Bollard et al., 2000; Duarte et al., 2005; Rooney et al., 2003; Wang et al., 2003). The sensitivity and resolution of HR-MAS NMR spectroscopy is

comparatively lower than MS techniques. However, the main advantage of HR-MAS NMR spectroscopy over MS and liquid state NMR techniques is that it requires minimal sample preparation and the metabolic space covered is independent of the choice of solvent(s) used for extraction of metabolites from tissues (Beckonert et al., 2010; Schenetti et al., 2006).

In this chapter, HR-MAS NMR spectroscopy has been used as an analytical platform for the non-targeted metabolic profiling of CRC and normal tissue specimens obtained from CRC patients. The HR-MAS NMR analysis, data pre-treatment and pre-processing by Matlab were carried out by our collaborators at the Imperial College London, UK. Raw spectral data analysis by Chenomx, multivariate statistics by SIMCA and pathway mapping of marker metabolites using KEGG were carried out at the Department of Pharmacy, NUS, Singapore.

4.2. Experimental

4.2.1. Clinical population and tissue samples

The same cohort of clinical samples (described in Table 3.1. of Chapter 3) which was used for GC/MS analysis, was used for HR-MAS NMR spectroscopy analysis. However due to limited size of each tissue block, all the tissues (n=63) were analyzed using GC/MS, while 47 tissues were analyzed using HR-MAS NMR spectroscopy, of which 18 pairs were matched samples. The anatomical and clinicopathological characteristics of the clinical tissue samples analyzed by HR-MAS NMR spectroscopy are summarized in Table

4.1. Collection, handling and storage of tissue samples were carried out in the same manner as described in section 3.2.1. of Chapter 3. About 10 mg of each tissue specimen was accurately weighed and kept at -80ºC until HR-MAS NMR spectroscopy analysis.

Table 4.1. Summary of anatomical and clinicopathological characteristics of the clinical tissue samples analyzed by HR-MAS NMR spectroscopy.

Normal[a]	CRC[a]	CRC anatomical site	Histology	Grade[b]	TNM Stage	Dukes Stage
M23	T23	Caecum	Adenocarcinoma	MD	T3N0M0	B
-	T7	Caecum	Adenocarcinoma	MD	T3N2M0	C
M4	T4	Ascending colon	Adenocarcinoma	MD	T3N1M0	C
M1	-	Transverse colon	Adenocarcinoma	MD	T3N2M0	C
M30	T30	Transverse colon	Adenocarcinoma	MD	T3N0M0	B
M31	T31	Descending colon	Adenocarcinoma	MD	T3N0M0	B
M19	-	Descending colon	Adenocarcinoma	PD	T4N1M0	C
M6	-	Sigmoid colon	Adenocarcinoma	PD	T2N1M0	C
M33	T33	Sigmoid colon	Adenocarcinoma	MD	T3N1M0	C
M24	T24	Sigmoid colon	Adenocarcinoma	MD	T3N1M0	C
M28	T28	Sigmoid colon	Adenocarcinoma	MD	T3N0M0	B
M29	T29	Sigmoid colon	High-grade dysplasia	MD	T2N0M0	A
M32	T32	Sigmoid colon	Adenocarcinoma	WD	T4N0M0	B
M27	T27	Sigmoid colon	Mucinous	M	T3N1M0	C
-	T17	Sigmoid colon	Adenocarcinoma	MD	T3N1M0	C
M3	T3	Rectosigmoid colon	Adenocarcinoma	MD	T2N0M1	D
M15	-	Rectosigmoid colon	Adenocarcinoma	MD	T1N0M0	A
M11	-	Rectosigmoid colon	Adenocarcinoma	WD	T3N1M0	C
M25	T25	Rectum	Adenocarcinoma	MD	T3N2M0	C
M10	T10	Rectum	Adenocarcinoma	MD	T3N1M1	D
-	T5	Rectum	Adenocarcinoma	MD	T2N0M0	B
M12	-	Rectum	Adenocarcinoma	MD	T2N0M0	A
M26	T26	Rectum	Adenocarcinoma	MD	T3N0M0	B
M22	T22	Rectum	Adenocarcinoma	MD	T3N0M0	A
M9	T9	Rectum	Adenocarcinoma	MD	T2N0M0	B
M13	-	Rectum	Adenocarcinoma	MD	T4N0M1	D
M20	T20	Rectum	Mucinous	M	T3N1M0	C
M21	T21	Rectum	Adenocarcinoma	MD	T3N0M0	B
M18	-	Rectum	Adenocarcinoma	MD	T3N0M1	D

[a] T (CRC) tissue, M (normal) tissue.

[b] MD, WD, M and PD are moderately differentiated, well-differentiated, mucinous and poorly differentiated, respectively.

4.2.2. HR-MAS NMR spectroscopy analysis

HR-MAS NMR spectroscopic analysis including sample pretreatment was carried out at the Imperial College London, UK, as per the validated protocol which has been recently published (Beckonert et al., 2010). Each accurately weighed intact tissue (about 10 mg) was bathed in D_2O solution for 15 s. The tissue was inserted into a zirconium oxide 4 mm outer diameter rotor with an additional drop of D_2O to provide a field-frequency lock for the NMR spectrometer. An insert was placed into the rotor to make a spherical sample volume of 25 µL. A cap was finally added as a closure of the rotor and the assembled device was used immediately for NMR analysis. All samples were randomized during analysis to reduce any potential systematic errors.

All ^{1}H NMR spectra were recorded on a Bruker AV-600 NMR spectrometer (Rheinstetten, Germany) operating at 600.11 MHz for ^{1}H, equipped with a HR-MAS at a spin rate of 5000 Hz. Sample temperature was regulated using cooled N_2 gas at 10 ºC during the acquisition of spectra to minimize spectral degradation. Two different types of ^{1}H NMR experiments were carried out for each sample, a one-dimensional (1D) Nuclear Overhauser effect spectroscopy (NOESY) experiment with water suppression and a 1D Carr-Purcell-Meiboom-Gill (CPMG) spin-echo experiment. CPMG pulse sequence is widely used to measure spin-spin relaxation time T2 and thus the CPMG sequence generated spectra can be edited by T2 relaxation times to reduce signals from high molecular weight species or systems in intermediate chemical exchange (Zhang and Hirasaki, 2003). 1D NOESY is a selective 1-D experiment that uses shaped pulses to selectively excite specific resonances

in order to observe isolated dipolar couplings. The 1D NOESY experiment generates a corresponding unedited spectrum with improved solvent peak suppression (Teahan et al., 2006). The CPMG spin-echo experiment gave the clearest signature of metabolic changes between the cancer and normal tissues, with little extra information contained in the higher molecular weight components. As such, results obtained from the CPMG experiments were used for further data analysis. CPMG spin-echo spectra were obtained using the pulse sequence [recycle delay (RD)-90º-(τ-180º-τ)n - acquire FID], with a spin-spin relaxation delay, 2nτ, of 240 ms. The RD was 2 s. The 90º pulse length was 6.9-9.0 μs. A total of 256 transients were collected into 32 K data points with a spectral width of 20 ppm. ^{1}H MAS NMR spectra of tissues were manually phased and baseline corrected using XwinNMR 3.5 (Bruker Analytik, Rheinstetten, Germany). The ^{1}H NMR spectra were referenced to the methyl resonance of alanine at δ 1.47. The total analysis time (including sample preparation, optimization of NMR parameters and data acquisition) of HR-MAS NMR spectroscopy for each sample was approximately 40 min. Although a greater mass of the tissue (> 20 mg) is recommended to fill the rotor space for MAS analysis, the ~10 mg tissue used in our experiments generated good signal sensitivity and resolution. For assignment purposes, two-dimensional (2D) correlation spectroscopy (COSY) and J-resolved (JRES) NMR spectra were acquired on selected samples.

4.2.3. HR-MAS NMR spectroscopy data analysis

The data generated from HR-MAS NMR spectroscopy were analyzed in two different ways –

1. Using Matlab (Version 7, The Mathworks, Inc., Natwick, MA, USA) followed by manual identification of metabolites and statistical analyses.

2. Using Chenomx NMR suite software (Version 6.1., Chenomx Inc., Alberta, Canada) followed by statistical analyses.

4.2.3.1. HR-MAS NMR spectroscopy data analysis using Matlab and manual identification of metabolites

The spectra over the range of δ -1.0 to 10.0 were imported into Matlab using in-house script developed by Dr. Rachel Cavill, Dr. Tim Ebbels and Dr. Hector Keun at the Imperial College London, UK. All spectra were "binned" into 0.01 ppm regions. Probabilistic quotient normalization of the spectra using the median spectrum to estimate the most probable quotient was carried out before chemometric and statistical analyses (Dieterle et al., 2006). The binned data were analyzed initially by OPLS-DA using SIMCA-P software (Umetrics, Umeå, Sweden), generating a model classifying normal from tumor [3 LV, R^2Y = 0.843, Q^2(cum) = 0.653] and the correlated loadings were used to help identify the spectral regions discriminating between these groups. These differential spectra regions were subsequently confirmed via visual inspection of the NMR spectra. The marker metabolites were assigned subsequently. The peak intensities of the spectra region related to the marker

metabolites were integrated from the full-resolution data. All processed data were mean-centered and Pareto-scaled during chemometric data analysis. A secondary OPLS-DA model was created using the marker metabolite intensities as variables. The residual water resonance signal (δ 4.50-5.19) and the spectral region (δ 1.0 to 0.5) were removed prior to analysis. The peak intensities of the spectra region related to the marker metabolites were integrated in Matlab using the full-resolution data and a local linear baseline correction. An independent 't' test with Welch's correction was used for the comparison of the marker metabolite levels to determine their statistical significant differences between the CRC and normal mucosa groups ($p < 0.05$ was considered to be statistically significant). ROC analysis was performed using GraphPad Prism software (Version 5.02., GraphPad Software Inc., La Jolla, CA, USA) to validate the robustness of the OPLS-DA model(s) using the cross-validated (7-fold) predicted Y-values.

4.2.3.2. HR-MAS NMR spectroscopy data analysis using Chenomx NMR suite software

Processed NMR spectra for all the samples present in the form of Bruker '1r' files were imported and converted to Chenomx NMR suite format (.cnx) using the processor module of Chenomx NMR suite. As no chemical shape indicator (CSI) was present in the samples, all the NMR spectra were referenced to the methyl resonance of alanine at δ 1.47. After conversion of the NMR spectra of all the samples into .cnx format, metabolite identification and quantification were carried out using the in-built spectral library of the profiler module of

Chenomx NMR software. The resulting data were normalized before chemometric analyses. The normalized data were analyzed using PCA followed by OPLS-DA using SIMCA-P software (Umetrics, Umeå, Sweden). All processed data were mean-centered and unit-variance (UV) scaled during chemometric data analysis. An independent 't' test with Welch's correction was used for the comparison of the marker metabolite levels to determine their significant differences between the CRC and normal tissues groups ($p < 0.05$ was considered as statistically significant). ROC analysis was performed using GraphPad Prism to validate the robustness of the OPLS-DA model using the cross-validated (7-fold) predicted Y-values.

4.3. Results and discussion

In total, 22 tumor samples and 25 normal tissues obtained from 29 CRC patients were analyzed by HR-MAS NMR spectroscopy (Table 4.1.). The representative HR-MAS NMR spectra of CRC and normal tissue are shown in Figure 4.1. The marker metabolites which were identified from NMR data processed using Matlab followed by manual metabolite assignment, are summarized in Table 4.2. The corresponding OPLS-DA model [3 LV, $R^2(Y)$ = 0.622, $Q^2(cum)$ = 0.518] and the ROC curve (AUC = 0.9542) are shown in Figures 4.2. and 4.3., respectively. The set of marker metabolites identified from NMR data processed by Chenomx NMR suite software is shown in Table 4.3. The HMDB (Wishart et al., 2009) and the KEGG (Kanehisa and Goto, 2000) were referred to acquire information on the identified marker metabolites and related metabolic pathways, respectively.

Lipids and glucose were found to be present at higher levels in normal tissues compared to CRC tissues, while choline-containing compounds (ChoCC), taurine, scyllo-inositol, glycine, phosphoethanolamine (PE), lactate and phosphocholine (PC) were present at higher levels in the CRC specimens. Our HR-MAS NMR results indicated clearly higher levels of both saturated and unsaturated lipids and/or fatty acids in normal tissues compared to CRC specimens (Table 4.2.). The lower lipid levels in the CRC specimens were likely to be associated with higher metabolic turnover and demand in membrane biosynthesis for cell propagation leading to a higher utilization rate of lipids, particularly triglycerides. Another class of compounds that were found to be perturbed in tumors is the choline-containing compounds (ChoCC) such as choline, PC, phosphatidylcholine, glycerophosphocholine and PE, all important precursors of constituents of cell membranes (Glunde et al., 2006; Griffin and Shockcor, 2004). Consistent with earlier observations, (Moreno et al., 1993) PC and PE were found in our study to be present at higher levels in the CRC specimens based on the results of HR-MAS NMR spectroscopy (Tables 4.2. and 4.3.). Taurine is important in osmoregulation and its level was found to be increased in several tumors including CRC (Griffin and Shockcor, 2004; Moreno et al., 1993). Scyllo-inositol is an osmolyte that was found to be higher in normal human colon as compared to the different longitudinal levels of the healthy gut (Wang et al., 2007). Our results showed that scyllo-inositol was further elevated in CRC compared to normal colon tissues and suggested the localized change in osmotic regulation in CRC tumor. Like GC/MS, HR-MAS NMR data also showed that levels of lactate and glycine were consistently higher in CRC specimens while glucose was consistently lower.

Finally, OPLS-DA was performed using the full-resolution data with different combinations of anatomical sites and Dukes stages of CRC specimens as test classifiers. For this experiment, the data related to the normal tissues were excluded during analysis.

Figure 4.1. HR-MAS NMR spectra of representative CRC and normal tissue.

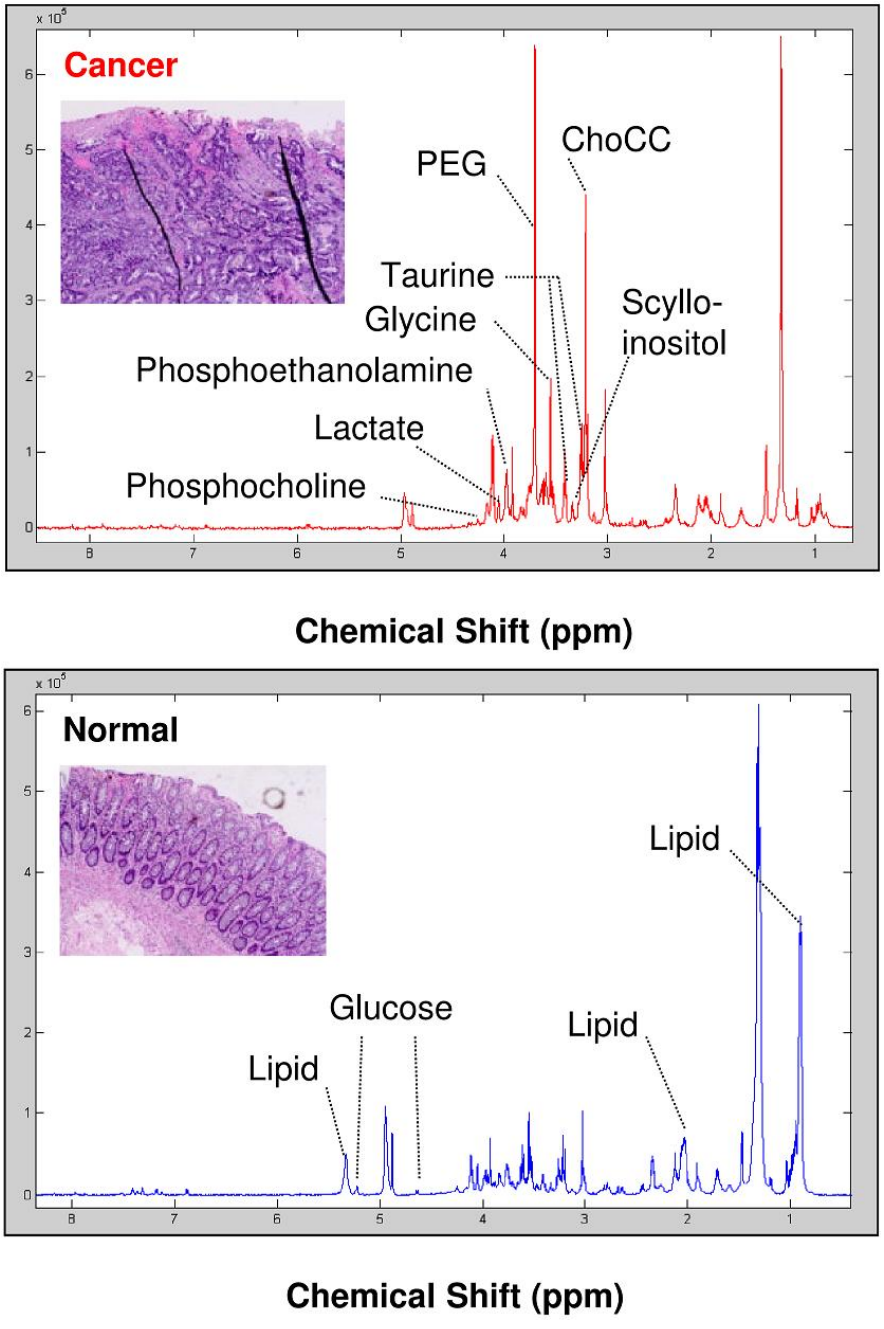

Table 4.2. Marker metabolites identified by HR-MAS NMR spectroscopy (data processed by Matlab with manual metabolite assignment).

Metabolite	δ ^{1}H (ppm)	Group	Multiplicity[a]	Identified by	% fold change of cancer from normal[b]	p value[c]
Lipids	0.90	CH_3	M	1D	-83.3	<0.01
	2.00	CH_2-C=C	M		-48.0	<0.05
	5.28-5.44	-CH=CH-	M		-84.5	<0.01
ChoCC[d]	3.21	$N(CH_3)_3$	s (multiple)	1D, COSY	82.7	<0.05
Taurine	3.25	NCH_2	T	1D, JRES,	115.8	<0.0001
	3.42	SCH_2	T	COSY	152.3	<0.0001
Scyllo-inositol	3.34	Half δ-CH_2	S	1D, JRES	39.1	<0.05
Glycine	3.55	CH_2	S	1D, JRES	24.4	0.1751
PE[d]	3.99	OCH_2	M	1D, JRES, COSY	46.0	0.0541
Lactate	4.11	α-CH	Q	1D, JRES, COSY	65.0	<0.01
PC[d]	4.19	OCH_2	T	1D, JRES, COSY	75.6	<0.01
Glucose	4.64	1-CH	D	1D, JRES, COSY	-45.8	<0.05
	5.23	1-CH	D	1D, JRES, COSY	-63.3	<0.01

a. d, m, q, s and t are doublet, multiplet, quartet, singlet and triplet, respectively.
b. Positive and negative percentages indicate higher levels of metabolites in CRC and normal tissues, respectively.
c. p value calculated using the independent 't'-test with Welch's correction (significance at $p < 0.05$).
d. ChoCC, PE and PC are choline-containing compounds, phosphoethanolamine and phosphocholine, respectively.

Table 4.3. Marker metabolites identified by HR-MAS NMR spectroscopy (data processed by Chenomx NMR suite).

Metabolite	δ ^{1}H (ppm)	Identified By	% fold change of cancer from normal[a]	p value[b]
ChoCC[d]	3.2, 3.5, 4.0	Chenomx library	55.3	<0.0005
Taurine	3.3, 3.4	Chenomx library	72.0	<0.0001
Glycine	3.6	Chenomx library	47.6	<0.005
PE[c]	3.2, 4.0	Chenomx library	51.7	<0.0005
Lactate	1.3, 4.1	Chenomx library	55.4	<0.0001
PC[c]	3.2, 3.6, 4.2	Chenomx library	58.8	<0.0005
Glucose	3.2, 3.4, 3.5, 3.7, 3.8, 3.9, 4.6, 5.2	Chenomx library	-129.2	<0.05

a. Positive and negative percentages indicate higher levels of metabolites in CRC and normal tissues, respectively.
b. p value calculated using the independent 't'-test with Welch's correction (significance at $p < 0.05$).
c. ChoCC, PE and PC are choline-containing compounds, phosphoethanolamine and phosphocholine, respectively.

The colon class comprised all samples obtained from ceacum, ascending, transverse and descending colon and sigmoid colon, while the rectum class consisted of samples obtained from the rectosigmoid colon and rectum. Figure 4.6 shows the OPLS-DA model scores generated from the NMR data (processed by Matlab with manual metabolite assignment) using anatomical sites as classifiers [7 LV, $R^2(Y) = 0.983$, $Q^2(cum) = 0.625$]. The corresponding ROC curve (AUC = 1.00) is shown in Figure 4.7. Normal tissue samples did not show any clustering trend based on anatomical site when subjected to PCA. Our results suggested that CRC harbors distinct metabolic phenotype according to the anatomical location of the tumor. However the NMR data processed by Chenomx was unable to generate any such OPLS-DA model which may be due to the unavailability of marker metabolites such as lipid and

Figure 4.2. OPLS-DA scores plot discriminating CRC from normal tissues based on marker metabolites detected by HR-MAS NMR (data processed by Matlab with manual metabolite assignment).

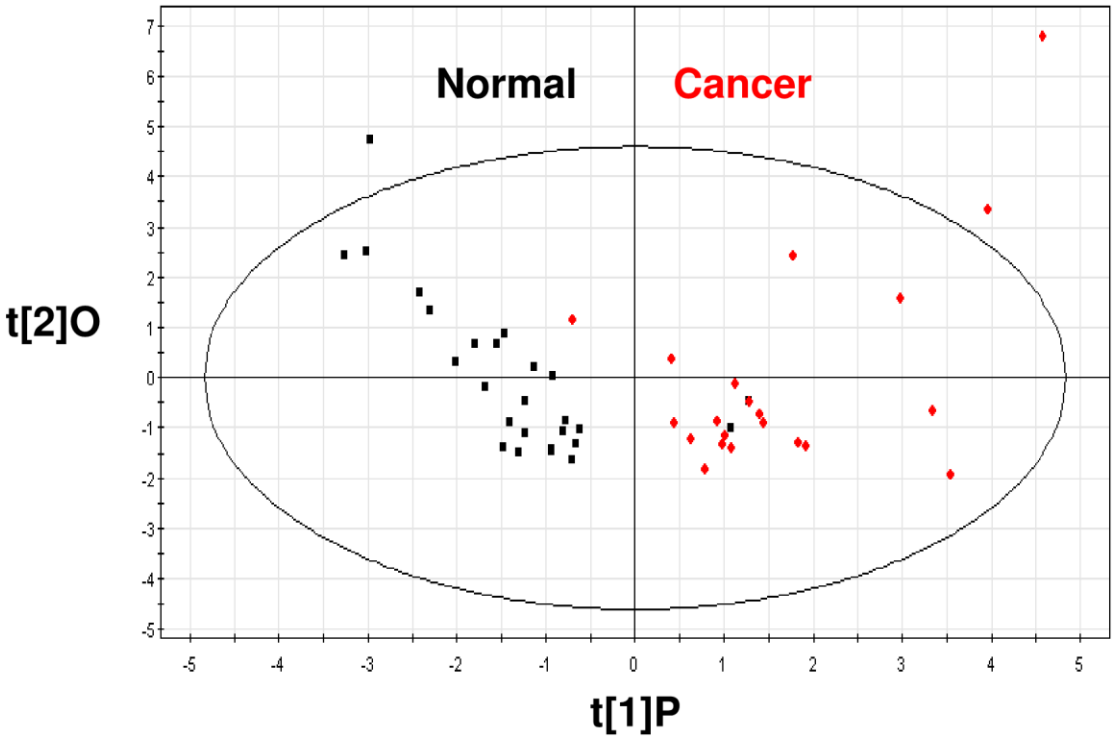

Figure 4.3. ROC curve determined using the cross-validated predicted Y-values of the HR-MAS NMR OPLS-DA model (data processed by Matlab with manual metabolite assignment).

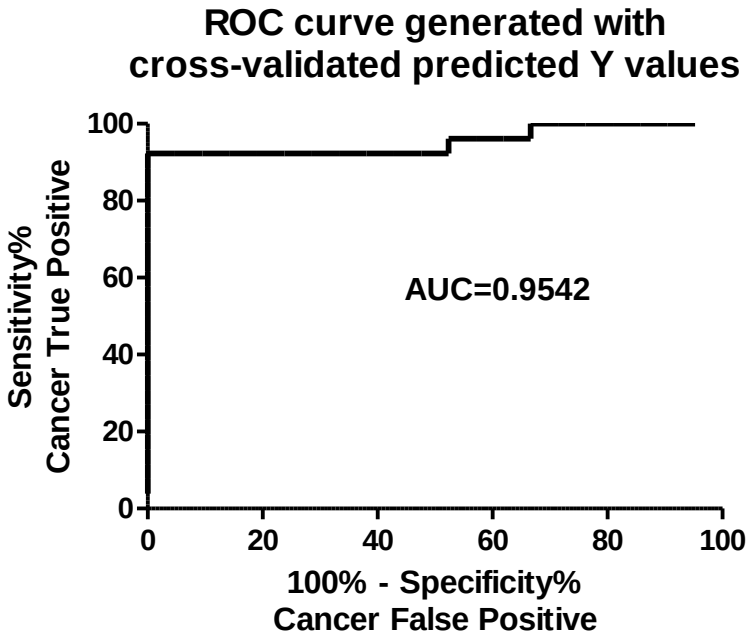

Figure 4.4. OPLS-DA scores plot discriminating CRC from normal tissues based on marker metabolites detected by HR-MAS NMR (data processed by Chenomx NMR suite).

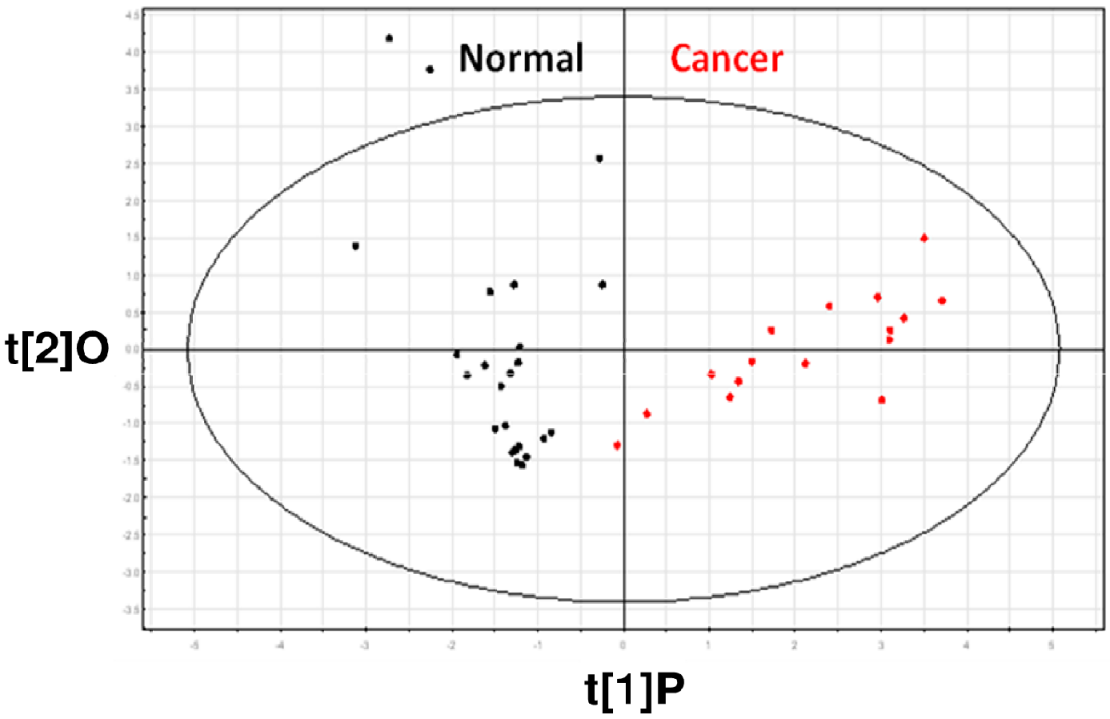

Figure 4.5. ROC curve determined using the cross-validated predicted Y-values of the HR-MAS NMR OPLS-DA model (data processed by Chenomx NMR suite).

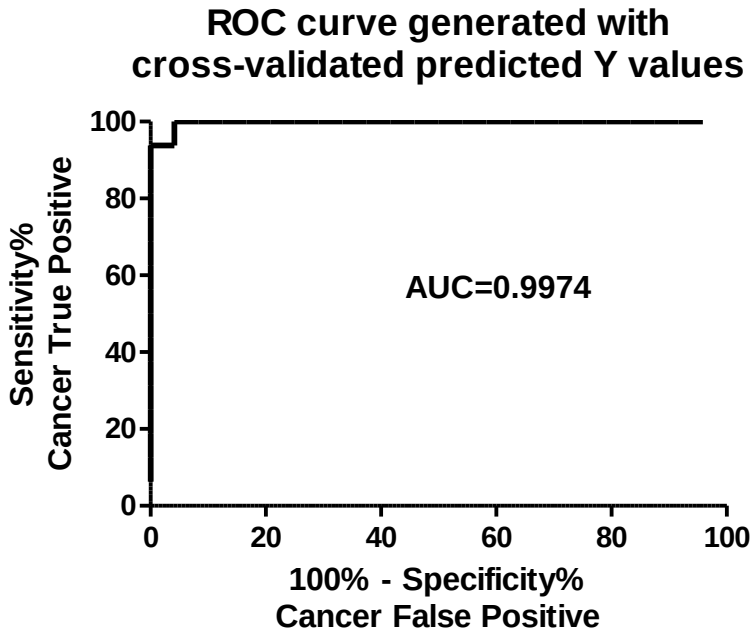

Figure 4.6. OPLS-DA scores plot discriminating colon from rectal cancers based on HR-MAS NMR data (processed by Matlab with manual metabolite assignment).

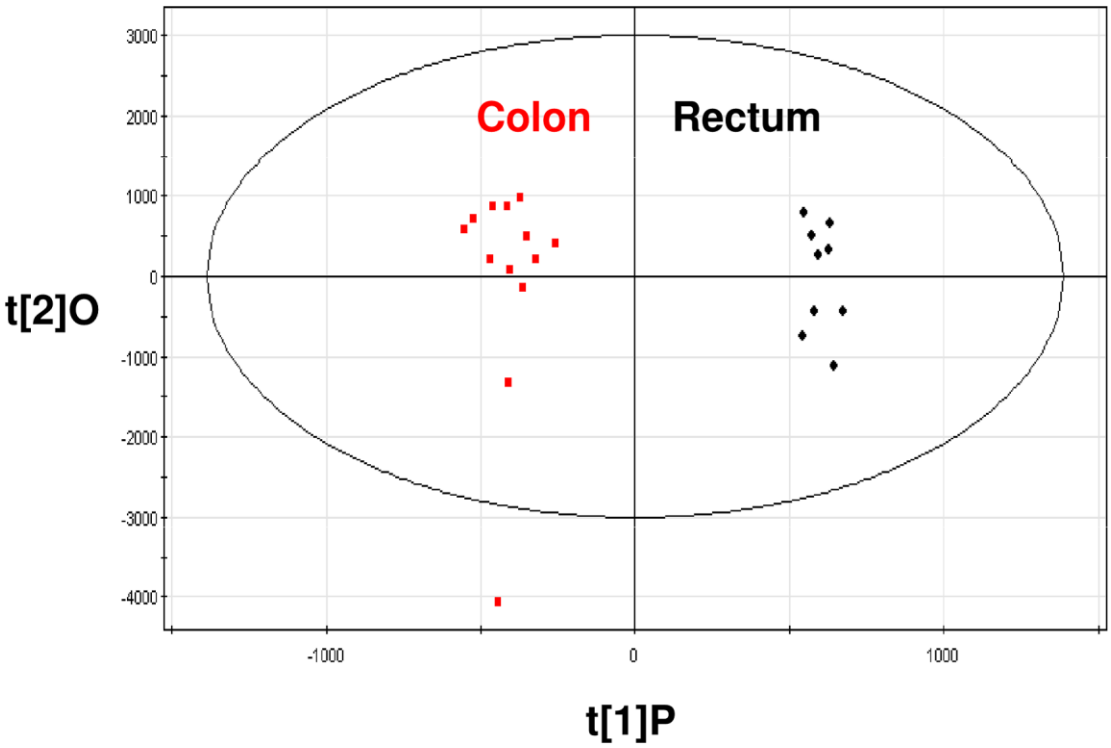

Figure 4.7. ROC curve determined using the cross-validated predicted Y-values of the HR-MAS NMR OPLS-DA model with anatomical site as classifier.

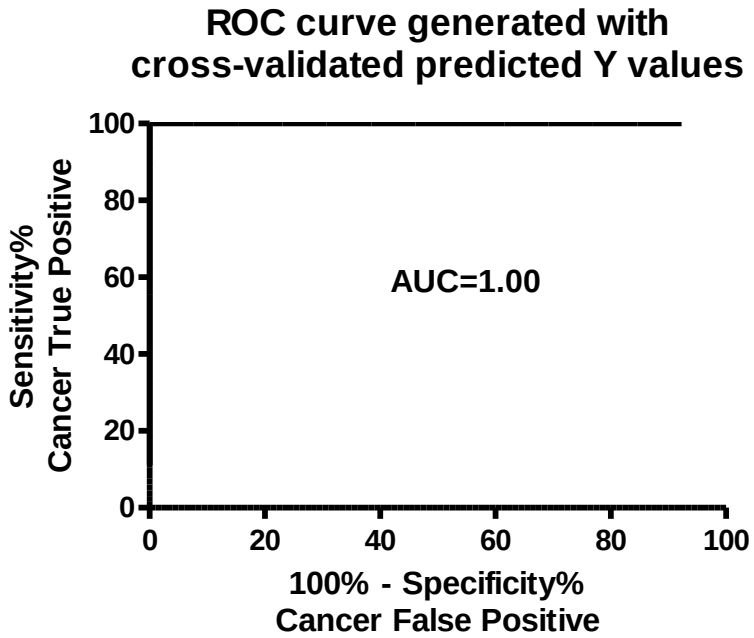

scyllo-inositol in the Chenomx library. No valid OPLS-DA model was obtained when the Duke stages were used as classifier.

4.4. Conclusion

HR-MAS NMR spectroscopy-based non-targeted metabolic profiling generated pertinent data using CRC and normal biopsied tissue specimens obtained from CRC patients. The data thus obtained was subjected to chemometric analyses which in turn generated OPLS-DA models capable of discriminating CRC from normal tissues as well as the anatomical site of tumors. The high AUC values of the respective ROC curves confirmed that the OPLS-DA models were robust in nature. The marker metabolites identified by HR-MAS NMR spectroscopy indicated deregulations in tissue hypoxia, glycolysis, nucleotide biosynthesis, osmoregulation and lipid metabolism. However, the HR-MAS NMR spectroscopy data was unable to generate any OPLS-DA model capable of separating the different stages of CRC.

CHAPTER 5

NON-TARGETED METABOLIC PROFILING OF COLORECTAL CANCER USING GC×GC/TOFMS

5.1. Introduction

GC×GC/TOFMS consists of two capillary columns having complementary stationary phases. The primary or first-dimension column is non-polar in nature allowing separation of large number of compounds belonging to different chemical classes. As a result, each individual narrow chromatographic fraction eluting out of the primary column consists of analytes with closely similar volatilities. The secondary or second-dimension column is polar in nature which allows fast separation of analytes having close volatilities. Therefore, the two columns operate orthogonally generating a 2D plane of separation for the analytes and resulting in a synergistically enhanced peak capacity obtained by the two individual columns. The modulator device which acts as the interface between the two columns performs three main functions - 1. accumulation and trapping of eluent of primary column, 2. refocusing and 3. rapid release of the adjacent fractions of the primary column into the secondary column. Cryogenic modulators are typically used for this purpose (Beens et al., 2001; Khummueng et al., 2006). TOFMS are the preferred detectors for GC×GC as they can acquire 50 or more mass spectra per second necessary for proper reconstruction of the very fast eluted second-dimension peaks, and enable reliable spectral deconvolution of co-eluting peaks. Although the analysis time of GC×GC/TOFMS is usually shorter as

compared to GC/MS, the amount of information provided per sample per unit time is not compromised. Apart from the increased number of detectable peaks as compared to GC/MS, spectral purity is much improved in GC×GC/TOFMS, which in turn aids in mass spectral deconvolution and compound identification. Despite the many advantages of using GC×GC/TOFMS in non-targeted metabolic profiling, one of its biggest challenges is the complexity and large volume of the generated data (Adahchour et al., 2008; Dimandja et al., 2003; Ryan et al., 2005). GC×GC/TOFMS has already been successfully utilized in non-targeted metabolic profiling (Koek et al., 2007; Mohler et al., 2006; Pasikanti et al., 2010; Sinha et al., 2004; Welthagen et al., 2005). Thus it is pertinent to explore GC×GC/TOFMS as an analytical platform for non-targeted metabolic profiling of CRC in order to gain greater metabolic space coverage as compared to GC/MS and HR-MAS NMR spectroscopy. This chapter deals with the non-targeted metabolic profiling of CRC using GC×GC/TOFMS.

5.2. Experimental

5.2.1. Clinical population and tissue samples

The same cohort of tissue specimens that was used for GC/MS analysis was subjected to analysis by GC×GC/TOFMS. Please refer to Table 3.1. of Chapter 3 for the anatomical and clinicopathological characteristics of the tissue samples.

5.2.2. Validation of analytical performance of GC×GC/TOFMS

As the same set of samples which were analyzed by GC/MS was used for GC×GC/TOFMS analysis and the same sample preparation protocol (section 2.2.3. of Chapter 2) was followed, separate sample stability studies were not further performed. The different sample stability studies were carried out while validating our GC/MS method and are described in Chapter 2. Due to the large number of chromatographic peaks generated by GC×GC/TOFMS (about 800 peaks in the case of colon tissue samples) and inherent 2D nature of separation, the applicability and feasibility of conventional analytical method validation parameters is limited. Therefore to evaluate the analytical performance of GC×GC/TOFMS we adopted an alternative approach in which we used quality control (QC) samples in conjunction with chemometric analyses. The QC samples were prepared by processing about 20 mg aliquots of a normal colon tissue sample, as per our developed sample preparation protocol (section 2.2.3. of Chapter 2). These QC samples were injected periodically during analysis of the clinical samples. After analysis, the chromatographic data generated for the QC samples were subjected to chemometric analyses along with that of the clinical samples. The analytical performance of GC×GC/TOFMS was considered as satisfactory if the QC samples were found to be clustered together in the PCA plot.

5.2.3. GC×GC/TOFMS analysis

Tissue samples for GC×GC/TOFMS analysis were prepared as per the procedure described in section 2.2.3 of Chapter 2. The samples were randomized to nullify any system effect before analysis. Analysis was carried out using a Pegasus GC×GC/TOFMS (Leco Corp., St. Joseph, MI, USA) system comprising an Agilent 7890 GC and Pegasus IV TOFMS. A dual-stage, quad jet thermal consumable free modulator was used. The N_2 gas for the modulator was chilled by a closed-loop immersion cooler (FTS, Stone Ridge, NY, USA) which was set at a temperature of -80°C. Helium was used as the carrier gas at a constant flow rate of 1.0 mL/min. An injection volume of 1 µL and an injector split ratio of 1:10 were used. A DB-1 [30 m × 250 µm (i.d.) × 0.25 µm] fused silica capillary column (Agilent J&W Scientific, Folsom, CA, USA) and a Rxi®-17 [1 m × 100 µm (i.d.) × 0.10 µm] fused silica capillary column (Restek Corp., Bellefonte, PA, USA) were used as the primary and secondary columns, respectively. The temperature gradient used for the primary column was 60ºC for 0.2 min, increased at 5ºC/min to 125ºC and further increased at 15ºC/min to 270ºC where it was kept for 25 min. The secondary column was always maintained at 10°C higher temperature than the primary column temperature. The modulator temperature offset was +20°C relative to the secondary column. The solvent acquisition delay was 500 s. A modulation period of 4 s with hot pulse time of 0.8 s was used. The injector, front inlet, transfer line, and ion source temperatures were kept constant at 250, 250, 270 and 200°C, respectively. The MS was operated using EI mode (70 eV) at a detector voltage of 1650 V. A scan range of *m/z* 50 to 650 and an

acquisition rate of 100 spectra/s were used for data acquisition. Chromatogram acquisition, noise reduction, baseline correction, smoothing, library matching and peak area calculation were carried out using the ChromaTOF software (Version 4.21, Leco Corp.). Only peaks having signal-to-noise ratio (s/n) greater than 100 were considered and peak area was computed by the software using unique mass. Peaks with SI more than 70% were assigned compound names while those having less than 70% SI were considered as unknown compound. Identities of selected metabolites were further confirmed by comparison of their mass spectra and R_t with those obtained using commercially available reference standards.

5.2.4. GC×GC/TOFMS data analysis

The Statistical Compare feature of ChromaTOF software was used to align analytes from chromatograms belonging to different samples and to generate data table consisting of sample names and area of analytes. The normalization of each sample was done by dividing the area of each analyte by the total peak area of all the analytes present in the sample. The normalized data was subjected to PCA to identify outliers and innate clustering trends using SIMCA-P software (Umetrics, Umeå, Sweden). The data were mean-centered and UV-scaled during chemometric data analysis. After PCA, OPLS-DA was performed to generate a model discriminating CRC from normal tissue specimens and to identify marker metabolites responsible for such discrimination. OPLS-DA was also carried out using anatomical site and Duke's stage of CRC as classifiers. An independent 't' test with Welch's

correction using SPSS software (Version 11.0, SPSS Inc., Chicago, IL, USA) was used for the comparison of the marker metabolite levels to determine their significant differences between the CRC and normal tissue groups ($p < 0.01$ was considered to be statistically significant). ROC analysis was also performed using GraphPad Prism software (Version 5.02., GraphPad Software Inc., La Jolla, CA, USA) to validate the robustness of the OPLS-DA model using the cross-validated predicted Y values.

5.3. Results and discussion

GC×GC/TOFMS was used for the non-targeted metabolic profiling of 31 tumor samples and 32 normal tissues obtained from 31 CRC patients. Figure 5.1. shows the surface and contour plots of a representative GC×GC/TOFMS chromatogram of human colon tissue. The analytical performance of GC×GC/TOFMS was found to be satisfactory as the PCA plot of all the samples showed that all the QC samples were clustered together (Figure 5.2.). The OPLS-DA model [2 LV, $R^2Y = 0.979$, $Q^2(cum) = 0.932$] generated from the GC×GC/TOFMS data and the corresponding ROC curve (AUC = 1.000) are shown in Figures 5.3. and 5.4., respectively. However no valid OPLS-DA model was obtained using anatomical site of CRC tumor or Duke's stage as classifier. The 44 marker metabolites identified on the basis of the OPLS-DA model (Figure 5.3.) and which were found to be significantly different between CRC and normal tissue group ($p < 0.01$, Welch 't' test) are summarized in Table 5.1. All the marker metabolites except squalene, AA, mannose, galactose, glucose, ribitol, fumarate, malate, oxalate and succinate,

Figure 5.1. A. Surface plot of GC×GC/TOFMS chromatogram of human colon tissue.
B. Contour plot of GC×GC/TOFMS chromatogram of human colon tissue (black dots indicate peaks).

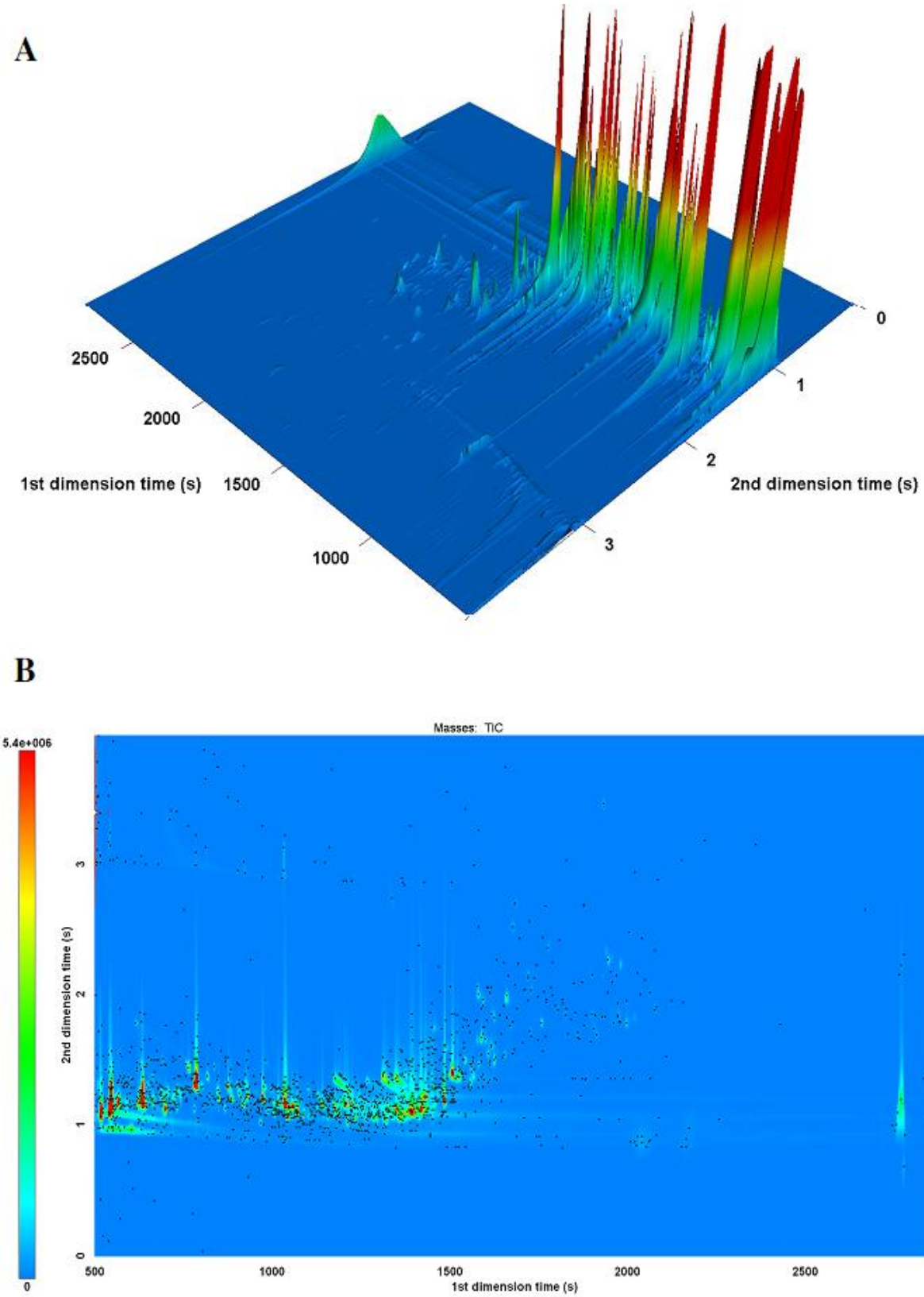

Figure 5.2. PCA plot of CRC and normal tissues along with QC samples based on GC×GC/TOFMS metabolic profiles.

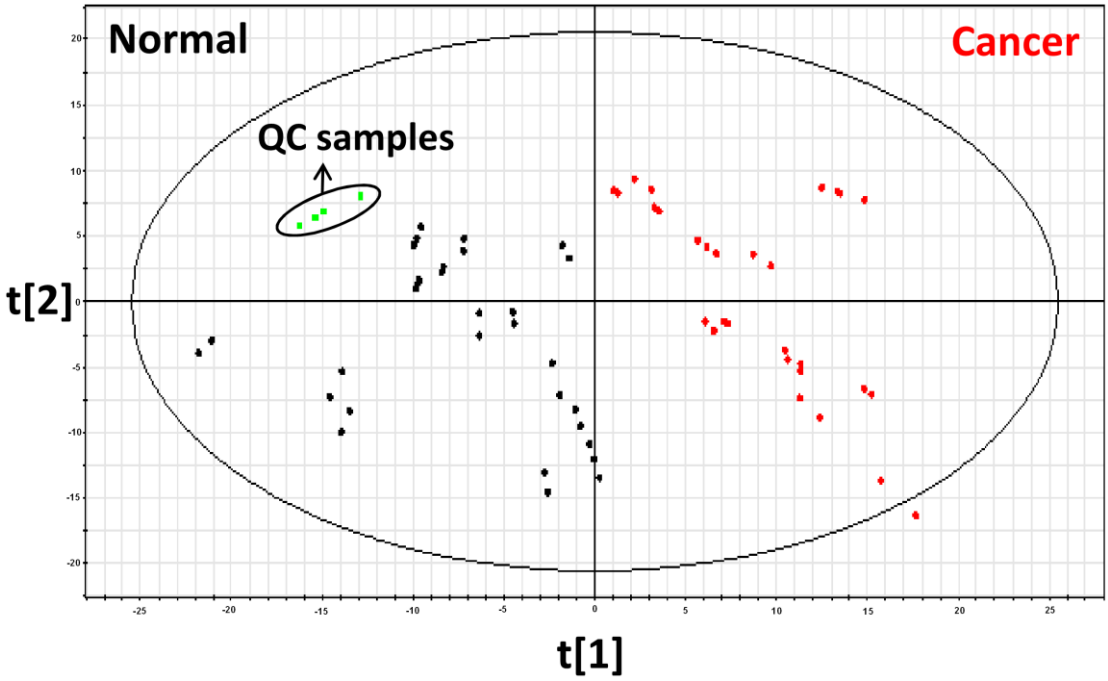

Figure 5.3. OPLS-DA scores plot discriminating CRC from normal tissues based on GC×GC/TOFMS metabolic profiles.

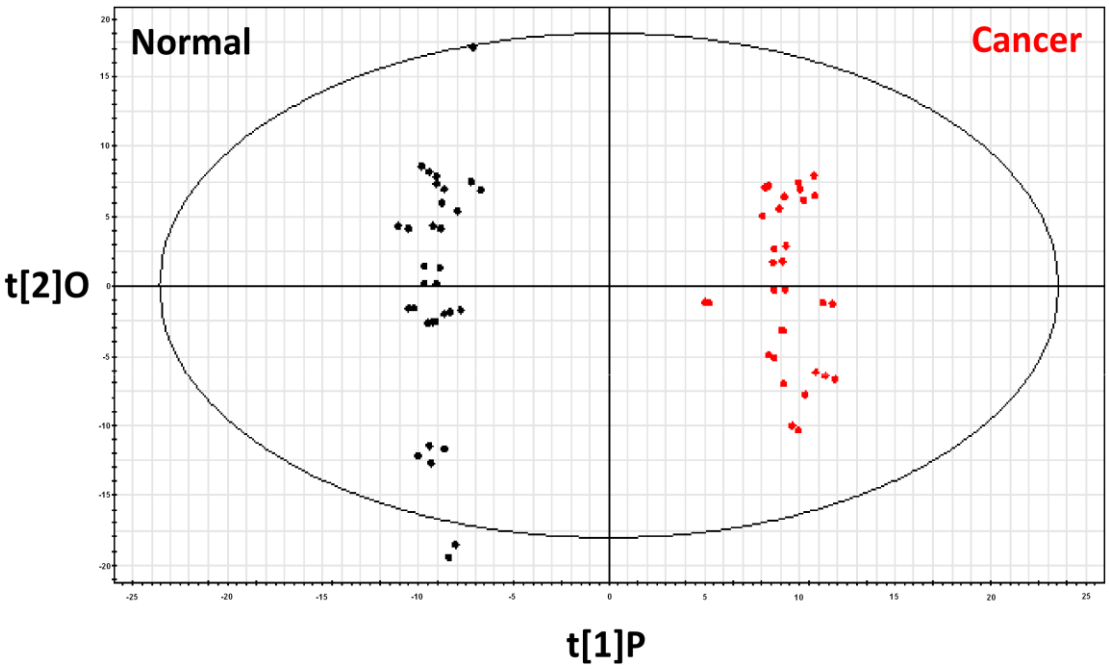

Figure 5.4. ROC curve determined using the cross-validated predicted Y values of the GC×GC/TOFMS OPLS-DA model.

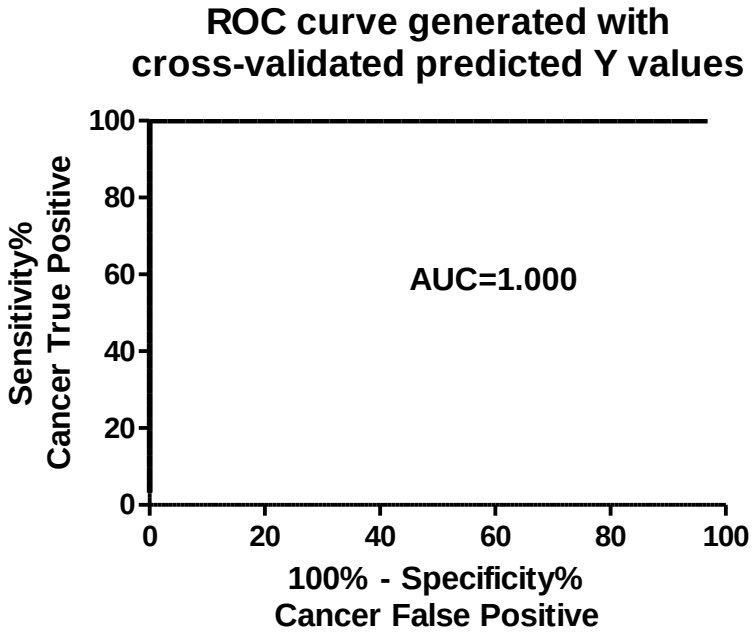

were found to be higher in CRC tissues as compared to normal tissues (Table 5.1.). Out of the 44 marker metabolites identified by GC×GC/TOFMS, 19 metabolites were also identified by GC/MS and 3 metabolites by HR-MAS NMR spectroscopy. The directions of fold changes of the common marker metabolites were found to be consistent across the three different analytical platforms reinforcing the clinical validity and robustness of these marker metabolites in characterizing CRC. In this section we focus our discussion only on those exclusive marker metabolites which were identified by GC×GC/TOFMS as the other marker metabolites identified by either GC/MS or HR-MAS NMR spectroscopy have been discussed in Chapters 3 and 4. The HMDB (Wishart et al., 2009) and the KEGG (Kanehisa and Goto, 2000) were utilized to get information about the identified marker metabolites and their related metabolic pathways, respectively.

Table 5.1. Marker metabolites identified by GC×GC/TOFMS.

Metabolite	Chemical class	Identified by[c]	% fold change of cancer from normal[d]	p value[e]
Glycine[b]	Amino acid	Standard	115.2	<0.0001
L-Proline[a]	Amino acid	Standard	83.3	<0.0001
L-Phenylalanine[a]	Amino acid	Standard	28.9	<0.01
L-Alanine	Amino acid	Standard	90.9	<0.001
L-Leucine	Amino acid	Standard	82.2	<0.0001
L-Valine	Amino acid	Standard	88.2	<0.001
L-Serine	Amino acid	Standard	42.3	<0.01
L-Threonine	Amino acid	Standard	95.5	<0.01
L-Isoleucine	Amino acid	Standard	148.7	<0.0001
Picolinic acid	Amino acid	NIST	94.1	<0.0001
L-Methionine	Amino acid	Standard	30.8	<0.01
L-Aspartic acid	Amino acid	Standard	28.9	<0.01
β-Alanine	Amino acid	NIST	184.9	<0.001
Aminomalonic acid	Amino acid	NIST	311.9	<0.0001
1-Methyl-hydantoin	Amino ketone	NIST	34.3	<0.001

[a] Profiled also by GC/MS.
[b] Profiled also by GC/MS and HR-MAS NMR spectroscopy.
[c] Metabolite identification using standard compound or NIST library search.
[d] Positive and negative percentages indicate higher levels of metabolites in cancer and normal tissues, respectively.
[e] Statistical p value calculated using the independent 't'-test with Welch's correction (significance at $p < 0.01$).

Table 5.1. Marker metabolites identified by GC×GC/TOFMS (continued).

Metabolite	Chemical class	Identified by[c]	% fold change of cancer from normal[d]	p value[e]
Palmitic acid[a]	Fatty acid	NIST	52.5	<0.0001
Margaric acid[a]	Fatty acid	NIST	21.6	<0.01
Oleic acid[a]	Fatty acid	NIST	118.4	<0.0001
Stearic acid[a]	Fatty acid	NIST	20.5	<0.001
Arachidonic acid[a]	Fatty acid	Standard	-38.7	<0.001
11-Eicosenoic acid[a]	Fatty acid	NIST	25.6	<0.01
Myristic acid	Fatty acid	NIST	86.1	<0.0001
Pentadecanoic acid	Fatty acid	NIST	71.1	<0.01
Linolenic acid	Fatty acid	NIST	128.2	<0.0001
Lignoceric acid	Fatty acid	NIST	122.9	<0.0001
Phosphate[a]	Inorganic acid	Standard	47.1	<0.0001
D-Mannose[a]	Monosaccharide	Standard	-50.9	<0.01
D-Galactose[a]	Monosaccharide	Standard	-72.6	<0.01
D-Glucose[b]	Monosaccharide	Standard	-91.0	<0.0001
L-Arabinose	Monosaccharide	NIST	54.5	<0.0001

[a] Profiled also by GC/MS.
[b] Profiled also by GC/MS and HR-MAS NMR spectroscopy.
[c] Metabolite identification using standard compound or NIST library search.
[d] Positive and negative percentages indicate higher levels of metabolites in cancer and normal tissues, respectively.
[e] Statistical p value calculated using the independent 't'-test with Welch's correction (significance at $p < 0.01$).

Table 5.1. Marker meabolites identified by GC×GC/TOFMS (continued).

Metabolite	Chemical class	Identified by[c]	% fold change of cancer from normal[d]	p value[e]
Lactate[b]	Organic acid	Standard	94.6	<0.0001
Fumarate[a]	Organic acid	Standard	-14.7	<0.01
Malate[a]	Organic acid	Standard	-64.3	<0.0001
Oxalate	Organic acid	Standard	-118.3	<0.001
Succinate	Organic acid	Standard	-62.5	<0.01
Maleic acid	Organic acid	Standard	43.6	<0.0005
Pantothenic acid	Organic acid	NIST	188.2	<0.005
Glycerol	Polyol	Standard	59.9	<0.0001
Ribitol	Polyol	Standard	-59.1	<0.005
1-Monooleoylglycerol[a]	Polyol derivative	NIST	97.5	<0.01
Uracil	Pyrimidine derivative	Standard	86.3	<0.0001
Uridine[a]	Pyrimidine nucleoside	Standard	141.0	<0.0001
Cholesterol[a]	Steroid	Standard	65.5	<0.0001
Squalene	Triterpene	NIST	-34.5	<0.01

[a] Profiled also by GC/MS.
[b] Profiled also by GC/MS and HR-MAS NMR spectroscopy.
[c] Metabolite identification using standard compound or NIST library search.
[d] Positive and negative percentages indicate higher levels of metabolites in cancer and normal tissues, respectively.
[e] Statistical p value calculated using the independent 't'-test with Welch's correction (significance at $p < 0.01$).

Recent studies suggest that the enzyme phosphoglycerate dehydrogenase (PHGDH) which oxidizes the glycolytic intermediate 3-phosphoglycerate to initiate serine biosynthesis, is over-expressed in breast cancer and helps cancer cells to proliferate rapidly (Locasale, et al., 2011; Possemato et al., 2011). This further implies that the suppression of PHGDH can be a new therapeutic target. Using GCxGC/TOFMS we observed higher levels of L-serine and glycine in cancer tissues which indicated branching of serine biosynthetic pathway from glycolysis and its upregulation, the end product of which is glycine. Our findings using human CRC tissue samples, were actually made before the findings by Locasale et al. and Possemato et al. and suggested that there is also a possible existence of this particular form of metabolic deregulation in human CRC.

Squalene acts as the metabolic precursor of cholesterol. Reduced level of squalene justifies the corresponding increase in cholesterol in CRC tissues. Moreover squalene has been shown to possess chemopreventive effect in rat models of CRC. It is a constituent of dietary oils like olive oil and this finding further emphasizes the influence of diet in CRC development (Rao et al., 1998). The endogenous levels of several fatty acids (myristic acid, pentadecanoic acid, lignoceric acid, linolenic acid in addition to those detected by GC/MS except AA), glycerol, cholesterol and polyol derivatives (Table 5.1.) were found to be significantly elevated in CRC tissue. This indicated the high biosynthetic rate of these metabolites to meet energy demand and rapid generation of lipid bio-components of cell membrane in fast proliferating tumor cells (Garber, 2006; Ong et al., 2010). Apart from this, previous studies have shown that such fatty acids act as tumor promoters in

murine cancer models and increase the risk of CRC in humans (Reddy, 1986, 1992). Lignoceric acid is a very long chain fatty acid (24 carbon atoms long) which acts as a tissue marker of peroxisomal disorder and is associated with perturbation in lipid metabolism (Wishart et al., 2009). This metabolite was found in higher levels in CRC tissues than in normal tissues suggesting definite alteration of lipid metabolism in CRC.

In accordance with other studies (Denkert et al., 2008; Ong et al., 2010), we also found that several proteinogenic amino acids were significantly elevated in CRC tissues (Table 5.1.). This observation can be attributed to increased protein synthesis in malignant cells as seen in different forms of cancer including CRC (Griffin and Shockcor, 2004). β-Alanine and L-proline play important role in osmoregulation (Burg and Ferraris, 2008). Higher levels of these two amino acids along with taurine and scyllo-inositol (identified by HR-MAS NMR spectroscopy) in CRC suggested altered osmoregulation. Aminomalonic acid is an amino acid which originates from defects in protein synthesis. Higher level of this metabolite in CRC suggested the possible existence of erratic protein synthesis (Wishart et al., 2009).

Picolinic acid is produced under inflammatory conditions and acts as an inducer of some inflammatory cytokines (Bosco et al., 2000; Wishart et al., 2009). Elevated levels of picolinic acid along with reduced levels of AA (major metabolic precursor of eicosanoids which act as inflammatory mediators) in CRC tissue further emphasize the significant association of inflammation with CRC (Kashfi and Rigas, 2005; Sano et al., 1995; Shureiqi and Lippman, 2001; Smith, 1992; Soslow et al., 2000; Soumaoro et al., 2006).

Succinate and oxalate were found to be reduced in CRC tissues along with fumarate and malate (also identified by GC/MS). This finding corroborated with the perturbation of TCA cycle in response to altered energy demand in CRC.

Higher level of pantothenic acid (vitamin B5) was found in CRC as compared to normal colon tissues. Similar observation was obtained previously in a rat model of colon adenocarcinoma (Baker et al., 1981) suggesting that high vitamin B5 content is required for catalysis of metabolism associated with rapid proliferation of tumors.

A comparison of the three analytical platforms that we used for the non-targeted metabolic profiling of CRC is presented in Table 5.2. Although GC×GC/TOFMS was found to be superior to GC/MS and HR-MAS NMR in terms of metabolic space coverage, HR-MAS NMR spectroscopy proved to be more advantageous in terms of the ease of sample preparation and the shorter total analysis time. Moreover, HR-MAS NMR spectroscopy was the only platform which was able to discriminate anatomical site of CRC tumor while the other two platforms failed to do so. It was not possible to cover all the metabolite classes using the three analytical platforms. Therefore it is always recommended to use multiple and complimentary analytical platforms to cover as much metabolic space as possible. Metabolite classes such as lyso-phospholipids, sphingolipids, oxylipins, glycolipids, glycerolipids, glucoronides, pterins, quinones, lipoamides, carnitines, retinoids are some of the metabolite classes that have not been covered by the three analytical platforms.

In some cases metabolite identification was not possible because of low SI. These “missed” or “unknown” metabolites constituted about 17% of the total metabolites analyzed by the method. However this amount can be an overestimate particularly in case of GCxGC/TOFMS data because second dimensional separation can split a single peak of an unknown analyte into multiple peaks resulting in an apparent increase in the number of unknown analytes. The unknown metabolites constitute a constant challenge in the field of metabolic profiling. Online databases such as the Golm’s database and the HMDB database could be used to identify the unknowns in some cases but the coverage of such databases is still limited and in future collaborative efforts are required to build more comprehensive databases which can aid in finding the identity of unknowns. Even if any unknown metabolite contributed significantly to the chemometric separation of CRC and normal tissue, it was not considered to be significant as it did not provide any useful information regarding metabolic pathway or aided in biological interpretation of metabolic profiling results.

In order to enhance the information obtained from non-targeted metabolic profiling of CRC, it was pertinent to map and cross-compare the marker metabolites identified using all the three analytical platforms with regards to the human metabolic pathways. For this purpose the KegArray application (Version 1.2.3) of KEGG was used. This application facilitated the association of metabolites with organism specific KEGG metabolic pathway maps. The findings about the key sets of marker metabolites, related metabolic pathways and their biological relevance are summarized in Table 5.3.

5.4. Conclusion

GC×GC/TOFMS was able to provide coverage of comparatively more metabolic space as evident from the identification of 44 marker metabolites belonging to various chemical classes. A robust OPLS-DA model capable of discriminating CRC from normal tissue groups was generated on the basis of GC×GC/TOFMS metabolic profiles. However no valid OPLS-DA model was obtained using the Dukes stage or anatomical site of CRC as classifier. The marker metabolites identified using all the three analytical platforms were associated with perturbations in metabolic pathways such as glycolysis, TCA cycle, lipid metabolism, amino acid metabolism and nucleotide metabolism. Deregulation of these metabolic pathways suggested the existence of conditions like tissue hypoxia, altered osmoregulation, rapid proliferation, high energy demand of cancer cells and inflammatory environment in CRC. These perturbations of metabolic pathways shed light on the carcinogenesis of CRC and may yield potential therapeutic targets with further research.

Table 5.2. Comparison of different analytical platforms used for non-targeted metabolic profiling of CRC.

Parameters	**HR MAS NMR**	**GC/MS**	**GC×GC/TOFMS**
Sample preparation	simple	tedious	tedious
Total analysis time	40 min	200 min	190 min
No. of chromatographic peaks	not applicable	~75	~800
No. of marker metabolites	9	19	44
Chemical class of metabolites	acyl phosphate, lipid, amino acid, monosaccharide, polyol, organic acid, choline containing compounds	monosaccharide, amino acid, steroid, organic acid, fatty acid, polyol, polyol derivative, inorganic acid, pyrimidine nucleoside.	monosaccharide, amino acid, triterpene, amino ketone, steroid, organic acid, fatty acid, polyol derivative, inorganic acid, pyrimidine derivative, pyrimidine nucleoside.
Q^2(cum) of OPLS-DA model (CRC vs. Normal)	0.779	0.784	0.934
Q^2(cum) of OPLS-DA model (Anatomical site of tumor)	0.625	no valid model	no valid model

Table 5.3. Metabolites, metabolic pathways and biological relevance in CRC.

Metabolite[a]	Metabolic pathway[b]	Major metabolic process[b]	Biological relevance
D-Mannose (↓)	Fructose and mannose metabolism	Carbohydrate metabolism	Enhanced carbohydrate metabolism especially glycolytic pathway to meet high energy demand of cancer cells under hypoxic conditions
D-Galactose (↓)	Galactose metabolism	Carbohydrate metabolism	
D-Glucose (↓)	Glycolysis	Carbohydrate metabolism	
Lactate (↑)	Glycolysis	Carbohydrate metabolism	
Ribitol (↓)	Pentose and glucuronate interconversions	Carbohydrate metabolism	
Fumarate (↓)	TCA cycle	Carbohydrate metabolism	Deregulation of TCA cycle caused by altered energy demand in cancer cells
Malate (↓)	TCA cycle	Carbohydrate metabolism	
Succinate (↓)	TCA cycle	Carbohydrate metabolism	
Oxalate (↓)	Glyoxylate and dicarboxylate metabolism	Carbohydrate metabolism	
Palmitic acid (↑)	Fatty acid biosynthesis	Lipid metabolism	Increased biosynthesis of lipid components of cell membrane to cope up with rapid growth of cancer cells
Oleic acid (↑)	Fatty acid biosynthesis	Lipid metabolism	
Stearic acid (↑)	Fatty acid biosynthesis	Lipid metabolism	
γ-Linolenic acid (↑)	Fatty acid biosynthesis	Lipid metabolism	
Lignoceric acid (↑)	Fatty acid biosynthesis	Lipid metabolism	
Myristic acid (↑)	Fatty acid biosynthesis	Lipid metabolism	
Pentadecanoic acid (↑)	Fatty acid biosynthesis	Lipid metabolism	
Margaric acid (↑)	Fatty acid biosynthesis	Lipid metabolism	
Glycerol (↑)	Glycerolipid metabolism	Lipid metabolism	
Phosphocholine (↑)	Glycerophospholipid metabolism	Lipid metabolism	
Phosphoethanolamine (↑)	Glycerophospholipid metabolism	Lipid metabolism	
Cholesterol[c] (↑)	Steroid biosynthesis	Lipid metabolism	
Squalene (↓)	Steroid biosynthesis	Lipid metabolism	
Cholesterol[c] (↑)	Primary bile acid biosynthesis	Lipid metabolism	Bile acids may act as tumor promoters or carcinogens in CRC

[a] Metabolites are grouped together on basis of biological relevance, (↑): Elevated in CRC (↓): Reduced in CRC

[b] Related to metabolites using KEGG

[c] Metabolites found to be involved in more than one relevant metabolic pathway

Table 5.3. Metabolites, metabolic pathways and biological relevance in CRC (continued).

Metabolite[a]	Metabolic pathway[b]	Major metabolic process[b]	Biological relevance
L-Aspartic acid (↑)	Alanine, aspartate and glutamate metabolism	Amino acid metabolism	Increased synthesis of proteins to meet demand of rapidly proliferating cancer cells
L-Alanine (↑)	Alanine, aspartate and glutamate metabolism	Amino acid metabolism	
N-Methyl-hydantoin (↑)	Arginine and proline metabolism	Amino acid metabolism	
Glycine[c] (↑)	Glycine, serine and threonine metabolism	Amino acid metabolism	
L-Serine (↑)	Glycine, serine and threonine metabolism	Amino acid metabolism	
L-Threonine (↑)	Glycine, serine and threonine metabolism	Amino acid metabolism	
L-Methionine (↑)	Methionine biosynthesis	Amino acid metabolism	
L-Phenylalanine (↑)	Phenylalanine biosynthesis	Amino acid metabolism	
L-Proline[c] (↑)	Proline biosynthesis	Amino acid metabolism	
L-Leucine (↑)	Valine, leucine and isoleucine biosynthesis	Amino acid metabolism	
L-Isoleucine (↑)	Valine, leucine and isoleucine biosynthesis	Amino acid metabolism	
L-Valine (↑)	Valine, leucine and isoleucine biosynthesis	Amino acid metabolism	
L-Proline[c] (↑)	ATP-binding cassette (ABC) transport	Membrane transport	Osmoregulation to maintain the homeostasis of rapidly proliferating cancer cells
β-Alanine[c] (↑)	β-Alanine metabolism	Amino acid metabolism	
Scyllo inositol (↑)	Inositol phosphate metabolism	Carbohydrate metabolism	
Taurine (↑)	Taurine and hypotaurine metabolism	Amino acid metabolism	
Glycine (↑)	Purine metabolism	Nucleotide metabolism	Increased nucleotide biosynthesis to meet demand of rapidly proliferating cancer cells
Uracil (↑)	Pyrimidine metabolism	Nucleotide metabolism	
Uridine (↑)	Pyrimidine metabolism	Nucleotide metabolism	
β-Alanine[c] (↑)	Pyrimidine metabolism	Nucleotide metabolism	
Arachidonic acid (↓)	Eicosanoid biosynthesis	Lipid metabolism	Inflammation associated with CRC development
Picolinic acid (↑)	Tryptophan metabolism	Amino acid metabolism	

[a] Metabolites are grouped together on basis of biological relevance, (↑): Elevated in CRC (↓): Reduced in CRC

[b] Related to metabolites using KEGG

[c] Metabolites found to be involved in more than one relevant metabolic pathway

CHAPTER 6

DEVELOPMENT AND VALIDATION OF AN UPLC/MS/MS METHOD FOR TARGETED PROFILING OF EICOSANOIDS AND ARACHIDONIC ACID IN COLORECTAL CANCER

6.1. Introduction

Different analytical platforms such as enzyme immunoassay (EIA) (Nicosia et al., 1992), radioimmunoassay (RIA) (Levine, 1986; Pugh and Thomas, 1994; Rigas et al., 1993; Rigas and Levine, 1984), GC/MS, gas chromatography tandem mass spectrometry (GC/MS/MS) (Capdevila et al., 1981, 1992; Catella et al, 1990; Hubbard et al., 1986; Tsikas, 1998; Tsukamoto et al, 2002), capillary electrophoresis with ultraviolet detection (Vandernoot and VanRollins, 2002), HPLC with fluorescence detection (Maier et al., 2000; Nithipatikom et al., 2000; Yue et al., 2004), LC/MS and liquid chromatography tandem mass spectrometry (LC/MS/MS) (Bolcato et al., 2003; Hishinuma et al., 2007; Kempen et al., 2001; Margalit et al., 1996; Takabatake et al., 2002; Yang et al., 2006; Yue et al., 2007), have been used to determine selected sub-sets of the eicosanoids. Although GC/MS and GC/MS/MS with negative ion chemical ionization are the most commonly used techniques for the eicosanoids, tedious sample preparation steps including derivatization are necessary before analysis. EIAs and RIAs cannot determine eicosanoids simultaneously and are affected by cross reactivity. Moreover RIAs suffer from the disadvantage of radiation hazards. Fluorescent HPLC method is applicable but it suffers from long elution time and high

background noise (Yue et al., 2004). Although various LC/MS or LC/MS/MS methods have been used for identification and quantification of eicosanoids in different biological matrices such as microsomal incubates (Bolcato et al., 2003), human synovial cell-culture (Takabatake et al., 2002), human blood (Margalit et al., 1996), rat brain tissue (Yue et al., 2007), mouse prostate tissue (Yang et al., 2006), human lung cancer cells, rat leukemia cells (Kempen et al., 2001) and mouse bone marrow-derived mast cells (Hishinuma et al., 2007), they have not been explored for the determination of eicosanoids in human colon tissue. Unlike LC/MS, RIA (Pugh and Thomas, 1994; Rigas et al., 1993) and GC/MS (Bennett et al., 1987; Giardiello et al., 1998; Yang et al., 1998) were reported for the determination of eicosanoids in human colon tissue.

In this chapter, we report the development and validation of an UPLC/MS/MS method for the simultaneous and fast determination of AA and biologically relevant eicosanoids in human colorectal tissue viz. prostaglandin E_2 (PGE_2), prostacyclin (PGI_2) [assayed as its stable hydrolytic product 6-keto-prostaglandin$_{1\alpha}$ (6-k-$PGF_{1\alpha}$)], prostaglandin D_2 (PGD_2), leukotriene B_4 (LTB_4), thromboxane A_2 (TXA_2) [assayed as its stable breakdown product thromboxane B_2 (TXB_2)], 13S-hydroxy-9Z,11E-octadecadienoic acid (13S-HODE), 12-hydroxy-5Z,8Z,10E,14Z-eicosatetraenoic acid (12-HETE) and 8-hydroxy-5Z,9E,11Z,14Z-eicosatetraenoic acid (8-HETE). As prostaglandin $F_{2\alpha}$ ($PGF_{2\alpha}$) does not play a role in CRC carcinogenesis, it was not profiled in our study (Wang and Dubois, 2008). As 15-LOX-2 which catalyze the conversion of AA to 15-hydroxy eicosatetraenoic acid (15-HETE) is not expressed in human colon tissue, 15-HETE was also excluded from our study

(Ikawa et al., 1999). Although 13S-HODE is not a metabolic product of AA, it was included in our study as it has shown anticarcinogenic effect in CRC cells (Shureiqi et al., 1999).

6.2. Experimental

6.2.1. Materials

Butylated hydroxyl toluene (BHT), PGE_2, 6-k-$PGF_{1\alpha}$, PGD_2, LTB_4, TXB_2, 13S-HODE, 12-HETE, 8-HETE and deuterated prostaglandin E_2 (PGE_2-d_4) were purchased from Cayman Chemical Company (Ann Arbor, MI, USA). PGE_2-d_4 was used as the internal standard (IS). AA and citric acid were obtained from Sigma-Aldrich Inc. (St. Louis, MO, USA). HPLC-grade methanol and acetonitrile (ACN) were purchased from Tedia Company Inc. (Fairfield, OH, USA). HPLC-grade ethyl acetate and n-hexane were purchased from Fisher Scientific (Leicestershire, UK). Ammonium acetate and formic acid (FA), both of 99% purity, were purchased from VWR International Ltd. (Leicestershire, UK). Ultra pure grade phosphate buffer saline (PBS) was obtained from 1st Base Private Limited (Singapore). Water used for the study was purified with a Milli-Q water purification system (Millipore, Billerica, MA, USA). Bovine serum albumin (BSA) and Coomassie® Brilliant Blue G-250 dye were obtained from Bio-Rad Laboratories (Hercules, CA, USA).

6.2.2. Human colon tissue samples

Human colon tissues were provided by the Department of Colorectal Surgery, SGH, Singapore. The utilization of human tissue was approved by the SingHealth Centralised Institutional Review Board (CIRB), Singapore (CIRB reference number 2009/723/B). For method development and validation, one representative normal colon tissue (3 g) was snap-frozen immediately following surgery and then stored at -80ºC until processing. The tissue was subsequently cut and divided into tissue masses of about 10 mg each for the UPLC/MS/MS method development and validation.

6.2.3. Sample preparation

For the development of the sample preparation protocol, previously reported sample preparation strategies were used as references (Kempen et al., 2001; Yang et al., 2006). About 10 mg of each human colon tissue was weighed accurately and transferred to a 2 mL Eppendorf tube and 500 µL of ice-cold PBS containing 0.1% BHT was added to each sample. 20 µL of 1N citric acid and 10 µL of a 500 ng/mL stock solution of PGE_2-d_4 (IS) were added to each sample. The samples were then homogenized for 2 min at a frequency of 25 Hz using 4 mm inner diameter metal balls in a Retsch MM400 ball mill (Haan, Germany). Each homogenate was subsequently transferred to a 15 mL glass centrifuge tubes. 1 mL of n-hexane:ethyl acetate (1:1, v/v) was added to the aqueous homogenate and vortex-mixed for 2 min. Each sample was then centrifuged at 1800 g units for 3 min. The upper organic layer was collected

and the extraction process was repeated two more times. After extraction, 10 µL of the lower aqueous layer was kept aside for protein assay as the amount of individual eicosanoids and AA in each tissue was normalized with respect to the total protein content. The organic phases obtained from three extractions were pooled and then evaporated to dryness under a stream of nitrogen at room temperature (24°C) using a Turbovap LV (Caliper Life Sciences, Hopkinton, MA, USA). Each sample was then reconstituted in 50 µL of methanol and used for UPLC/MS/MS analysis.

6.2.4. Protein assay

The protein content in tissue samples was determined using the Bradford assay via a 96 well plate format. The dye reagent was prepared by diluting 1 part of Coomassie® Brilliant Blue G-250 dye concentrate with 4 parts of water followed by filtration to remove particulates. Protein standard solution of BSA (100 µg/mL) was prepared in PBS containing 0.1% BHT. For preparation of calibration curve, 2, 5, 10, 20 and 50 µL of the protein standard solution with corresponding 98, 95, 90, 80 and 50 µL of PBS containing 0.1% BHT were added in separate wells followed by addition of 25 µL of dye reagent to each well. For tissue samples, 10 µL of the lower aqueous layer obtained during sample preparation, 90 µL of PBS containing 0.1% BHT and 25 µL of dye reagent were added to each well. Solutions were mixed using a microplate mixer and incubated at room temperature (24ºC) for 5 min. The absorbance was then measured at 595 nm using a Tecan Infinite M200 microplate reader

(Tecan Group Ltd., Männedorf, Switzerland). The protein content in each sample was determined from the standard calibration curve.

6.2.5. UPLC/MS/MS analysis

Analysis of AA and eicosanoids was performed using an ACQUITY UPLC system (Waters, Milford, MA, USA) coupled to a 3200 QTRAP hybrid triple quadrupole linear ion trap mass spectrometer (Applied Biosystems, Foster City, CA, USA) equipped with a Turbo Ion Spray electrospray ionization (ESI) source. Multiple reaction monitoring (MRM) experiments were performed using negative ESI ionization mode. The dwell time used for all MRM experiments was 50 ms. The optimized source-dependent and compound-dependent MS parameters for the analytes are shown in Table 6.1. The collision-activated dissociation (CAD) gas was set to 'Medium' throughout the experiments. The interface heater was kept on to maximize the ion signal and to avoid contamination of the ion optics. Chromatographic separations were carried out on an ACQUITY UPLC BEH C_{18} (1.7 µm 100 × 2.1 mm i.d.) column (Waters, Milford, MA, USA). The column and autosampler temperature were maintained at 45 and 4 °C, respectively. The optimized mobile phase consisted of 0.1% FA in water (solvent A) and 0.1% FA in ACN (solvent B). The mobile phase flow rate was 0.4 mL/min. The optimized elution condition is shown in Table 6.2. A partial loop with needle overfill injection mode was used and the injection volume was 2 µL. The analysis time for each sample was 5.5 min. Data acquisition and processing

were performed using the Analyst software (Version 1.4.2, Applied Biosystems, Foster City, CA, USA).

6.2.6. Method validation

US-FDA guidelines for bioanalytical method validation and International Conference on Harmonization (ICH) guidelines on analytical method validation with suitable modifications were followed for the method validation studies (FDA, 2001; ICH 1994, 1996). During method validation, parameters such as selectivity, sensitivity, matrix effect, linearity, accuracy, precision, extraction efficiency and autosampler stability of samples were investigated. Calculations of method validation results were carried out using the Microsoft Excel 2007 software.

6.2.6.1. Selectivity

Selectivity of the developed UPLC/MS/MS method was investigated by comparing the chromatograms of blank and standard samples. The blank sample comprising 500 µL of ice-cold PBS containing 0.1% BHT was subjected to sample preparation as described earlier. The standard sample containing all the standard metabolites (at concentrations of 10 pg/mg and 5 ng/mg of colon tissue for eicosanoids and AA, respectively) was used for checking background chromatographic interferences, if any.

Table 6.1. Optimized source- and compound-dependent MS parameters

Source-dependent parameters					
Curtain gas (psi)	15				
Ion spray voltage (V)	-4500				
Temperature (°C)	500				
Nebulizer gas 1 (psi)	40				
Nebulizer gas 2 (psi)	45				
Compound-dependent parameters					
Metabolite	**MRM transition (m/z)**	**DP[a] (V)**	**EP[b] (V)**	**CE[c] (V)**	**CXP[d] (V)**
6-k $PGF_{1\alpha}$	369.2→163.0	-55	-6	-38	-1
TXB_2	369.1→169.2	-35	-4	-26	-1
PGE_2	351.3→271.2	-19	-6	-27	-1
PGE_2-d_4 (IS)	355.1→275.3	-30	-5	-27	-2
PGD_2	351.3→189.2	-20	-4	-28	-1
LTB_4	335.1→195.2	-48	-4	-23	-1
13S-HODE	295.1→277.0	-30	-7	-21	-1
8-HETE	319.2→155.2	-30	-5	-22	-1
12-HETE	319.1→179.0	-30	-7	-21	-1
AA	303.1→259.0	-45	-5	-21	-1

[a] Declustering potential; [b] Entrance potential; [c] Collision energy; [d] Collision cell exit potential

Table 6.2. Optimized UPLC elution conditions

Time (min)	**% Solvent A[a]**	**% Solvent B[a]**	**Curve[b]**
0.00	50	50	6
3.70	5	95	4
4.35	5	95	6
4.50	50	50	6
5.50	50	50	6

[a] Solvent A: 0.1% FA in water, solvent B: 0.1% FA in ACN
[b] Different curves of the UPLC gradient were used to optimize the chromatographic resolution of the analytes.

6.2.6.2. Sensitivity

The limit of detection (LOD) and limit of quantification (LOQ) of each metabolite were determined as per ICH guidelines (ICH, 1994, 1996). The LODs and LOQs of metabolites were calculated using equations 1 and 2 with regards to three calibration curves.

LOD = 3.3 × (SD of y intercept) ÷ average slope (equation 1)

LOQ = 10 × (SD of y intercept) ÷ average slope (equation 2)

In addition to the determination of the LOD and LOQ of individual metabolites, it was important to determine the minimal amount of colon tissue that was required to produce a reasonably sensitive profiling of endogenous eicosanoids and AA. In our method development, different weights of colon tissue (5, 10 and 20 mg) were processed and analyzed to determine an optimal balance between tissue weight and sensitivity limit of the UPLC/MS/MS assay.

6.2.6.3. Matrix effect

The matrix effect was investigated using the post-extraction spike method (spiked in matrix extract) in which the peak areas of standard metabolites in neat solvent were compared to that obtained from standard metabolites spiked in matrix post-extraction (Bottcher et al., 2007). As all the eicosanoids and AA profiled in our study were present endogenously in human colon tissue, it was

impossible to obtain ‘blank’ human colon tissue devoid of these metabolites. To negate the endogenous occurrence of these metabolites which could interfere with our evaluation of matrix effect, the peak area observed in the case of standard metabolites spiked in matrix post-extraction was corrected by subtracting the basal peak area of metabolites in unspiked matrix. For this purpose, one representative normal colon tissue was divided into aliquots of about 10 mg each and homogenized in a ball mill using 500 µL of ice-cold PBS containing 0.1% BHT for each sample. The homogenates thus obtained were pooled and mixed so that a matrix homogenate with uniform basal amount of endogenous metabolites was obtained. The homogenate was further redistributed into 500 µL aliquots. Each aliquot was then subjected to extraction as per our sample preparation method. Standard metabolites were spiked subsequently into the matrix extract at low (30 pg/mg and 15 ng/mg of colon tissue for eicosanoids and AA, respectively), medium (300 pg/mg and 40 ng/ mg of colon tissue for eicosanoids and AA, respectively) and high (4000 pg/mg and 300 ng/mg of colon tissue for eicosanoids and AA, respectively) concentration levels. Three replicates were used for each concentration level. The basal peak areas of the metabolites in matrix were determined using three replicates of 500 µL of matrix homogenate devoid of any standard metabolite. The matrix effect was then evaluated using equation 3.

Matrix effect = $[1-(A_1 – A_2) \div A_3] \times 100$ (equation 3)

where,

A_1 = mean peak area of sample consisting of matrix extract spiked with standard metabolite

A_2 = mean basal peak area of metabolite present in matrix

A_3 = mean peak area of standard metabolite in neat solvent

6.2.6.4. Linearity and accuracy

Stock solutions of standard metabolites were prepared in methanol containing 0.1% BHT. Due to the unavailability of metabolite-free 'blank' matrix, the standard addition method was adopted to study the linearity and accuracy of our assay. The calibration standards and quality control (QC) samples were prepared by spiking standard metabolites into 500 µL aliquots of matrix homogenate (prepared as per method described in "matrix effect" section and having uniform basal amount of metabolites) and then subjecting them to sample preparation as described earlier. The concentrations of the metabolites in the calibration standards and QC samples were calculated with reference to 10 mg of colon tissue. For instance, a spiked amount of 500 pg of an eicosanoid was considered equivalent to a concentration of 500 pg of eicosanoid per 10 mg of colon tissue or 50 pg/mg of colon tissue. The concentration range used for calibration of the 8 eicosanoids was 10-5000 pg/mg of colon tissue whereas that for AA was 5-500 ng/mg of colon tissue. As per FDA guidelines for bioanalytical method validation QC samples should be used at three different concentrations (Bansal and DeStefano, 2007; FDA, 2001):

- Low QC: three times the lower limit of quantification (prepared QC: 3 times 10 pg/mg i.e 30 pg/mg)

- Medium QC: ~mid value of calibration range (prepared QC: 300 pg/mg)
- High QC: ~70-85% of higher limit of quantification (prepared QC: 80% of 5000 pg/mg i.e. 4000 pg/mg).

Similarly, as per guidelines the QC samples for AA were prepared at three concentrations of 15, 40 and 300 ng/mg of colon tissue. The basal peak area of a metabolite (determined using three replicates of 500 µL of matrix homogenate devoid of any standard metabolite) was subtracted from the observed peak areas of the metabolite in calibration samples to account for the endogenous occurrence of each metabolite in the matrix. The resulting peak areas were divided by the IS peak areas and the ratios were plotted against nominal concentration to construct calibration curve for each metabolite. The constructed calibration curves were used to determine the concentrations of the metabolites in the QC samples. The observed concentration of a metabolite in QC sample was corrected by subtracting the basal concentration of the metabolite (determined using three replicates of 500 µL of matrix homogenate devoid of any standard metabolite). The accuracy of the developed method was determined by measuring the percentage deviations of the observed concentrations of calibration samples and corrected concentrations of the QC samples from the nominal concentrations. A percentage deviation within ±15% was considered acceptable.

6.2.6.5. Intra- and inter-day precision

Both intra- and inter-day precision were determined using QC samples (prepared by standard addition method) at three different nominal concentrations viz. 30, 300 and 4000 pg/mg of colon tissue for the 8 eicosanoids and 15, 40 and 300 ng/mg of colon tissue for AA, respectively. The observed concentration of a metabolite in QC sample was corrected as discussed previously. The inter-day precision values were determined on three different days (first, second and third day of method validation). A relative standard deviation (RSD) of 15% was considered as satisfactory in our method validation.

6.2.6.6. Autosampler stability

In order to evaluate the stability of the extracted metabolites in the autosampler of the UPLC system, 6 human colon tissues of about 10 mg each were processed. The extracted samples were injected into the UPLC/MS/MS system (0 h), kept in the autosampler (4ºC) and re-injected after 24 h. The autosampler stability was determined by comparing the peak area of each metabolite measured at 0 and 24 h. A relative stability of 100 ± 15% was considered acceptable.

6.2.6.7. Extraction efficiency

The extraction efficiency was estimated at three concentration levels viz. 30, 300 and 4000 pg/mg of colon tissue for the 8 eicosanoids and 15, 40 and 300 ng/mg of colon tissue for AA. The standard metabolites were spiked into aliquots of 500 µL of matrix homogenate and processed as per our sample preparation protocol. The peak area of a metabolite obtained in the case of spiked samples was corrected by subtraction of basal peak area of the metabolite (determined using three replicates of 500 µL of matrix homogenate devoid of any standard metabolite) and was compared to the peak area of the unextracted standard metabolite to determine the extraction efficiency.

6.3. Results and discussion

During our preliminary UPLC/MS/MS method development, different mobile phase combinations comprising methanol, 0.1% FA in water, 0.1% FA in ACN and 10 mM ammonium acetate were attempted. Based on the quality of peak shape and resolution of metabolites, it was confirmed that mobile phase comprising 0.1% FA in water and 0.1% FA in ACN yielded the best results. A representative UPLC/MS/MS chromatogram of a sample comprising all the standard metabolites is shown in Figure 6.1. The total analysis time for each sample was short (5.5 min) as compared to previously reported methods (Hishinuma et al., 2007; Hubbard et al., 1986; Kempen et al., 2001; Maier et al., 2000; Takabatake et al., 2002; Tsukamoto et al., 2002; Yang et al., 2006; Yue et al., 2004, 2007). This supported the potential profiling of human CRC

samples by clinical laboratories where a short turn-around time is expected from the physicians.

The developed UPLC/MS/MS method was found to be selective with regards to all the MRM transitions, as considerable interferences were not observed when a blank sample was compared with a sample containing all the standard metabolites. While this finding was not unexpected due to the high selectivity of MRM experiments, it was pertinent to confirm that the profiled metabolites were derived from endogenous AA and eicosanoids and not other impurities or co-metabolites. The high selectivity of the method is essential to ensure that the observed perturbations in the levels of the inflammatory marker metabolites were related to the pathology of CRC and not due to chance correlation. The minimal amount of fresh colon tissue required to generate a reasonably sensitive profiling of endogenous AA and eicosanoids was found to be 10 mg. The establishment of this parameter would help guide clinician scientists in understanding and accommodating the requirement of the targeted profiling assay in addition to other tests such as histopathological assessment and genomic profiling of the colon tissues. While evaluating matrix effect (Figure 6.2.), we observed concentration-independent ion suppression for all the profiled analytes. The ion suppression due to matrix effect was found to be minimal ranging from 5 to 13 % across the three investigated concentration levels.

The calculated values of LOQ and LOD for all the eicosanoids and AA are shown in Table 6.3. Although the LOQ and LOD values were found to be higher than previously reported methods (Hubbard et al., 1986; Tsukamoto et al., 2002; Yue et al., 2004, 2007), our method was found to be sufficiently

sensitive as the profiled endogenous levels of AA and eicosanoids in human colon tissue were above the respective LOQs and LODs. The UPLC/MS/MS method was validated over a calibration range of 10-5000 pg/mg of colon tissue for the 8 eicosanoids and 5-500 ng/mg of colon tissue for AA. All the analytes showed satisfactory linearity of response as evident from their average correlation coefficients of greater than 0.99 (Table 6.3.). The accuracy of the developed method was found to be satisfactory as the percentage deviations of the observed concentrations of calibration and QC samples from the nominal concentrations were all within the acceptable limit of ±15% for all the metabolites. The RSDs of all the metabolites in terms of intra- and inter-day precision were found to be less than 15% (Table 6.4.). In addition, the relative stability of each metabolite was found to be within the acceptable limits of 100 ± 15% when kept in the autosampler at 4ºC for 24 h (Table 6.4.). Our results implied that batch analysis of clinical samples can be performed for up to 260 processed samples without compromising the chemical integrity of each metabolite. The extraction efficiencies of all the metabolites were consistent as indicated by the low SD values (0.94-6.25) and this is critical for developing a reliable method for the targeted profiling of AA and eicosanoids (Table 6.5.).

Figure 6.1. Representative UPLC/MS/MS chromatogram of a sample comprising all the standard metabolites.

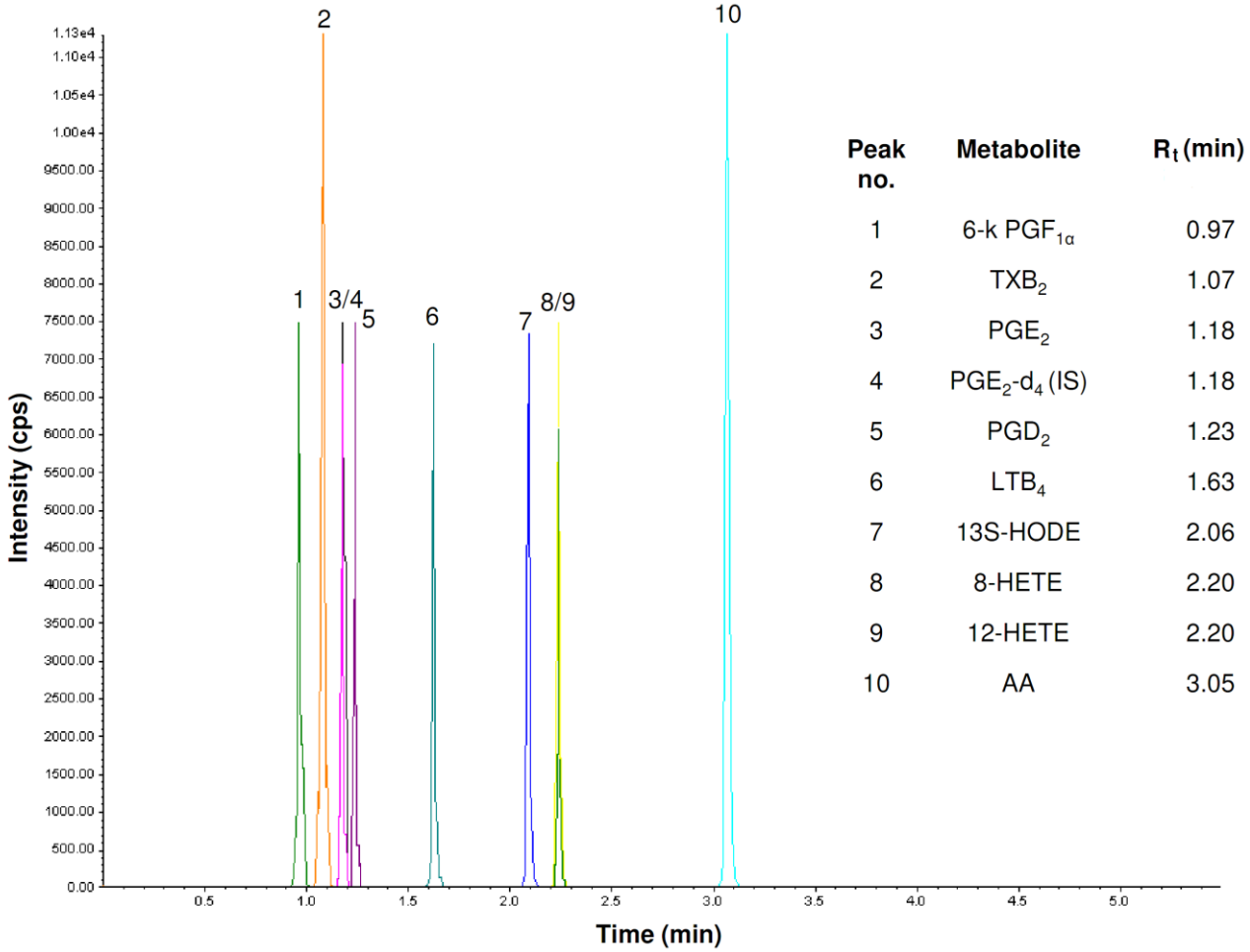

Peak no.	Metabolite	R_t (min)
1	6-k $PGF_{1\alpha}$	0.97
2	TXB_2	1.07
3	PGE_2	1.18
4	PGE_2-d_4 (IS)	1.18
5	PGD_2	1.23
6	LTB_4	1.63
7	13S-HODE	2.06
8	8-HETE	2.20
9	12-HETE	2.20
10	AA	3.05

Figure 6.2. Matrix effect on profiled metabolites (represented by mean percentage ion suppression with error bars depicting standard deviation).

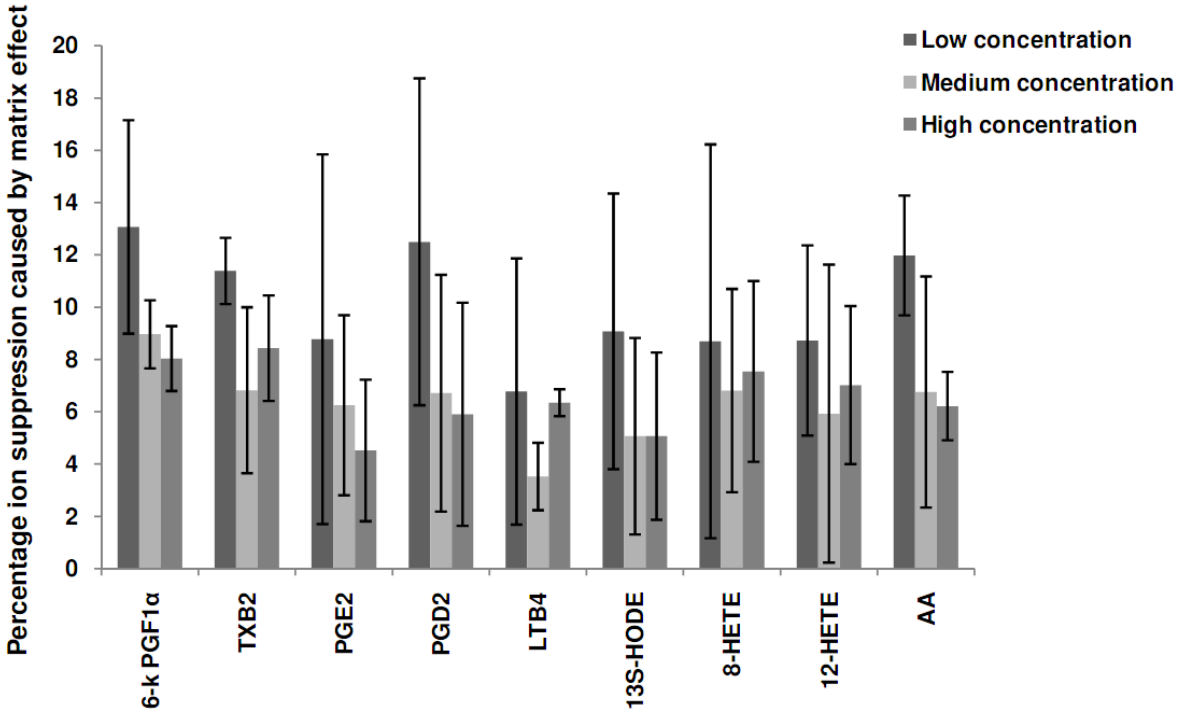

Table 6.3. Linearity, LOD and LOQ of eicosanoids and AA

Metabolite	**Calibration range**[a]	**Average r^2 (n=3)**	**LOD**[a]	**LOQ**[a]
6-k $PGF_{1\alpha}$	10-5000	0.9998	1.52	4.61
TXB_2	10-5000	0.9996	2.73	8.29
PGE_2	10-5000	0.9998	1.74	5.27
PGD_2	10-5000	0.9999	2.43	7.35
LTB_4	10-5000	0.9997	3.19	9.68
13S-HODE	10-5000	0.9998	2.28	6.91
8-HETE	10-5000	0.9998	1.24	3.75
12-HETE	10-5000	0.9997	2.59	7.84
	Calibration range[b]	**Average r^2 (n=3)**	**LOD**[b]	**LOQ**[b]
AA	5-500	0.9910	1.24	3.75

[a] pg/mg of colon tissue; [b] ng/mg of colon tissue

Table 6.4. Validation of assay precision and autosampler stability of metabolites

Metabolite	Intra-day precision (% RSD)			Inter-day precision (% RSD)			Auto-sampler stability[c]
	4000[a] (n=9)	**300[a] (n=9)**	**30[a] (n=9)**	**4000[a] (n=9)**	**300[a] (n=9)**	**30[a] (n=9)**	**(%) (n=6)**
6-k $PGF_{1\alpha}$	2.69	4.80	6.22	4.36	5.54	7.21	96.44±3.77
TXB_2	1.89	2.07	5.74	4.41	4.48	5.54	91.77±6.09
PGE_2	3.07	1.99	4.57	2.84	6.46	7.28	94.34±3.67
PGD_2	3.34	3.04	5.83	3.80	6.25	9.79	97.34±1.65
LTB_4	0.63	2.85	2.72	5.31	5.63	4.99	95.32±3.98
13S-HODE	1.45	3.65	5.41	3.17	3.84	8.07	98.86±6.55
8-HETE	3.03	3.28	2.39	6.69	5.29	7.49	89.89±3.92
12-HETE	6.04	2.42	4.05	5.81	3.47	8.46	90.57±2.41
	300[b] (n=9)	**40[b] (n=9)**	**15[b] (n=9)**	**300[b] (n=9)**	**40[b] (n=9)**	**15[b] (n=9)**	
AA	2.55	3.67	7.02	3.41	3.76	8.00	87.42±0.82

[a] pg/mg of colon tissue; [b] ng/mg of colon tissue;
[c] Values are expressed as mean % stability ± SD

Table 6.5. Extraction efficiency of eicosanoids and AA

Metabolite	Extraction efficiency (%)[a]		
	30[b] (n=3)	**300[b] (n=3)**	**4000[b] (n=3)**
6-k $PGF_{1\alpha}$	79.74±6.30	83.85±1.77	86.55±1.58
TXB_2	82.28±4.56	85.53±4.82	85.44±3.33
PGE_2	78.30±3.12	79.02±2.65	81.37±1.58
PGD_2	79.17±9.55	80.70±4.15	83.71±1.84
LTB_4	78.78±5.09	85.12±1.53	85.73±1.51
13S-HODE	75.98±5.27	81.54±3.55	86.62±3.27
8-HETE	81.16±6.64	85.13±2.54	86.09±2.21
12-HETE	79.37±4.96	82.63±4.95	85.84±4.26
	15[c] (n=3)	**40[c] (n=3)**	**300[c] (n=3)**
AA	79.65±7.52	79.87±4.63	83.63±3.65

[a] Values are expressed as mean ± SD; [b] pg/mg of colon tissue; [c] ng/mg of colon tissue

6.4. Conclusion

An UPLC/MS/MS-based analytical platform was developed and validated successfully (in terms of selectivity, sensitivity, matrix effect, precision, accuracy, extraction efficiency, linear response and sample stability) for the simultaneous profiling of AA and 8 eicosanoids in human colon tissue. Our rapid profiling method has the potential to be applied in clinical trials to determine the effect of NSAIDs on the endogenous levels of eicosanoids so as to better elucidate the mechanism and value of NSAID-based adjuvant therapy in improving the prognosis of human CRC.

CHAPTER 7

TARGETED PROFILING OF EICOSANOIDS AND ARACHIDONIC ACID IN COLORECTAL CANCER USING UPLC/MS/MS

7.1. Introduction

Cumulative evidences indicate an association between inflammation and CRC. IBD is an important risk factor for the development of CRC. Inflammation is also likely to be involved with other forms of sporadic as well as heritable CRC (Coussens and Werb, 2002; Mantovani et al., 2008; Kraus and Arber, 2009; Terzic et al., 2010). The link between CRC and inflammation is further reinforced by the preventive effect of NSAIDs in the development of CRC. NSAIDs exert their pharmacological effect primarily by inhibiting COX enzyme (Chan et al., 2005; Smalley and DuBois, 1997). The expression of COX-2 and LOX enzymes which are involved in the biosynthesis of eicosanoids gets perturbed in CRC. As a consequence fluctuations in the endogenous levels of these eicosanoids are expected which in turn play a prominent role in inflammation mediated development of CRC (Kashfi and Rigas, 2005; Melstrom et al., 2008; Sano et al., 1995; Soslow et al., 2000; Soumaoro et al., 2006; Steele et al., 1999; Wang and Dubois, 2008, 2010). The pathways of AA metabolism are shown in Figure 7.1. Therefore, the targeted and simultaneous profiling of biologically relevant eicosanoids viz. PGE_2, PGI_2 [assayed as its stable hydrolytic product 6-k-$PGF_{1\alpha}$ (Brash et al., 2007)], PGD_2, LTB_4, TXA_2 [assayed as its stable breakdown product TXB_2 (Needleman et al., 1976)], 13S-HODE, 12-HETE, 8-HETE and their major

metabolic precursor AA, could shed molecular insight into the role of inflammation in CRC carcinogenesis and progression.

In this chapter the targeted profiling of endogenous AA and eicosanoids in matched pairs of CRC and normal tissues obtained from 36 CRC patients is described. For this purpose, the UPLC/MS/MS method that we developed and validated as described in Chapter 6 was utilized.

7.2. Experimental

7.2.1. Clinical population and tissue samples

Because of ethical reasons, the amount of tissue that can be removed from patients while performing colonoscopy or surgery is limited. The first cohort of tissue samples obtained was fully utilized for non-targeted metabolic profiling study and this necessitated the use of a second cohort for our targeted profiling study. Clinical data such as age, gender, ethnicity, location of primary tumor, histological staging and grade were obtained from a prospectively maintained computerized database from the Singapore Polyposis Registry & the Colorectal Cancer Research Laboratory, Department of Colorectal Surgery, SGH. The anatomical and clinicopathological characteristics of the clinical tissue samples analyzed by UPLC/MS/MS are summarized in Table 7.1. The study population comprised 36 patients with a mean age of 59 ± 19 years at the time of cancer diagnosis. There were 20 males (56%) and 16 females (44%). The majority (80.5%) of the patients were Chinese (n = 29), while the remaining comprised 5 Malays (C10, C21, C31,

C33, C34), 1 Indian (C11) and 1 of other ethnicity (C5). There were 28 left-sided tumors (defined as those arising distal to the splenic flexure) of which 19 were in the rectosigmoid or rectum. This study was approved by the CIRB at the SGH (CIRB reference number 2009/723/B). Matched CRC and normal tissues (n = 72) were obtained from the 36 CRC patients during surgery. Fresh tumor tissue and normal tissue were snap-frozen immediately following excision of the specimen at surgery, then stored at -80 °C until processing. Resection of tissue samples were carried out by trained personnel at Singapore General Hospital. Tumor specimens were carefully micro-dissected to ensure that at least 90% of the analyzed tissue contained cancer cells. Matched normal tissues were taken at least 5-10 cm away from the edges of the tumor. All CRC tissues and matched normal tissues were cut and weighed accurately where approximately 10 mg of each tissue were reserved for UPLC/MS/MS analysis. The samples were kept at -80 °C until analysis.

7.2.2. UPLC/MS/MS analysis

Tissue samples for UPLC/MS/MS analysis were prepared as per the procedure described in section 6.2.3. of chapter 6. The protein content of each tissue sample was determined as per the method described in section 6.2.4. of Chapter 6. The same UPLC/MS/MS conditions as mentioned in section 6.2.5. of Chapter 6 were used for analysis.

7.2.3. UPLC/MS/MS data analysis

The amount of individual eicosanoids and AA in tissue samples as determined by UPLC/MS/MS were normalized with respect to total protein content. The normalized data were subjected to paired samples 't' test using SPSS software (Version 11.0, SPSS Inc., Chicago, IL, USA) to identify metabolites significantly different between the CRC and normal tissue groups ($p < 0.05$ was considered to be statistically significant). In order to verify any probable association between the endogenous levels of metabolites and Dukes stage of CRC or anatomical site of tumor, Spearman's correlation analysis was also carried out using the SPSS software.

7.3. Results and discussion

The endogenous levels of AA and 8 eicosanoids in 36 matched pairs of CRC and normal colon tissues are shown in Figure 7.2. and summarized in Table 7.2. The levels of these inflammatory mediators in CRC and normal tissues were compared statistically using paired samples 't' test. Among the metabolites, 6-k $PGF_{1\alpha}$, PGE_2, 12-HETE, 13S-HODE and AA were found to be significantly different between CRC and normal colon tissues ($p<0.05$). These inflammatory metabolic markers are therefore important in characterizing the phenotype of human CRC. However, it was noted that no significant correlation was found between the levels of the profiled inflammatory mediators and the Duke's stage of CRC or anatomical site of tumor.

Figure 7.1. Pathways for Arachidonic acid metabolism.
COX: cyclooxygenase; LOX: lipoxygenase; AA: arachidonic acid; PG: prostaglandin; PGI_2: prostacyclin; 6-k$PGF_{1\alpha}$: 6-keto-prostaglandin$_{1\alpha}$; HETE: hydroxy-eicosatetraenoic acid; EET: epoxy-eicosatrienoic acid; DiHETE: dihydroxy-eicosatetraenoic acid; 13S-HODE: 13*S*-hydroxy-9*Z*,11*E*-octadecadienoic acid; LTB_4: leukotriene B_4, TX: thromboxane.

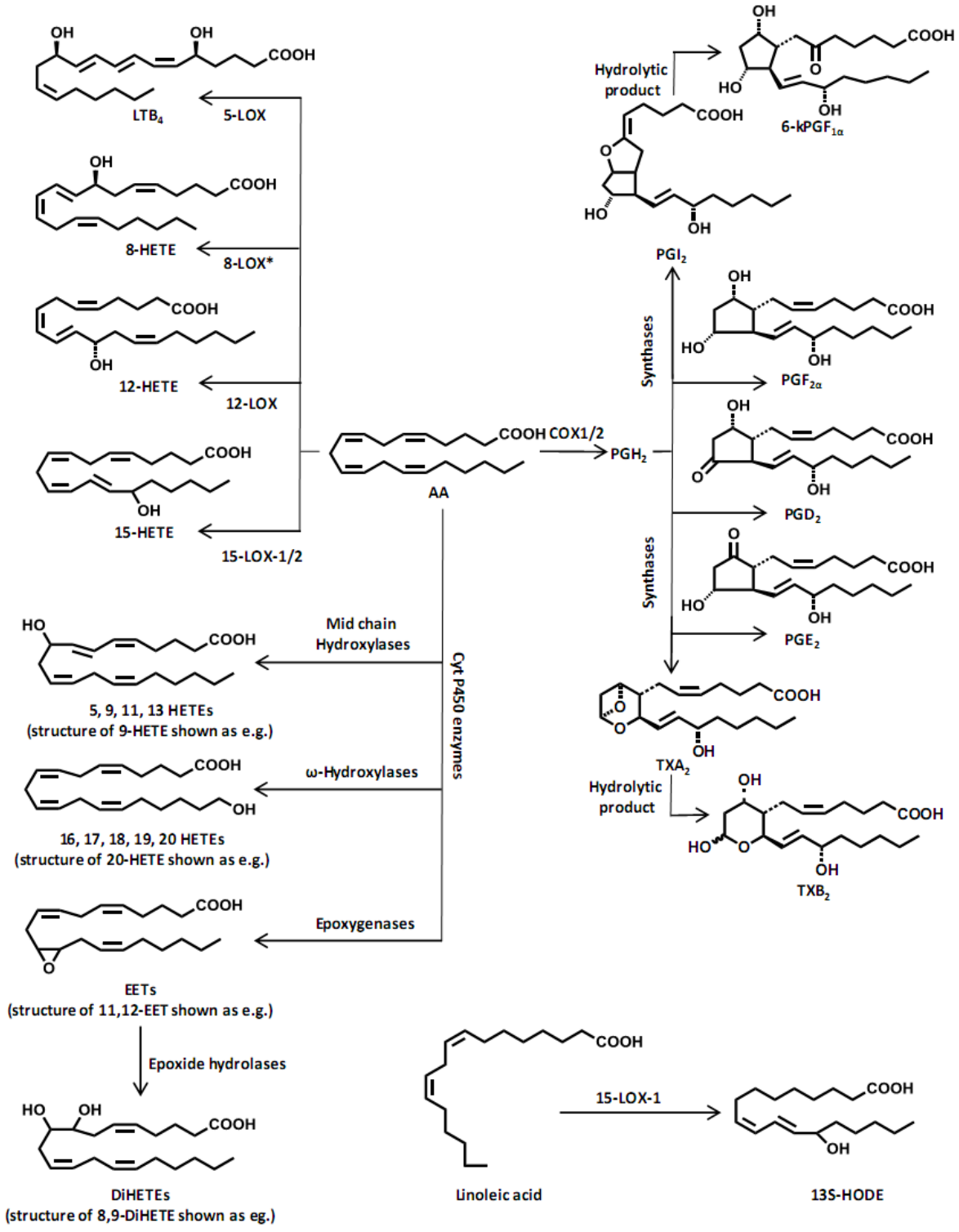

Table 7.1. Summary of clinicopathological characteristics of CRC patients

Normal[a]	CRC[a]	CRC anatomical site	Histology	Grade[b]	TNM stage	Duke stage
N1	C1	Sigmoid	Adenocarcinoma	MD	T2N2M0	C
N2	C2	Sigmoid	Adenocarcinoma	MD	T3N2M0	C
N3	C3	Hepatic flexure	Adenocarcinoma	PD	T3N2M0	C
N4	C4	Rectosigmoid	Adenocarcinoma	MD	T3N0M0	B
N5	C5	Rectum	Adenocarcinoma	MD	T2N0M0	A
N6	C6	Rectum	Adenocarcinoma	MD	T3N1M0	C
N7	C7	Ascending colon	Adenocarcinoma	MD	T3N0M0	B
N8	C8	Rectum	Adenocarcinoma	MD	T3N0M0	B
N9	C9	Rectosigmoid	Adenocarcinoma	WD	T3N0M0	B
N10	C10	Ascending colon	Mucinous	M	T2N1M0	C
N11	C11	Rectum	Mucinous	M	T4N1M0	C
N12	C12	Rectum	Adenocarcinoma	PD	T3N1M0	C
N13	C13	Rectum	Adenocarcinoma	MD	T3N0M0	B
N14	C14	Sigmoid	Adenocarcinoma	MD	T3N0M0	B
N15	C15	Rectum	Adenocarcinoma	MD	T3N0M0	B
N16	C16	Caecum	Adenocarcinoma	MD	T3N0M0	B
N17	C17	Rectum	Adenocarcinoma	MD	T3N0M0	B
N18	C18	Sigmoid	Adenocarcinoma	MD	T4N0M0	B
N19	C19	Caecum	Adenocarcinoma	WD	T3N1M0	C
N20	C20	Rectum	Adenocarcinoma	MD	T3N2M0	C
N21	C21	Hepatic flexure	Adenocarcinoma	MD	T3N1M0	C
N22	C22	Caecum	Adenocarcinoma	MD	T3N0M0	B
N23	C23	Rectum	Adenocarcinoma	MD	T2N0M0	A
N24	C24	Sigmoid	Adenocarcinoma	MD	T2N1M0	C
N25	C25	Sigmoid	Adenocarcinoma	PD	T2N1M0	C
N26	C26	Rectum	Adenocarcinoma	PD	T3N0M0	B
N27	C27	Rectum	Adenocarcinoma	MD	T3N0M0	B
N28	C28	Sigmoid	Adenocarcinoma	MD	T3N0M0	B
N29	C29	Rectosigmoid	Adenocarcinoma	WD	T2N0M0	A
N30[c]	C30[c]	-	Adenocarcinoma	MD	-	-
N31	C31	Sigmoid	Adenocarcinoma	MD	T4N2M0	C
N32	C32	Rectosigmoid	Adenocarcinoma	MD	T4N2M0	C
N33	C33	Rectum	Adenocarcinoma	MD	T3N0M0	C
N34	C34	Sigmoid	Adenocarcinoma	MD	T3N1M0	B
N35	C35	Rectosigmoid	Adenocarcinoma	MD	T3N0M0	B
N36	C36	Ascending colon	Adenocarcinoma	MD	T3N0M0	B

[a] For each C (CRC) sample, matched N (normal) tissue was provided.
[b] MD, WD, PD and M are moderately differentiated, well-differentiated, poorly differentiated and mucinous, respectively.
[c] 5 lesions were removed from multiple site, stage not determined

6-k $PGF_{1\alpha}$, a stable non-enzymatic hydrolytic product of unstable PGI_2, was found to be higher in normal colon as compared to CRC colon tissue. This finding corroborated with the previous results published by Rigas et al. (1993). PGI_2 showed cytoprotective activity on gastric mucosal surfaces and was determined to be important for maintaining normal vasculature (Wang and Dubois, 2008). PGI_2 and its stable synthetic analogues such as Cicaprost were shown to prevent lung and liver metastases in murine models of prostate (Schirner and Schneider, 1992), ovarian (Schirner and Schneider, 1991), mammary (Schirner et al., 1994; Schirner and Schneider, 1992), skin (Costantini et al., 1988) and lung (Lapis et al., 1990; Sava et al., 1989) carcinomas. In addition, these compounds demonstrated inhibitory effect on the growth of established micrometastases after the removal of primary mammary tumors in rats (Schirner and Schneider, 1997). Mechanistic studies have further revealed that PGI_2 and its analogues exhibited both direct and indirect antimetastatic effects by interfering with tumor cell-host interactions and potentiating host immune competency (Schirner et al., 1998). Recently it has been shown that platelets play an important role in metastasis and the antimetastatic effect of PGI_2 could be partially attributed to its inherent antiplatelet property (Gay and Felding-Habermann, 2011).

In this study, a significantly higher content of PGE_2 was found in CRC compared to normal colon tissue. This finding was consistent with the results of previous studies (Bennett et al., 1987; Rigas et al., 1993). The role of PGE_2 is quite dominant in the promotion CRC growth. The COX-2/PGE synthase-dependent

Figure 7.2. Endogenous levels of eicosanoids and AA in 36 pairs of CRC and normal tissues

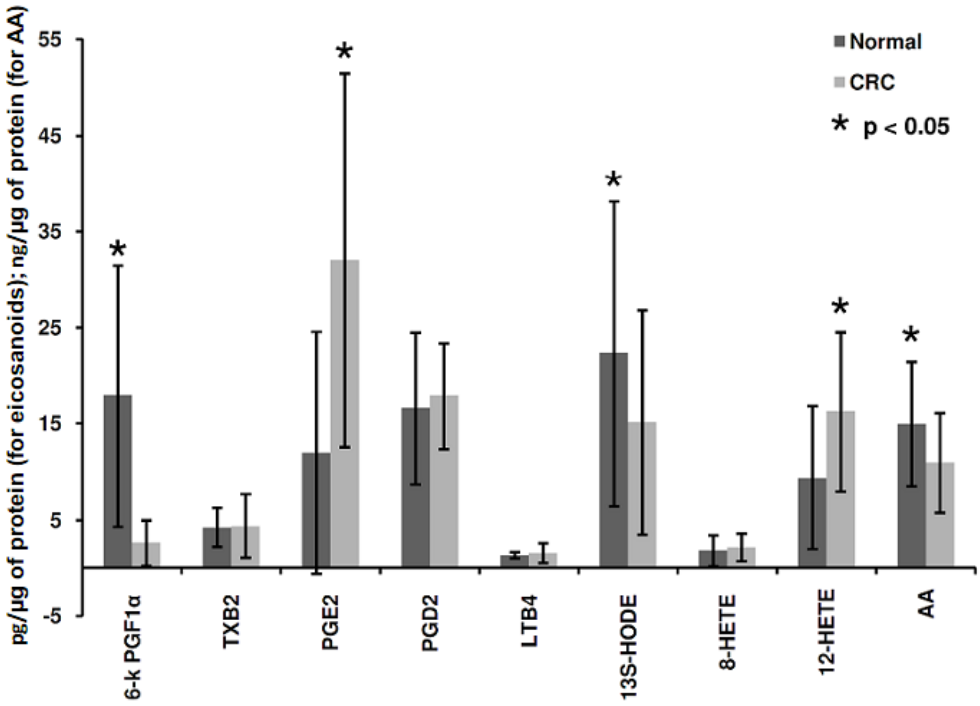

Table 7.2. Endogenous levels of eicosanoids and AA in 36 pairs of CRC and normal tissues

Metabolite	Normal[a] (pg/µg of protein)	CRC (pg/µg of protein)	p value[b]	% fold change of CRC from normal[c]
6-k $PGF_{1\alpha}$	17.91±13.56	2.59±2.41	<0.00001	-590.8
TXB_2	4.23±2.08	4.38±3.34	0.798	3.3
PGE_2	11.98±12.60	32.01±19.46	0.00001	62.6
PGD_2	16.62±7.89	17.86±5.52	0.489	7.0
LTB_4	1.27±0.32	1.51±1.02	0.221	15.5
13S-HODE	22.30±15.84	15.11±11.71	0.040	-47.5
8-HETE	1.74±1.59	2.09±1.42	0.357	16.8
12-HETE	9.36±7.43	16.27±8.28	0.00007	42.5
	Normal[a] (ng/µg of protein)	**CRC (ng/µg of protein)**	**p value[b]**	**% fold change of CRC from normal[c]**
AA	14.93±6.41	10.92±5.13	0.001	-36.7

[a] Values are expressed as mean±SD

[b] Statistical p value calculated using paired samples 't' test (significance at $p<0.05$)

[c] Positive and negative percentages indicate higher levels of analytes in CRC and normal tissues, respectively.

biosynthesis of PGE_2 and 15-hydroxyprostaglandin dehydrogenase (15-PGDH)-dependent degradation of PGE_2, determine its steady-state cellular levels. The expression of 15-PGDH was found to be reduced in CRC (Backlund et al., 2005; Yan et al., 2004) whereas the levels of COX-2 and PGE synthase were elevated (Yoshimatsu et al., 2001). The fluctuations of these enzymes resulted subsequently in the elevated levels of PGE_2 in CRC tissue which in turn contributed to CRC development by promoting angiogenesis (Tsujii et al., 1998), metastasis (Tsujii et al., 1997), immunosuppression (Kojima et al., 2001), proliferation (Sheng et al., 2001) and inhibiting apoptosis (Sheng et al., 1998). These effects exerted by PGE_2 are mediated through the activation of various signaling pathways. PGE_2 causes up-regulation of β-catenin transcriptional activity and phosphorylation of the EGF receptor resulting in activation of oncogenic phosphatidyl-inositol-3-kinase (PI3K), serine/threonine protein kinase (Akt) and rat sarcoma viral oncogene-mitogen activated protein kinase (RAS-MAPK) cascade (Pai et al., 2002). PGE_2 also activates the peroxisome proliferator activated receptor-δ (PPARδ) via stimulation of PI3K and stimulates expression of the angiogenic factor VEGF, the proliferation promoting factor cyclin D1 and the anti-apoptotic factor bcl-2 (Wang and Dubois, 2008, 2010). PGE_2 causes activation of Tcf-4 transcription factors via stabilization of β-catenin in CRC cells and consequently also activates the Wnt signaling pathway (Castellone et al., 2005). Moreover several downstream pathways of PGE_2 may act as a positive feedback loop and cause further upregulation of COX-2 expression (Chan and Giovannucci, 2010).

Our study further demonstrated that the endogenous levels of 12-HETE was significantly higher in CRC as compared to normal colon tissue. Evidences from *in vitro* studies indicated that 12-HETE enhanced adhesion, migration and metastasis of cancer cells (Chopra et al., 1991; Honn et al., 1992; Liu et al., 1995; Nie et al., 1998). Moreover *in vivo* studies have shown that 12-HETE plays an important role in carcinogenesis in murine skin tumor (Krieg et al., 1995) and human prostate cancer (Shureiqi and Lippman, 2001).

13S-HODE was found to be significantly higher in normal tissues as compared to CRC samples. This observation is corroborated by other studies (Shureiqi et al., 1999, 2010). *In vitro* studies in CRC cell lines have shown that 13S-HODE exerts an antitumorigenic effect by promoting apoptosis and causing cell cycle arrest (Shureiqi and Lippman, 2001). Moreover linoleic acid which acts as the metabolic precursor of 13S-HODE has been shown to have an inhibitory effect in murine model of skin cancer (Fischer et al., 1996). Interestingly, various *in vitro* studies have shown that the tumor promoting effects of 12-HETE, are counteracted by 13S-HODE as well as PGI_2 and its analogues (Grossi et al., 1989; Honn et al., 1992; Liu et al., 1991; Tang et al., 1993). These observations suggested that stable PGI_2 analogues and LOX modulators could also be investigated as potential chemotherapeutic agents in CRC.

Finally, we observed that the level of AA was significantly decreased in CRC colon tissue. This observation was consistent with our earlier findings where CRC was profiled using GC×GC/TOFMS- and GC/MS-based metabolic profiling platforms (Chan et al., 2009). The depleted levels of AA in CRC tissue could be attributed to the overexpression of COX-2 enzyme which

catalyzes the conversion of AA to eicosanoids (Kashfi and Rigas, 2005; Sano et al., 1995; Soslow et al., 2000).

7.4. Conclusion

Targeted profiling of eicosanoids and AA in 36 matched pairs of CRC and normal tissues were carried out using UPLC/MS/MS. The results indicated significantly higher levels of AA and antitumorigenic eicosanoids such as PGI_2 (assayed as its stable product 6-k $PGF_{1\alpha}$) and 13S-HODE in normal tissues whereas pro-tumorigenic eicosanoids such as PGE_2 and 12-HETE were found to be higher in CRC tissue specimens. However no significant association was observed between the endogenous levels of the profiled metabolites with CRC stage or anatomical site of tumor. The findings implied definite deregulation of eicosanoid biosynthetic pathways and suggested that a complicated interplay between eicosanoids is involved in inflammation mediated CRC development.

CHAPTER 8

CONCLUSION AND FUTURE DIRECTIONS

8.1. Conclusion

In my PhD project, both non-targeted metabolic profiling and targeted metabolic profiling of eicosanoids and AA in CRC using biopsied tissue specimens obtained from CRC patients were carried out. For global non-targeted metabolic profiling of CRC, three different analytical platforms namely GC/MS, HR-MAS NMR spectroscopy and GC×GC/TOFMS were explored. Prior to its application for non-targeted profiling the GC/MS method was developed and validated successfully in terms of sample stability, reproducibility, selectivity, linear response and sensitivity. HR-MAS NMR spectroscopic analysis including sample pretreatment was carried out at the Imperial College London, UK, as per the validated protocol which has been published recently (Beckonert et al., 2010). For validation of analytical performance of GC×GC/TOFMS an alternative approach involving QC samples and multivariate statistical analyses was used successfully. Although GC×GC/TOFMS proved to be better than GC/MS and HR-MAS NMR spectroscopy with respect to the extent of metabolic space coverage, HR-MAS NMR spectroscopy proved to be more advantageous in terms of sample preparation and total analysis time. The data generated by the three analytical platforms in conjunction with chemometric analysis led to the identification of marker metabolites belonging to diverse chemical classes such as monosaccharides, amino acids, triterpenes, amino ketones, steroids, organic

acids, fatty acids, fatty acid esters, polyols, polyol derivatives, pyrimidine derivatives, pyrimidine nucleosides, acyl phosphates, lipids and choline containing compounds. Although the OPLS-DA models generated on the basis of profiled data using the three analytical platforms were capable of discriminating normal tissues from malignant ones, no valid OPLS-DA model was obtained using CRC stage as classifier. This implied that the metabolic phenotype associated with CRC, although distinct from that of normal tissue, is not sensitive enough to discriminate the different stages of CRC. Of the three analytical methods used, only HR-MAS NMR spectroscopy-based metabolic profiling was able to produce a valid OPLS-DA model capable of discriminating anatomical site of tumor. This finding is interesting as the hazard of recurrence and metastasis in rectal cancer is 1.5 times that in colon cancer (Li et al., 2007). Thus, our results suggested that CRC harbors distinct metabolic signatures according to the anatomical location of tumor which may be exploited in future to better understand the distinction between colon and rectal cancers. The identified marker metabolites when linked to metabolic pathways using KEGG database revealed perturbations of biochemical processes such as glycolysis, TCA cycle, amino acid metabolism, fatty acid biosynthesis, steroid biosynthesis, eicosanoid biosynthesis, bile acid biosynthesis, nucleotide metabolism and osmoregulation. Majority of these observations can be attributed to the high energy demand, tissue hypoxia and altered synthetic rate of cellular components of rapidly proliferating tumor cells. Moreover our non-targeted metabolic profiling study using GCxGC/TOFMS suggested the branching of serine biosynthetic pathway from glycolysis and its upregulation, the end product of which is glycine. Recent

studies suggest that the enzyme phosphoglycerate dehydrogenase (PHGDH) which oxidizes the glycolytic intermediate 3-phosphoglycerate to initiate serine biosynthesis, is over-expressed in breast cancer and helps cancer cells to proliferate rapidly (Locasale, et al., 2011; Possemato et al., 2011). This further implies that the suppression of PHGDH could be a new therapeutic target. Our findings using human CRC tissue samples, were actually made before the findings by Locasale et al. and Possemato et al. and suggested that there is also a possible existence of this particular form of metabolic deregulation in human CRC. In addition to this, altered eicosanoid biosynthetic pathway as indicated by reduced AA levels in CRC tissues and presence of comparatively higher levels of picolinic acid in CRC tissues, implied an association of inflammatory environment with CRC development.

The strong evidence of association between inflammation and CRC and the significant role played by eicosanoids in it, as well as the altered expression of COX-2 and LOX enzymes involved in eicosanoid biosynthesis in CRC, formed our objective to carry out targeted metabolic profiling of 8 biologically relevant eicosanoids and the major metabolic precursor AA to record the fluctuations of these inflammatory metabolites and to understand their implicated roles in inflammation mediated CRC carcinogenesis better. For this purpose an UPLC/MS/MS-based method was developed and validated successfully (in terms of selectivity, sensitivity, precision, accuracy, extraction efficiency, linear response and sample stability) for the simultaneous profiling of AA and 8 eicosanoids in human colorectal tissue. Targeted profiling of eicosanoids and AA in 36 matched pairs of CRC and normal tissues revealed significantly higher levels of 6-k $PGF_{1\alpha}$ (stable hydrolytic product of unstable

PGI_2), 13S-HODE and AA in normal tissues whereas PGE_2 and 12-HETE were found to be higher in CRC tissue specimens. However, no significant correlation was obtained between the endogenous levels of the profiled metabolites with CRC stage or anatomical site of tumor. Both non-targeted profiling of CRC using GC×GC/TOFMS and GC/MS and targeted profiling showed diminished levels of AA in CRC tissues which could be attributed to the overexpression of COX-2 enzyme in CRC. These findings suggested deregulation of eicosanoid biosynthetic pathways and suggested that a complex interaction between pro-tumorigenic eicosanoids such as PGE_2 and 12-HETE and antitumorigenic eicosanoids such as PGI_2 and 13S-HODE is intimately involved in inflammation-associated CRC carcinogenesis.

8.2. Future directions

As one of our aims was to elucidate the metabolic phenotype associated with CRC and to verify its potential to be utilized for staging and prognosis of CRC, we used biopsied tissue specimens for our non-targeted metabolic profiling experiments. This is due to the fact that tissue provides site specific information and is less susceptible to variation as compared to serum, urine or faeces. During the progress of our project, concurrent studies were conducted by other research groups which involved non- targeted metabolic profiling of CRC using other biomatrices like serum (Ma et al., 2010; Ludwig et al., 2009; Qiu et al., 2009), urine (Qiu et al., 2010; Wang et al., 2010) and faecal water extracts (Monleón et al., 2009). Such findings have opened the way for utilizing non-targeted metabolic profiling as a minimally invasive or non-

invasive diagnostic tool for CRC. However, large scale clinical studies are required in the future to establish and validate such metabolic profiling-based diagnostic methods as suitable alternatives to existing diagnostic methods of CRC. With the development of LC/NMR/MS hybrid techniques (Lindon et al., 2000, 2004), it will be interesting to explore such analytical platforms for non-targeted metabolic profiling of CRC in the future so as to expand the metabolic space covered currently by the existing methods. Other biomatrices such as saliva and dried blood spot can also be investigated for non-targeted metabolic profiling of CRC. Proteomic study of exosomes from CRC ascites (Choi et al., 2011) has paved the way for future metabolic profiling studies of such exosomes. In our non-targeted metabolic profiling study we found metabolic perturbations related to lipid metabolism which also warrants lipidomic study of CRC in future to gain additional insight.

The results obtained from our targeted profiling of eicosanoids supported the concept of using aspirin and other NSAIDs as preventive agents or adjuvant therapeutic agents as they act primarily by inhibiting COX enzyme. However, verification of the mechanistic aspect of NSAID-based therapy in CRC requires large scale clinical trials to be conducted in future. In fact an international, multi-centre, double-blind randomized phase III clinical trial (ASCOLT, http://indox.org.uk/research/clinical/ascolt) that utilizes Aspirin as an adjuvant treatment for CRC is currently being conducted by our collaborators at SGH, Singapore. Our rapid UPLC/MS/MS profiling method has the potential to be applied in such clinical trials to determine the effect of aspirin or other NSAIDs on the endogenous levels of eicosanoids so as to better elucidate the mechanism and value of NSAID-based adjuvant therapy in

improving the prognosis of human CRC. Our targeted profiling results also implied that PGI_2 analogs and LOX modulators can also be explored in the future as potential chemotherapeutic agents in CRC. Future studies can also be carried out to elucidate the possible association of antiplatelet property of PGI_2 with its antimetastatic function (Gay and Felding-Habermann, 2011). Moreover, targeted metabolic profiling of other key metabolic pathways like components of amino acid, fatty acid, carbohydrate or nucleotide metabolism that get altered in CRC can be carried out in future so as to better elucidate the molecular mechanisms involved in CRC development and to identify potential metabolite-based biomarkers of disease progression or targets for therapeutic intervention.

REFERENCES

Adahchour M, Beens J, Brinkman UA. 2008. Recent developments in the application of comprehensive two-dimensional gas chromatography. J Chromatogr A 1186(1-2):67-108.

Astler VA, Coller FA. 1954. The prognostic significance of direct extension of carcinoma of the colon and rectum. Ann Surg 139:846-852.

Atherton HJ, Bailey NJ, Zhang W, Taylor J, Major H, Shockcor J, Clarke K, Griffin JL. 2006. A combined 1H-NMR spectroscopy- and mass spectrometry-based metabolomic study of the PPAR-alpha null mutant mouse defines profound systemic changes in metabolism linked to the metabolic syndrome. Physiol Genomics 27:178-186.

Backlund MG, Mann JR, Holla VR, Buchanan FG, Tai HH, Musiek ES, Milne GL, Katkuri S, DuBois RN. 2005. 15-Hydroxyprostaglandin dehydrogenase is down-regulated in colorectal cancer. J Biol Chem 280(5):3217-3223.

Backshall A, Allferez D, Telchert F, Wilson ID, Wilkinson RW, Goodlad RA, Keun HC. 2009. Detection of metabolic alterations in non-tumor gastrointestinal tissue of the Apc (Min/+) mouse by H-1 MAS NMR spectroscopy. J Proteome Res 8(3):1423-1430.

Baker H, Frank O, Chen T, Feingold S, DeAngelis B, Baker ER. 1981. Elevated vitamin levels in colon adenocarcinoma as compared with metastatic liver adenocarcinoma from colon primary and normal adjacent tissue. Cancer 47(12):2883-2886.

Ballinger AB, Anggiansah C. 2007. Colorectal cancer. BMJ 335(7622):715-718.

Bansal S, DeStefano A. 2007. Key elements of bioanalytical method validation for small molecules. The AAPS Journal 9(1) article 11.

Bao Y, Zhao T, Wang X, Qiu Y, Su M, Jia W. 2009. Metabonomic variations in the drug-treated type 2 diabetes mellitus patients and healthy volunteers. J Proteome Res 8(4):1623-1630.

Barbas C, Adeva N, Aguilar R, Rosillo M, Rubio T, Castro M. 1998. Quantitative determination of short-chain organic acids in urine by capillary electrophoresis. Clin Chem 44(6 Pt 1):1340-1342.

Barbas C, Moraes EP, Villasenor A. 2011. Capillary electrophoresis as a metabolomics tool for non-targeted fingerprinting of biological samples. J Pharm Biomed Anal 55(4):823-831.

Barton SJ, Howe FA, Tomlins AM, Cudlip SA, Nicholson JK, Bell BA, Griffiths JR. 1999. Comparison of in vivo 1H MRS of human brain tumours with 1H HR-MAS spectroscopy of intact biopsy samples in vitro. MAGMA 8(2):121-128.

Beckonert O, Coen M, Keun HC, Wang Y, Ebbels TM, Holmes E, Lindon JC, Nicholson JK. 2010. High-resolution magic-angle-spinning NMR spectroscopy for metabolic profiling of intact tissues. Nat Protoc 5(6):1019-1032.

Beens J, Adahchour M, Vreuls RJ, van Altena K, Brinkman UA. 2001. Simple, non-moving modulation interface for comprehensive two-dimensional gas chromatography. J Chromatogr A 919:127-132.

Bennett A, Civier A, Hensby CN, Melhuish PB, Stamford IF. 1987. Measurement of arachidonate and its metabolites extracted from human normal and malignant gastrointestinal tissues. Gut 28(3):315-318.

Bi X, Lin Q, Foo TW, Joshi S, You T, Shen HM, Ong CN, Cheah PY, Eu KW, Hew CL. 2006. Proteomic analysis of colorectal cancer reveals alterations in metabolic pathways: mechanism of tumorigenesis. Mol Cell Proteomics 5(6):1119-1130.

Bolcato CA, Frye RF, Zemaitis MA, Poloyac SM. 2003. Determination of 20-hydroxyeicosatetraenoic acid in microsomal incubates using high-performance liquid chromatography-mass spectrometry (HPLC-MS). J Chromatogr B Analyt Technol Biomed Life Sci 794(2):363-372.

Bollard ME, Garrod S, Holmes E, Lindon JC, Humpfer E, Spraul M, Nicholson JK. 2000. High-resolution (1)H and (1)H-(13)C magic angle spinning NMR spectroscopy of rat liver. Magn Reson Med 44(2):201-207.

Bollard ME, Murray AJ, Clarke K, Nicholson JK, Griffin JL. 2003. A study of metabolic compartmentation in the rat heart and cardiac mitochondria using high-resolution magic angle spinning 1H NMR spectroscopy. FEBS Lett 553(1-2):73-78.

Bollard ME, Xu J, Purcell W, Griffin JL, Quirk C, Holmes E, Nicholson JK. 2002. Metabolic profiling of the effects of D-galactosamine in liver spheroids using (1)H NMR and MAS-NMR spectroscopy. Chem Res Toxicol 15(11):1351-1359.

Bosco MC, Rapisarda A, Massazza S, Melillo G, Young H, Varesio L. 2000. The tryptophan catabolite picolinic acid selectively induces the chemokines macrophage inflammatory protein-1 alpha and -1 beta in macrophages. J Immunol 164(6):3283-3291.

Bottcher C, Roepenack-Lahaye EV, Willscher E, Scheel D, Clemens S. 2007. Evaluation of matrix effects in metabolite profiling based on capillary liquid chromatography electrospray ionization quadrupole time-of-flight mass spectrometry. Anal Chem 79(4):1507-1513.

Boudonck KJ, Mitchell MW, Nemet L, Keresztes L, Nyska A, Shinar D, Rosenstock M. 2009. Discovery of metabolomics biomarkers for early detection of nephrotoxicity. Toxicol Pathol 37(3):280-292.

Brash AR, Jackson EK, Saggese CA. 1983. Metabolic disposition of prostacyclin in humans. J Pharmacol Exp Ther. 226, 78-87.

Brenner DE, Rennert G. 2005. Fecal DNA biomarkers for the detection of colorectal neoplasia: attractive, but is it feasible? J Natl Cancer Inst 97(15):1107-1109.

Broadhurst D, Kell DB. 2006. Statistical strategies for avoiding false discoveries in metabolomics and related experiments. Metabolomics 2, 171-196.

Burg MB, Ferraris JD. 2008. Intracellular organic osmolytes: function and regulation. J Biol Chem 283(12):7309-7313.

Buyse M, Piedbois Y, Piedbois P, Gray R. 2000a. Tumour site, sex, and survival in colorectal cancer. Lancet 356(9232):858.

Buyse M, Thirion P, Carlson RW, Burzykowski T, Molenberghs G, Piedbois P. 2000b. Relation between tumour response to first-line chemotherapy

and survival in advanced colorectal cancer: a meta-analysis. Meta-Analysis Group in Cancer. Lancet 356(9227):373-378.

Bylesjö M, Rantalainen M, Cloarec O, Nicholson JK, Holmes E, Trygg J. 2006. OPLS discriminant analysis: combining the strengths of PLS-DA and SIMCA classification. J Chemometrics 20:341-351.

Capdevila J, Chacos N, Werringloer J, Prough RA, Estabrook RW. 1981. Liver microsomal cytochrome P-450 and the oxidative metabolism of arachidonic acid. Proc Natl Acad Sci USA 78(9):5362-5366.

Capdevila J, Wei S, Yan J, Karara A, Jacobson HR, Falck JR, Guengerich FP, DuBois RN. 1992. Cytochrome P-450 arachidonic acid epoxygenase. Regulatory control of the renal epoxygenase by dietary salt loading. J Biol Chem 267(30):21720-21726.

Castellone MD, Teramoto H, Williams BO, Druey KM, Gutkind JS. 2005. Prostaglandin E_2 promotes colon cancer cell growth through a Gs-axin-beta-catenin signaling axis. Science 310(5753):1504-1510.

Catella F, Lawson JA, Fitzgerald DJ, FitzGerald GA. 1990. Endogenous biosynthesis of arachidonic acid epoxides in humans: increased formation in pregnancy-induced hypertension. Proc Natl Acad Sci USA 87(15):5893-5897.

Chan AT, Giovannucci EL. 2010. Primary prevention of colorectal cancer. Gastroenterology 138(6):2029-2043.

Chan AT, Giovannucci EL, Meyerhardt JA, Schernhammer ES, Curhan GC, Fuchs CS. 2005. Long-term use of aspirin and nonsteroidal anti-inflammatory drugs and risk of colorectal cancer. JAMA 294(8):914-923.

Chan EC, Koh PK, Mal M, Cheah PY, Eu KW, Backshall A, Cavill R, Nicholson JK, Keun HC. 2009. Metabolic profiling of human colorectal cancer using high-resolution magic angle spinning nuclear magnetic resonance (HR-MAS NMR) spectroscopy and gas chromatography mass spectrometry (GC/MS). J Proteome Res 8(1):352-361.

Chang KL, New LS, Mal M, Goh CW, Aw CC, Browne ER, Chan EC. 2011. Metabolic profiling of 3-nitropropionic acid early-stage Huntington's disease rat model using gas chromatography time-of-flight mass spectrometry. J Proteome Res 10(4):2079-2087.

Cheah PY. 1990. Hypotheses for the etiology of colorectal cancer-an overview. Nutr Cancer 14(1):5-13.

Chen C, Gonzalez FJ, Idle JR. 2007. LC-MS-based metabolomics in drug metabolism. Drug Metab Rev 39(2-3):581-597.

Chen X, Xu F, Wang Y, Pan Y, Lu D, Wang P, Ying K, Chen E, Zhang W. 2007. A study of the volatile organic compounds exhaled by lung cancer cells in vitro for breath diagnosis. Cancer 110(4):835-844.

Cheng LL, Anthony DC, Comite AR, Black PM, Tzika AA, Gonzalez RG. 2000. Quantification of microheterogeneity in glioblastoma multiforme with ex vivo high-resolution magic-angle spinning (HRMAS) proton magnetic resonance spectroscopy. Neuro Oncol 2(2):87-95.

Cheng LL, Burns MA, Taylor JL, He W, Halpern EF, McDougal WS, Wu CL. 2005. Metabolic characterization of human prostate cancer with tissue magnetic resonance spectroscopy. Cancer Res 65(8):3030-3034.

Cheng LL, Lean CL, Bogdanova A, Wright SC, Jr., Ackerman JL, Brady TJ, Garrido L. 1996. Enhanced resolution of proton NMR spectra of malignant lymph nodes using magic-angle spinning. Magn Reson Med 36(5):653-658.

Cheng LL, Ma MJ, Becerra L, Ptak T, Tracey I, Lackner A, Gonzalez RG. 1997. Quantitative neuropathology by high resolution magic angle spinning proton magnetic resonance spectroscopy. Proc Natl Acad Sci USA 94(12):6408-6413.

Chopra H, Timar J, Chen YQ, Rong XH, Grossi IM, Fitzgerald LA, Taylor JD, Honn KV. 1991. The lipoxygenase metabolite 12(S)-HETE induces a cytoskeleton-dependent increase in surface expression of integrin α IIb β 3 on melanoma cells. Int J Cancer 49 (5):774-786.

Choi DS, Park JO, Jang SC, Yoon YJ, Jung JW, Choi DY, Kim JW, Kang JS, Park J, Hwang D, Lee KH, Park SH, Kim YK, Desiderio DM, Kim KP, Gho YS. 2011. Proteomic analysis of microvesicles derived from human colorectal cancer ascites. Proteomics 11(13):2745-2751.

Cloarec O, Campbell A, Tseng LH, Braumann U, Spraul M, Scarfe G, Weaver R, Nicholson JK. 2007. Virtual chromatographic resolution enhancement in cryoflow LC-NMR experiments via statistical total correlation spectroscopy. Anal Chem 79(9):3304-3311.

Coen M, Holmes E, Lindon JC, Nicholson JK. 2008. NMR-based metabolic profiling and metabonomic approaches to problems in molecular toxicology. Chem Res Toxicol 21(1):9-27.

Costantini V, Fuschiotti P, Allegrucci M, Agnelli G, Nenci GG, Fioretti MC. 1988. Platelet-tumor cell interaction: Effect of prostacyclin and a

synthetic analog on metastasis formation. Cancer Chemother Pharmacol 22(4):289-293.

Coussens LM, Werb Z. 2002. Inflammation and cancer. Nature 420(6917):860-867.

Crawford NP, Colliver DW, Galandiuk S. 2003. Tumor markers and colorectal cancer: utility in management. J Surg Oncol 84(4):239-248.

Cunningham D, Atkin W, Lenz HJ, Lynch HT, Minsky B, Nordlinger B, Starling N. 2010. Colorectal cancer. Lancet 375(9719):1030-1047.

Daykin CA, Corcoran O, Hansen SH, Bjornsdottir I, Cornett C, Connor SC, Lindon JC, Nicholson JK. 2001. Application of directly coupled HPLC NMR to separation and characterization of lipoproteins from human serum. Anal Chem 73(6):1084-1090.

Deans GT, Parks TG, Rowlands BJ, Spence RA. 1992. Prognostic factors in colorectal cancer. Br J Surg 79:608-613.

Denkert C, Budczies J, Kind T, Weichert W, Tablack P, Sehouli J, Niesporek S, Konsgen D, Dietel M, Fiehn O. 2006. Mass spectrometry-based metabolic profiling reveals different metabolite patterns in invasive ovarian carcinomas and ovarian borderline tumors. Cancer Res 66(22):10795-10804.

Denkert C, Budczies J, Weichert W, Wohlgemuth G, Scholz M, Kind T, Niesporek S, Noske A, Buckendahl A, Dietel M, Fiehn O. 2008. Metabolite profiling of human colon carcinoma--deregulation of TCA cycle and amino acid turnover. Mol Cancer 7:72.

de Noo ME, Tollenaar RA, Deeldar AM, Bouwman LH. 2006. Current status and prospects of clinical proteomics studies on detection of colorectal cancer: Hopes and fears. World J Gastroenterology 12:6594-6601.

Dieterle F, Ross A, Schlotterbeck G, Senn H. 2006. Probabilistic quotient normalization as robust method to account for dilution of complex biological mixtures. Application in 1H NMR metabonomics. Anal Chem 78(13):4281-4290.

Dimandja JM, Clouden GC, Colon I, Focant JF, Cabey WV, Parry RC. 2003. Standardized test mixture for the characterization of comprehensive two-dimensional gas chromatography columns: the Phillips mix. J Chromatogr A 1019(1-2):261-272.

Dolcet X, Llobet D, Pallares J, Matias-Guiu X. 2005. NF-kB in development and progression of human cancer. Virchows Arch 446(5):475-482.

Dong SM, Lee EJ, Jeon ES, Park CK, Kim KM. 2005. Progressive methylation during the serrated neoplasia pathway of the colorectum. Mod Pathol 18(2):170-178.

Duarte IF, Stanley EG, Holmes E, Lindon JC, Gil AM, Tang H, Ferdinand R, McKee CG, Nicholson JK, Vilca-Melendez H, Heaton N, Murphy GM. 2005. Metabolic assessment of human liver transplants from biopsy samples at the donor and recipient stages using high-resolution magic angle spinning 1H NMR spectroscopy. Anal Chem 77(17):5570-5578.

Duffy MJ, van Dalen A, Haglund C, Hansson L, Holinski-Feder E, Klapdor R, Lamerz R, Peltomaki P, Sturgeon C, Topolcan O. 2007. Tumour

markers in colorectal cancer: European Group on Tumour Markers (EGTM) guidelines for clinical use. Eur J Cancer 43(9):1348-1360.

Dukes CE. 1932. The classification of cancer of the rectum. J Path Bact 35:323-332.

Dunn WB, Bailey NJ, Johnson HE. 2005. Measuring the metabolome: current analytical technologies. Analyst 130(5):606-625.

Dunn WB, Ellis DI. 2005. Metabolomics: Current analytical platforms and methodologies. Trends in Anal Chem 24:285-294.

Ferlay J, Shin HR, Bray F, Forman D, Mathers C, Parkin DM. 2008. GLOBOCAN 2008 v1.2, Cancer Incidence and Mortality Worldwide: IARC, Lyon, France: Available from: http://globocan.iarc.fr.

FDA. 2001. Guidance for industry: bioanalytical method validation, FDA, US Department of Health and Human Services. Available: http://www.fda.gov/cder/guidance/4252fnl.pdf.

Fiehn O. 2001. Combining genomics, metabolome analysis, and biochemical modelling to understand metabolic networks. Comp Funct Genomics 2(3):155-168.

Filella X, Molina R, Grau JJ, Pique JM, Garcia-Valdecasas JC, Astudillo E, Biete A, Bordas JM, Novell A, Campo E, et al. 1992. Prognostic value of CA 19.9 levels in colorectal cancer. Ann Surg 216(1):55-59.

Fischer SM, Hagerman RA, Li-Stiles E, Lo HH, Maldve RE, Belury MA, Locniskar MF. 1996. Arachidonate has protumor-promoting action that is inhibited by linoleate in mouse skin carcinogenesis. J Nutr 126(4 Suppl):1099S-1104S.

Fleming I, Cooper J, Henson D. 1997. AJCC cancer staging manual. Lippincott-Raven, Philadelphia, USA.

Foxall PJ, Lenz EM, Lindon JC, Neild GH, Wilson ID, Nicholson JK. 1996. Nuclear magnetic resonance and high-performance liquid chromatography-nuclear magnetic resonance studies on the toxicity and metabolism of ifosfamide. Ther Drug Monit 18(4):498-505.

Fu TF, Rife JP, Schirch V. 2001. The role of serine hydroxymethyltransferase isozymes in one-carbon metabolism in MCF-7 cells as determined by (13)C NMR. Arch Biochem Biophys 393(1):42-50.

Gallagher M, Wysocki CJ, Leyden JJ, Spielman AI, Sun X, Preti G. 2008. Analyses of volatile organic compounds from human skin. Br J Dermatol 159(4):780-791.

Gamache PH, Meyer DF, Granger MC, Acworth IN. 2004. Metabolomic applications of electrochemistry/mass spectrometry. J Am Soc Mass Spectrom 15(12):1717-1726.

Garber K. 2006. Energy deregulation: licensing tumors to grow. Science 312(5777):1158-1159.

Gay LJ, Felding-Habermann B. 2011. Contribution of platelets to tumour metastasis. Nat Rev Cancer 11(2):123-134.

Giardiello FM, Spannhake EW, DuBois RN, Hylind LM, Robinson CR, Hubbard WC, Hamilton SR, Yang VW. 1998. Prostaglandin levels in human colorectal mucosa: effects of sulindac in patients with familial adenomatous polyposis. Dig Dis Sci 43(2):311-316.

Glunde K, Ackerstaff E, Mori N, Jacobs MA, Bhujwalla ZM. 2006. Choline phospholipid metabolism in cancer: consequences for molecular pharmaceutical interventions. Mol Pharm 3(5):496-506.

Goodacre R, Broadhurst D, Smilde AK, Kristal BS, Baker JD, Beger R, Bessant C, Connor S, Calmani G, Craig A, Ebbels T, Kell DB, Manetti C, Newton J, Paternostro G, Somorjai R, Sjostrom M, Trygg J, Wulfert F. 2007. Proposed minimum reporting standards for data analysis in metabolomics. Metabolomics 3, 231-241.

Graca G, Duarte IF, B JG, Carreira IM, Couceiro AB, Domingues Mdo R, Spraul M, Tseng LH, Gil AM. 2008. Metabolite profiling of human amniotic fluid by hyphenated nuclear magnetic resonance spectroscopy. Anal Chem 80(15):6085-6092.

Grady WM. 2004. Genomic instability and colon cancer. Cancer Metastasis Rev 23(1-2):11-27.

Griffin JL, Lehtimaki KK, Valonen PK, Grohn OH, Kettunen MI, Yla-Herttuala S, Pitkanen A, Nicholson JK, Kauppinen RA. 2003. Assignment of 1H nuclear magnetic resonance visible polyunsaturated fatty acids in BT4C gliomas undergoing ganciclovir-thymidine kinase gene therapy-induced programmed cell death. Cancer Res 63(12):3195-3201.

Griffin JL, Shockcor JP. 2004. Metabolic profiles of cancer cells. Nat Rev Cancer 4(7):551-561.

Groger T, Przyborowska AM, Waterman D, Bramley PM, Fraser PD, Tuchler M, Patel RKP, Halket JM. 2003. Ion trap LC/MS/MS and chemical

derivatization for metabolic profiling of GM foodstuffs. In: Proceedings of the 51st ASMS Conference, 8–12 June, Montreal.

Grossi IM, Fitzgerald LA, Umbarger LA, Nelson KK, Diglio CA, Taylor JD, Honn KV. 1989. Bidirectional control of membrane expression and/or activation of the tumor cell IRGpIIb/IIIa receptor and tumor cell adhesion by lipoxygenase products of arachidonic acid and linoleic acid. Cancer Res 49(4):1029-1037.

Gunderson LL, Sosin H. 1974. Areas of failure found at re-operation (second or symptomatic look) following "curative surgery" for adenocarcinoma of the rectum: clinicopathologic correlation and implications for adjuvant therapy. Cancer 34:1278-1292.

Halket JM, Waterman D, Przyborowska AM, Patel RK, Fraser PD, Bramley PM. 2005. Chemical derivatization and mass spectral libraries in metabolic profiling by GC/MS and LC/MS/MS. J Exp Bot 56(410):219-243.

Harrigan GG, Goodacre R. (eds). 2003. Metabolic Profiling: Its role in biomarker discovery and gene function analysis. Kluwer Academic Publishers, Boston, USA.

Harrigan GG, LaPlante RH, Cosma GN, Cockerell G, Goodacre R, Maddox JF, Luyendyk JP, Ganey PE, Roth RA. 2004. Application of high-throughput Fourier-transform infrared spectroscopy in toxicology studies: contribution to a study on the development of an animal model for idiosyncratic toxicity. Toxicol Lett 146(3):197-205.

Hentosh P, Yuh SH, Elson CE, Peffley DM. 2001. Sterol-independent regulation of 3-hydroxy-3-methylglutaryl coenzyme A reductase in tumor cells. Mol Carcinog 32(3):154-166.

Hishinuma T, Suzuki K, Saito M, Yamaguchi H, Suzuki N, Tomioka Y, Kaneko I, Ono M, Goto J. 2007. Simultaneous quantification of seven prostanoids using liquid chromatography/tandem mass spectrometry: the effects of arachidonic acid on prostanoid production in mouse bone marrow-derived mast cells. Prostaglandins Leukot Essent Fatty Acids 76(6):321-329.

Honn KV, Nelson KK, Renaud C, Bazaz R, Diglio CA, Timar J. 1992. Fatty acid modulation of tumor cell adhesion to microvessel endothelium and experimental metastasis. Prostaglandins 44 (5):413-429.

Hubbard WC, Litterst CL, Liu MC, Bleecker ER, Eggleston JC, McLemore TL, Boyd MR. 1986. Profiling of prostaglandin biosynthesis in biopsy fragments of human lung carcinomas and normal human lung by capillary gas chromatography-negative ion chemical ionization mass spectrometry. Prostaglandins 32(6):889-906.

Hurwitz H, Fehrenbacher L, Novotny W, Cartwright T, Hainsworth J, Heim W, Berlin J, Baron A, Griffing S, Holmgren E, Ferrara N, Fyfe G, Rogers B, Ross R, Kabbinavar F. 2004. Bevacizumab plus irinotecan, fluorouracil, and leucovorin for metastatic colorectal cancer. N Engl J Med 350(23):2335-2342.

ICH. 1994. International Conference on Harmonization (ICH) validation of analytical methods: definitions and terminology. ICH Q2 A, Geneva.

ICH. 1996. International Conference on Harmonization (ICH) validation of analytical methods: methodology. ICH Q2 B, Geneva.

Ikawa H, Kamitani H, Calvo BF, Foley JF, Eling TE. 1999. Expression of 15-lipoxygenase-1 in human colorectal cancer. Cancer Res 59(2):360-366.

Ippolito JE, Xu J, Jain S, Moulder K, Mennerick S, Crowley JR, Townsend RR, Gordon JI. 2005. An integrated functional genomics and metabolomics approach for defining poor prognosis in human neuroendocrine cancers. Proc Natl Acad Sci USA 102(28):9901-9906.

James CA, Breda M, Baratte S, Casati M, Grassi S, Pellegatta B, Sarati S, Frigerio E. 2004. Analysis of drugs and metabolites in tissues and other solid matrices. Chromatographia 59:S149.

Jasperson KW, Tuohy TM, Neklason DW, Burt RW. 2010. Hereditary and familial colon cancer. Gastroenterology 138(6):2044-2058.

Jass JR. 1999. Serrated adenoma and colorectal cancer. J Pathol 187(5):499-502.

Jass JR, Atkin WS, Cuzick J, Bussey HJ, Morson BC, Northover JM, Todd IP. 1986. The grading of rectal cancer: historical perspectives and a multivariate analysis of 447 cases. Histopathology 10(5):437-459.

Kabbinavar F, Hurwitz HI, Fehrenbacher L, Meropol NJ, Novotny WF, Lieberman G, Griffing S, Bergsland E. 2003. Phase II, randomized trial comparing bevacizumab plus fluorouracil (FU)/leucovorin (LV) with FU/LV alone in patients with metastatic colorectal cancer. J Clin Oncol 21(1):60-65.

Kaderbhai NN, Broadhurst DI, Ellis DI, Goodacre R, Kell DB. 2003. Functional genomics via metabolic footprinting: monitoring metabolite

secretion by Escherichia coli tryptophan metabolism mutants using FT-IR and direct injection electrospray mass spectrometry. Comp Funct Genomics 4(4):376-391.

Kashfi K, Rigas B. 2005. Is COX-2 a 'collateral' target in cancer prevention? Biochem Soc Trans 33(Pt 4):724-727.

Kanehisa M, Goto S. 2000. KEGG: Kyoto Encyclopedia of Genes and Genomes. Nucleic Acids Res 28:27-30.

Keun HC, Beckonert O, Griffin JL, Richter C, Moskau D, Lindon JC, Nicholson JK. 2002. Cryogenic probe 13C NMR spectroscopy of urine for metabonomic studies. Anal Chem 74(17):4588-4593.

Keun, HC, Ebbels TMD, Antti H, Bollard ME, Beckonert O, Holmes E, Lindon JC, Nicholson JK. 2003. Improved analysis of multivariate data by variable stability scaling: application to NMR-based metabolic profiling. Anal Chim Acta 490:265-276.

Khummueng W, Harynuk J, Marriott PJ. 2006. Modulation ratio in comprehensive two-dimensional gas chromatography. Anal Chem 78(13):4578-4587.

Kind T, Tolstikov V, Fiehn O, Weiss RH. 2007. A comprehensive urinary metabolomic approach for identifying kidney cancerr. Anal Biochem 363(2):185-195.

Koek MM, Muilwijk B, van Stee LL, Hankemeier T. 2008. Higher mass loadability in comprehensive two-dimensional gas chromatography-mass spectrometry for improved analytical performance in metabolomics analysis. J Chromatogr A 1186(1-2):420-429.

Kohne CH, Cunningham D, Di CF, Glimelius B, Blijham G, Aranda E, Scheithauer W, Rougier P, Palmer M, Wils J, Baron B, Pignatti F, Schoffski P, Micheel S, Hecker H. 2002. Clinical determinants of survival in patients with 5-fluorouracil-based treatment for metastatic colorectal cancer: results of a multivariate analysis of 3825 patients. Ann Oncol 13(2):308-317.

Kojima M, Morisaki T, Uchiyama A, Doi F, Mibu R, Katano M, Tanaka M. 2001. Association of enhanced cyclooxygenase-2 expression with possible local immunosuppression in human colorectal carcinomas. Ann Surg Oncol 8(5):458-465.

Kraus S, Arber N. 2009. Inflammation and colorectal cancer. Curr Opin Pharmacol 9(4):405-410.

Krieg P, Kinzig A, Ress-Loschke M, Vogel S, Vanlandingham B, Stephan M, Lehmann WD, Marks F, Furstenberger G. 1995. 12-lipoxygenase isoenzymes in mouse skin tumor development. Mol Carcinog 14(2):118-129.

Labianca R, Nordlinger B, Beretta GD, Brouquet A, Cervantes A. 2010. Primary colon cancer: ESMO Clinical Practice Guidelines for diagnosis, adjuvant treatment and follow-up. Ann Oncol 21 Suppl 5:v70-77.

Lakatos PL, Lakatos L. 2008. Risk for colorectal cancer in ulcerative colitis: changes, causes and management strategies. World J Gastroenterol 14(25):3937-3947.

Lapis K, Timar J, Papay J, Paku S, Szende B, Ladanyi A. 1990. Experimental metastasis inhibition by pretreatment of the host. Arch Geschwulstforsch 60 (2):97-102.

Lee R, Ptolemy AS, Niewczas L, Britz-McKibbin P. 2007. Integrative metabolomics for characterizing unknown low-abundance metabolites by capillary electrophoresis-mass spectrometry with computer simulations. Anal Chem 79(2):403-415.

Lenz EM, Wilson ID. 2007. Analytical strategies in metabonomics. J Proteome Res 6(2):443-458.

Leon C, Rodriguez-Meizoso I, Lucio M, Garcia-Canas V, Ibanez E, Schmitt-Kopplin P, Cifuentes A. 2009. Metabolomics of transgenic maize combining Fourier transform-ion cyclotron resonance-mass spectrometry, capillary electrophoresis-mass spectrometry and pressurized liquid extraction. J Chromatogr A 1216(43):7314-7323.

Levine L. 1986. Radioimmunoassay for leukotrienes: some applications and limitations. Adv Prostaglandin Thromboxane Leukot Res 16:339-351.

Li M, Li JY, Zhao AL, Gu J. 2007. Colorectal cancer or colon and rectal cancer? Clinicopathological comparison between colonic and rectal carcinomas. Oncology 73(1-2):52-57.

Li NJ, Liu WT, Li W, Li SQ, Chen XH, Bi KS, He P. 2010. Plasma metabolic profiling of Alzheimer's disease by liquid chromatography/mass spectrometry. Clin Biochem 43(12):992-997.

Lin CY, Huifeng W, Tjeerdema RS, Viant MR. 2007. Evaluation of metabolite extraction strategies from tissue samples using NMR metabolomics. Metabolomics 3:55-67.

Lindon JC, Holmes E, Nicholson JK. 2001. Pattern recognition methods and applications in biomedical magnetic resonance. Prog Nuc Magn Reson 39:1-40.

Lindon JC, Nicholson JK, Holmes E. 2007a. The handbook of metabonomics and metabolomics. Elsevier, The Netherlands.

Lindon JC, Nicholson JK, Wilson ID. 2000. Directly coupled HPLC-NMR and HPLC-NMR-MS in pharmaceutical research and development. J Chromatogr B Biomed Sci Appl 748(1):233-258.

Lindon JC, Holmes E, Bollard ME, Stanley EG, Nicholson JK. 2004. Metabonomics technologies and their applications in physiological monitoring, drug safety assessment and disease diagnosis. Biomarkers 9(1):1-31.

Lindon JC, Holmes E, Nicholson JK. 2007b. Metabonomics in pharmaceutical R&D. FEBS J 274(5):1140-1151.

Lindor NM, Rabe K, Petersen GM, Haile R, Casey G, Baron J, Gallinger S, Bapat B, Aronson M, Hopper J, Jass J, LeMarchand L, Grove J, Potter J, Newcomb P, Terdiman JP, Conrad P, Moslein G, Goldberg R, Ziogas A, Anton-Culver H, de Andrade M, Siegmund K, Thibodeau SN, Boardman LA, Seminara D. 2005. Lower cancer incidence in Amsterdam-I criteria families without mismatch repair deficiency: familial colorectal cancer type X. JAMA 293(16):1979-1985.

Lipkin M, Yang K, Edelmann W, Xue L, Fan K, Risio M, Newmark H, Kucherlapati R. 1999. Preclinical mouse models for cancer chemoprevention studies. Ann N Y Acad Sci 889:14-19.

Lisec J, Schauer N, Kopka J, Willmitzer L, Fernie AR. 2006. Gas chromatography mass spectrometry-based metabolite profiling in plants. Nat Protoc 1(1):387-396.

Liu B, Khan WA, Hannun YA, Timar J, Taylor JD, Lundy S, Butovich I, Honn KV. 1995. 12(S)-hydroxyeicosatetraenoic acid and 13(S)-hydroxyoctadecadienoic acid regulation of protein kinase C-alpha in melanoma cells: Role of receptor-mediated hydrolysis of inositol phospholipids. Proc Natl Acad Sci USA 92 (20):9323-9327.

Liu B, Timar J, Howlett J, Diglio CA, Honn KV. 1991. Lipoxygenase metabolites of arachidonic and linoleic acids modulate the adhesion of tumor cells to endothelium via regulation of protein kinase C. Cell Regul 2(12):1045-1055.

Locasale JW, Grassian AR, Melman T, Lyssiotis CA, Mattaini KR, Bass AJ, Heffron G, Metallo CM, Muranen T, Sharfi H, Sasaki AT, Anastasiou D, Mullarky E, Vokes NI, Sasaki M, Beroukhim R, Stephanopoulos G, Ligon AH, Meyerson M, Richardson AL, Chin L, Wagner G, Asara JM, Brugge JS, Cantley LC, Vander Heiden MG. 2011. Phosphoglycerate dehydrogenase diverts glycolytic flux and contributes to oncogenesis. Nat Genet 43(9):869-874.

Locker GY, Hamilton S, Harris J, Jessup JM, Kemeny N, Macdonald JS, Somerfield MR, Hayes DF, Bast RC, Jr. 2006. ASCO 2006 update of recommendations for the use of tumor markers in gastrointestinal cancer. J Clin Oncol 24(33):5313-5327.

Longley DB, Allen WL, Johnston PG. 2006. Drug resistance, predictive markers and pharmacogenomics in colorectal cancer. Biochim Biophys Acta 1766(2):184-196.

Ludwig C, Ward DG, Martin A, Viant MR, Ismail T, Johnson PJ, Wakelam MJ, Gunther UL. 2009. Fast targeted multidimensional NMR metabolomics of colorectal cancer. Magn Reson Chem 47 Suppl 1:S68-73.

Lynch HT, Lynch JF, Attard TA. 2009. Diagnosis and management of hereditary colorectal cancer syndromes: Lynch syndrome as a model. CMAJ 181(5):273-280.

Ma Y, Liu W, Peng J, Huang L, Zhang P, Zhao X, Cheng Y, Qin H. 2010. A pilot study of gas chromatograph/mass spectrometry-based serum metabolic profiling of colorectal cancer after operation. Mol Biol Rep 37(3):1403-1411.

Mahadevan S, Shah SL, Marrie TJ, Slupsky CM. 2008. Analysis of metabolomic data using support vector machines. Anal Chem 80(19):7562-7570.

Maier KG, Henderson L, Narayanan J, Alonso-Galicia M, Falck JR, Roman RJ. 2000. Fluorescent HPLC assay for 20-HETE and other P-450 metabolites of arachidonic acid. Am J Physiol Heart Circ Physiol 279(2):H863-871.

Mantovani A, Allavena P, Sica A, Balkwill F. 2008. Cancer-related inflammation. Nature 454(7203):436-444.

Marnett LJ. 1992. Aspirin and the potential role of prostaglandins in colon cancer. Cancer Res 52(20):5575-5589.

Margalit A, Duffin KL, Isakson PC. 1996. Rapid quantitation of a large scope of eicosanoids in two models of inflammation: development of an electrospray and tandem mass spectrometry method and application to biological studies. Anal Biochem 235(1):73-81.

Melstrom LG, Bentrem DJ, Salabat MR, Kennedy TJ, Ding XZ, Strouch M, Rao SM, Witt RC, Ternent CA, Talamonti MS, Bell RH, Adrian TA. 2008. Overexpression of 5-lipoxygenase in colon polyps and cancer and the effect of 5-LOX inhibitors in vitro and in a murine model. Clin Cancer Res 14(20):6525-6530.

Metrakos P. 2009. A "new era" in the treatment of colorectal cancer liver metastasis: the gloves are off! Ann Surg 249(6):887-888.

Mohler RE, Dombek KM, Hoggard JC, Young ET, Synovec RE. 2006. Comprehensive two-dimensional gas chromatography time-of-flight mass spectrometry analysis of metabolites in fermenting and respiring yeast cells. Anal Chem 78(8):2700-2709.

Moka D, Vorreuther R, Schicha H, Spraul M, Humpfer E, Lipinski M, Foxall PJ, Nicholson JK, Lindon JC. 1998. Biochemical classification of kidney carcinoma biopsy samples using magic-angle-spinning 1H nuclear magnetic resonance spectroscopy. J Pharm Biomed Anal 17(1):125-132.

Monleón D, Morales JM, Barrasa A, Lopez JA, Vazquez C, Celda B. 2009. Metabolite profiling of fecal water extracts from human colorectal cancer. NMR Biomed 22(3):342-348.

Moreno A, Rey M, Montane JM, Alonso J, Arus C. 1993. 1H NMR spectroscopy of colon tumors and normal mucosal biopsies; elevated

taurine levels and reduced polyethyleneglycol absorption in tumors may have diagnostic significance. NMR Biomed 6(2):111-118.

Morris M, Watkins SM. 2005. Focused metabolomic profiling in the drug development process: advances from lipid profiling. Curr Opin Chem Biol 9(4):407-412.

Needleman P, Moncada S, Bunting S. 1976. Identification of an enzyme in platelet microsomes which generates thromboxane A2 from prostaglandin endoperoxides. Nature 261, 558-560.

Nicholson JK, Foxall PJ, Spraul M, Farrant RD, Lindon JC. 1995. 750 MHz 1H and 1H-13C NMR spectroscopy of human blood plasma. Anal Chem 67(5):793-811.

Nicholson JK, Lindon JC, Holmes E. 1999. 'Metabonomics': understanding the metabolic responses of living systems to pathophysiological stimuli via multivariate statistical analysis of biological NMR spectroscopic data. Xenobiotica 29(11):1181-1189.

Nicosia S, Vigano T, Folco GC. 1992. Eicosanoids in allergic reactions: quantitative determination by enzyme immunoassay. Pharmacol Res 26 Suppl 2:116-117.

Nie D, Hillman GG, Geddes T, Tang K, Pierson C, Grignon DJ, Honn KV. 1998. Platelet-type 12-lipoxygenase in a human prostate carcinoma stimulates angiogenesis and tumor growth. Cancer Res 58 (18):4047-4051.

Nithipatikom K, Pratt PF, Campbell WB. 2000. Determination of EETs using microbore liquid chromatography with fluorescence detection. Am J Physiol Heart Circ Physiol 279(2):H857-862.

Ong ES, Zou L, Li S, Cheah PY, Eu KW, Ong CN. 2010. Metabolic profiling in colorectal cancer reveals signature metabolic shifts during tumorigenesis. Mol Cell Proteomics.

Pai R, Soreghan B, Szabo IL, Pavelka M, Baatar D, Tarnawski AS. 2002. Prostaglandin E2 transactivates EGF receptor: a novel mechanism for promoting colon cancer growth and gastrointestinal hypertrophy. Nat Med 8(3):289-293.

Pasikanti KK, Esuvaranathan K, Ho PC, Mahendran R, Kamaraj R, Wu QH, Chiong E, Chan EC. 2010. Noninvasive urinary metabonomic diagnosis of human bladder cancer. J Proteome Res 9(6):2988-2995.

Pasikanti KK, Ho PC, Chan EC. 2008. Gas chromatography/mass spectrometry in metabolic profiling of biological fluids. J Chromatogr B Analyt Technol Biomed Life Sci 871(2):202-211.

Pasikanti KK, Norasmara J, Cai S, Mahendran R, Esuvaranathan K, Ho PC, Chan EC. 2010. Metabolic footprinting of tumorigenic and nontumorigenic uroepithelial cells using two-dimensional gas chromatography time-of-flight mass spectrometry. Anal Bioanal Chem 398(3):1285-1293.

Petrik V, Loosemore A, Howe FA, Bell BA, Papadopoulos MC. 2006. OMICS and brain tumour biomarkers. Br J Neurosurg 20(5):275-280.

Pham-Tuan H, Kaskavelis L, Daykin CA, Janssen HG. 2003. Method development in high-performance liquid chromatography for high-

throughput profiling and metabonomic studies of biofluid samples. J Chromatogr B Analyt Technol Biomed Life Sci 789(2):283-301.

Possemato R, Marks KM, Shaul YD, Pacold ME, Kim D, Birsoy K, Sethumadhavan S, Woo HK, Jang HG, Jha AK, Chen WW, Barrett FG, Stransky N, Tsun ZY, Cowley GS, Barretina J, Kalaany NY, Hsu PP, Ottina K, Chan AM, Yuan B, Garraway LA, Root DE, Mino-Kenudson M, Brachtel EF, Driggers EM, Sabatini DM. 2011. Functional genomics reveal that the serine synthesis pathway is essential in breast cancer. Nature 476(7360):346-350.

Powell SM, Zilz N, Beazer-Barclay Y, Bryan TM, Hamilton SR, Thibodeau SN, Vogelstein B, Kinzler KW. 1992. APC mutations occur early during colorectal tumorigenesis. Nature 359(6392):235-237.

Price KE, Lunte CE, Larive CK. 2008. Development of tissue-targeted metabonomics. Part 1. Analytical considerations. J Pharm Biomed Anal 46(4):737-747.

Psychogios N, Hau DD, Peng J, Guo AC, Mandal R, Bouatra S, Sinelnikov I, Krishnamurthy R, Eisner R, Gautam B, Young N, Xia J, Knox C, Dong E, Huang P, Hollander Z, Pedersen TL, Smith SR, Bamforth F, Greiner R, McManus B, Newman JW, Goodfriend T, Wishart DS. 2011. The human serum metabolome. PLoS One 6(2):e16957.

Pugh S, Thomas GA. 1994. Patients with adenomatous polyps and carcinomas have increased colonic mucosal prostaglandin E_2. Gut 35(5):675-678.

Qiu Y, Cai G, Su M, Chen T, Liu Y, Xu Y, Ni Y, Zhao A, Cai S, Xu LX, Jia W. 2010. Urinary metabonomic study on colorectal cancer. J Proteome Res 9(3):1627-1634.

Qiu Y, Cai G, Su M, Chen T, Zheng X, Xu Y, Ni Y, Zhao A, Xu LX, Cai S, Jia W. 2009. Serum metabolite profiling of human colorectal cancer using GC-TOFMS and UPLC-QTOFMS. J Proteome Res 8(10):4844-4850.

Qizilbash AH. 1982. Pathologic studies in colorectal cancer. A guide to the surgical pathology examination of colorectal specimens and review of features of prognostic significance. Pathol Annu 17:1-46.

Rao CV, Newmark HL, Reddy BS. 1998. Chemopreventive effect of squalene on colon cancer. Carcinogenesis 19(2):287-290.

Reddy BS. 1986. Amount and type of dietary fat and colon cancer: animal model studies. Prog Clin Biol Res 222:295-309.

Reddy BS. 1992. Dietary fat and colon cancer: animal model studies. Lipids 27(10):807-813.

Ribic CM, Sargent DJ, Moore MJ, Thibodeau SN, French AJ, Goldberg RM, Hamilton SR, Laurent-Puig P, Gryfe R, Shepherd LE, Tu D, Redston M, Gallinger S. 2003. Tumor microsatellite-instability status as a predictor of benefit from fluorouracil-based adjuvant chemotherapy for colon cancer. N Engl J Med 349(3):247-257.

Ridge JA, Daly JM. 1985. Treatment of colorectal hepatic metastases. Surg Gynecol Obstet 161(6):597-607.

Rigas B, Goldman IS, Levine L. 1993. Altered eicosanoid levels in human colon cancer. J Lab Clin Med 122(5):518-523.

Rigas B, Levine L. 1984. Arachidonic acid metabolism by rat liver cells (the C-9 cell line). J Pharmacol Exp Ther 231(2):230-235.

Rooney OM, Troke J, Nicholson JK, Griffin JL. 2003. High-resolution diffusion and relaxation-edited magic angle spinning 1H NMR spectroscopy of intact liver tissue. Magn Reson Med 50(5):925-930.

Rozen P, Young GP, Levin B, Spann SJ. 2006. Colorectal cancer in clinical practice: prevention, early detection and management. Taylor and Francis, London, UK.

Ryan D, Morrison P, Marriott P. 2005. Orthogonality considerations in comprehensive two-dimensional gas chromatography. J Chromatogr A 1071(1-2):47-53.

Saltz LB, Meropol NJ, Loehrer PJ, Needle MN, Kopit J, Mayer RJ. 2004. Phase II trial of cetuximab in patients with refractory colorectal cancer that expresses the epidermal growth factor receptor. J Clin Oncol 22(7):1201-1208.

Sano H, Kawahito Y, Wilder RL, Hashiramoto A, Mukai S, Asai K, Kimura S, Kato H, Kondo M, Hla T. 1995. Expression of cyclooxygenase-1 and -2 in human colorectal cancer. Cancer Res 55(17):3785-3789.

Sava G, Perissin L, Zorzet S, Piccini P, Giraldi T. 1989. Antimetastatic action of the prostacyclin analog iloprost in the mouse. Clin Exp Metastasis 7(6):671-678.

Schenetti L, Mucci A, Parenti F, Cagnoli R, Righi V, Tosi MR, Tugnoli V. 2006. HR-MAS NMR spectroscopy in the characterization of human tissues: Application to healthy gastric mucosa. Concepts in Magnetic Resonance 28A:430-443.

Schirner M, Kraus C, Lichtner RB, Schneider MR, Hildebrand M. 1998. Tumor metastasis inhibition with the prostacyclin analogue cicaprost

depends on discontinuous plasma peak levels. Prostaglandins Leukot Essent Fatty Acids 58(4):311-317.

Schirner M, Lichtner RB, Schneider MR. 1994. The stable prostacyclin analogue cicaprost inhibits metastasis to lungs and lymph nodes in the 13762NF MTLN3 rat mammary carcinoma. Clin Exp Metastasis 12(1):24-30.

Schirner M, Schneider MR. 1991. Cicaprost inhibits metastases of animal tumors. Prostaglandins 42(5):451-461.

Schirner M, Schneider MR. 1992. The prostacyclin analogue cicaprost inhibits metastasis of tumours of R 3327 MAT Lu prostate carcinoma and SMT 2A mammary carcinoma. J Cancer Res Clin Oncol 118(7):497-501.

Schirner M, Schneider MR. 1997. Inhibition of metastasis by cicaprost in rats with established SMT2A mammary carcinoma growth. Cancer Detect Prev 21(1):44-50.

Seierstad T, Roe K, Sitter B, Halgunset J, Flatmark K, Ree AH, Olsen DR, Gribbestad IS, Bathen TF. 2008. Principal component analysis for the comparison of metabolic profiles from human rectal cancer biopsies and colorectal xenografts using high-resolution magic angle spinning H-1 magnetic resonance spectroscopy. Molecular Cancer 7: 33.

Shen H, Airiau CY, Brereton RG. 2002. Resolution of LC/1H NMR data applied to a three-component mixture of polyaromatic hydrocarbons. Chemom Intell Lab Syst 62, 61-78.

Sheng H, Shao J, Morrow JD, Beauchamp RD, DuBois RN. 1998. Modulation of apoptosis and Bcl-2 expression by prostaglandin E2 in human colon cancer cells. Cancer Res 58(2):362-366.

Sheng H, Shao J, Washington MK, DuBois RN. 2001. Prostaglandin E_2 increases growth and motility of colorectal carcinoma cells. J Biol Chem 276(21):18075-18081.

Shureiqi I, Chen D, Day RS, Zuo X, Hochman FL, Ross WA, Cole RA, Moy O, Morris JS, Xiao L, Newman RA, Yang P, Lippman SM. 2010. Profiling lipoxygenase metabolism in specific steps of colorectal tumorigenesis. Cancer Prev Res 3(7):829-838.

Shureiqi I, Lippman SM. 2001. Lipoxygenase modulation to reverse carcinogenesis. Cancer Res 61(17):6307-6312.

Shureiqi I, Wojno KJ, Poore JA, Reddy RG, Moussalli MJ, Spindler SA, Greenson JK, Normolle D, Hasan AA, Lawrence TS, Brenner DE. 1999. Decreased 13-S-hydroxyoctadecadienoic acid levels and 15-lipoxygenase-1 expression in human colon cancers. Carcinogenesis 20(10):1985-1995.

Sinha AE, Hope JL, Prazen BJ, Nilsson EJ, Jack RM, Synovec RE. 2004. Algorithm for locating analytes of interest based on mass spectral similarity in GC x GC-TOF-MS data: analysis of metabolites in human infant urine. J Chromatogr A 1058(1-2):209-215.

Sitter B, Lundgren S, Bathen TF, Halgunset J, Fjosne HE, Gribbestad IS. 2006. Comparison of HR MAS MR spectroscopic profiles of breast cancer tissue with clinical parameters. NMR Biomed 19(1):30-40.

Smalley WE, DuBois RN. 1997. Colorectal cancer and nonsteroidal anti-inflammatory drugs. Adv Pharmacol 39:1-20.

Smit S, van Breemen MJ, Hoefsloot HC, Smilde AK, Aerts JM, de Koster CG. 2007. Assessing the statistical validity of proteomics based biomarkers. Anal Chim Acta 592(2):210-217.

Smith WL. 1992. Prostanoid biosynthesis and mechanisms of action. Am J Physiol 263(2 Pt 2):F181-191.

Soga T. 2007. Capillary electrophoresis-mass spectrometry for metabolomics. Methods Mol Biol 358:129-137.

Soga T, Ohashi Y, Ueno Y, Naraoka H, Tomita M, Nishioka T. 2003. Quantitative metabolome analysis using capillary electrophoresis mass spectrometry. J Proteome Res 2(5):488-494.

Soslow RA, Dannenberg AJ, Rush D, Woerner BM, Khan KN, Masferrer J, Koki AT. 2000. COX-2 is expressed in human pulmonary, colonic, and mammary tumors. Cancer 89(12):2637-2645.

Soumaoro LT, Iida S, Uetake H, Ishiguro M, Takagi Y, Higuchi T, Yasuno M, Enomoto M, Sugihara K. 2006. Expression of 5-lipoxygenase in human colorectal cancer. World J Gastroenterol 12(39):6355-6360.

Sreekumar A, Poisson LM, Rajendiran TM, Khan AP, Cao Q, Yu J, Laxman B, Mehra R, Lonigro RJ, Li Y, Nyati MK, Ahsan A, Kalyana-Sundaram S, Han B, Cao X, Byun J, Omenn GS, Ghosh D, Pennathur S, Alexander DC, Berger A, Shuster JR, Wei JT, Varambally S, Beecher C, Chinnaiyan AM. 2009. Metabolomic profiles delineate potential role for sarcosine in prostate cancer progression. Nature 457(7231):910-914.

Steinberg SM, Barkin JS, Kaplan RS, Stablein DM. 1987. Prognostic indicators of colon tumors. The Gastrointestinal Tumor Study Group experience. Cancer 57:1866-1870.

Steele VE, Holmes CA, Hawk ET, Kopelovich L, Lubet RA, Crowell JA, Sigman CC, Kelloff GJ. 1999. Lipoxygenase inhibitors as potential cancer chemopreventives. Cancer Epidemiol Biomarkers Prev 8(5):467-483.

Sternberg A, Sibirsky O, Cohen D, Blumenson LE, Petrelli NJ. 1999. Validation of a new classification system for curatively resected colorectal adenocarcinoma. Cancer 86:782-792.

Stoler DL, Chen N, Basik M, Kahlenberg MS, Rodriguez-Bigas MA, Petrelli NJ, Anderson GR. 1999. The onset and extent of genomic instability in sporadic colorectal tumor progression. Proc Natl Acad Sci U S A 96(26):15121-15126.

Swanson MG, Keshari KR, Tabatabai ZL, Simko JP, Shinohara K, Carroll PR, Zektzer AS, Kurhanewicz J. 2008. Quantification of choline- and ethanolamine-containing metabolites in human prostate tissues using 1H HR-MAS total correlation spectroscopy. Magn Reson Med 60(1):33-40.

Swanson MG, Zektzer AS, Tabatabai ZL, Simko J, Jarso S, Keshari KR, Schmitt L, Carroll PR, Shinohara K, Vigneron DB, Kurhanewicz J. 2006. Quantitative analysis of prostate metabolites using 1H HR-MAS spectroscopy. Magn Reson Med 55(6):1257-1264.

Takabatake M, Hishinuma T, Suzuki N, Chiba S, Tsukamoto H, Nakamura H, Saga T, Tomioka Y, Kurose A, Sawai T, Mizugaki M. 2002.

Simultaneous quantification of prostaglandins in human synovial cell-cultured medium using liquid chromatography/tandem mass spectrometry. Prostaglandins Leukot Essent Fatty Acids 67(1):51-56.

Tang DG, Grossi IM, Chen YQ, Diglio CA, Honn KV. 1993. 12(S)-HETE promotes tumor-cell adhesion by increasing surface expression of alpha V beta 3 integrins on endothelial cells. Int J Cancer 54(1):102-111.

Tate AR, Foxall PJ, Holmes E, Moka D, Spraul M, Nicholson JK, Lindon JC. 2000. Distinction between normal and renal cell carcinoma kidney cortical biopsy samples using pattern recognition of (1)H magic angle spinning (MAS) NMR spectra. NMR Biomed 13(2):64-71.

Teahan O, Gamble S, Holmes E, Waxman J, Nicholson JK, Bevan C, Keun HC. 2006. Impact of analytical bias in metabonomic studies of human blood serum and plasma. Anal Chem 78(13):4307-4318.

Teichert F, Verschoyle RD, Greaves P, Edwards RE, Teahan O, Jones DJ, Wilson ID, Farmer PB, Steward WP, Gant TW, Gescher AJ, Keun HC. 2008. Metabolic profiling of transgenic adenocarcinoma of mouse prostate (TRAMP) tissue by 1H-NMR analysis: evidence for unusual phospholipid metabolism. Prostate 68(10):1035-1047.

Terzic J, Grivennikov S, Karin E, Karin M. 2010. Inflammation and colon cancer. Gastroenterology 138(6):2101-2114 e2105.

Tey J, Baggarley S, Lee KM. 2008. Cancer care in Singapore. Biomed Imaging Interv J 4(3):e38.

Tolstikov VV, Lommen A, Nakanishi K, Tanaka N, Fiehn O. 2003. Monolithic silica-based capillary reversed-phase liquid

chromatography/electrospray mass spectrometry for plant metabolomics. Anal Chem 75(23):6737-6740.

Trygg J, Holmes E, Lundstedt T. 2007. Chemometrics in metabonomics. J Proteome Res 6(2):469-479.

Tsikas D. 1998. Application of gas chromatography mass spectrometry and gas chromatography tandem mass spectrometry to assess in vivo synthesis of prostaglandins, thromboxane, leukotrienes, isoprostanes and related compounds in humans. J Chromatogr B 717:201-245.

Tsujii M, Kawano S, DuBois RN. 1997. Cyclooxygenase-2 expression in human colon cancer cells increases metastatic potential. Proc Natl Acad Sci USA 94(7):3336-3340.

Tsujii M, Kawano S, Tsuji S, Sawaoka H, Hori M, DuBois RN. 1998. Cyclooxygenase regulates angiogenesis induced by colon cancer cells. Cell 93(5):705-716.

Tsukamoto H, Hishinuma T, Mikkaichi T, Nakamura H, Yamazaki T, Tomioka Y, Mizugaki M. 2002. Simultaneous quantification of prostaglandins, isoprostane and thromboxane in cell-cultured medium using gas chromatography-mass spectrometry. J Chromatogr B 774:205-214.

Tugnoli V, Mucci A, Schenetti L, Righi V, Calabrese C, Fabbri A, Di Febo G, Tosi MR. 2006a. Ex vivo HR-MAS Magnetic Resonance Spectroscopy of human gastric adenocarcinomas: a comparison with healthy gastric mucosa. Oncol Rep 16(3):543-553.

Tugnoli V, Schenetti L, Mucci A, Parenti F, Cagnoli R, Righi V, Trinchero A, Nocetti L, Toraci C, Mavilla L, Trentini G, Zunarelli E, Tosi MR.

2006b. Ex vivo HR-MAS MRS of human meningiomas: a comparison with in vivo 1H MR spectra. Int J Mol Med 18(5):859-869.

Tzika AA, Astrakas L, Cao H, Mintzopoulos D, Andronesi OC, Mindrinos M, Zhang J, Rahme LG, Blekas KD, Likas AC, Galatsanos NP, Carroll RS, Black PM. 2007. Combination of high-resolution magic angle spinning proton magnetic resonance spectroscopy and microscale genomics to type brain tumor biopsies. Int J Mol Med 20(2):199-208.

Underwood BR, Broadhurst D, Dunn WB, Ellis DI, Michell AW, Vacher C, Mosedale DE, Kell DB, Barker RA, Grainger DJ, Rubinsztein DC. 2006. Huntington disease patients and transgenic mice have similar pro-catabolic serum metabolite profiles. Brain 129(Pt 4):877-886.

Urpi-Sarda M, Monagas M, Khan N, Llorach R, Lamuela-Raventos RM, Jauregui O, Estruch R, Izquierdo-Pulido M, Andres-Lacueva C. 2009. Targeted metabolic profiling of phenolics in urine and plasma after regular consumption of cocoa by liquid chromatography-tandem mass spectrometry. J Chromatogr A 1216(43):7258-7267.

Vandernoot VA, VanRollins M. 2002. Capillary electrophoresis of cytochrome P-450 epoxygenase metabolites of arachidonic acid. 2. Resolution of stereoisomers. Anal Chem 74(22):5866-5870.

Vigneau-Callahan KE, Shestopalov AI, Milbury PE, Matson WR, Kristal BS. 2001. Characterization of diet-dependent metabolic serotypes: analytical and biological variability issues in rats. J Nutr 131(3):924S-932S.

Vogelstein B, Fearon ER, Hamilton SR, Kern SE, Preisinger AC, Leppert M, Nakamura Y, White R, Smits AM, Bos JL. 1988. Genetic alterations during colorectal-tumor development. N Engl J Med 319(9):525-532.

Wachtershauser A, Akoglu B, Stein J. 2001. HMG-CoA reductase inhibitor mevastatin enhances the growth inhibitory effect of butyrate in the colorectal carcinoma cell line Caco-2. Carcinogenesis 22(7):1061-1067.

Wang C, Kong H, Guan Y, Yang J, Gu J, Yang S, Xu G. 2005. Plasma phospholipid metabolic profiling and biomarkers of type 2 diabetes mellitus based on high-performance liquid chromatography/electrospray mass spectrometry and multivariate statistical analysis. Anal Chem 77(13):4108-4116.

Wang D, DuBois RN. 2008. Pro-inflammatory prostaglandins and progression of colorectal cancer. Cancer Lett 267(2):197-203.

Wang D, Dubois RN. 2010. The role of COX-2 in intestinal inflammation and colorectal cancer. Oncogene 29(6):781-788.

Wang W, Feng B, Li X, Yin P, Gao P, Zhao X, Lu X, Zheng M, Xu G. 2010. Urinary metabolic profiling of colorectal carcinoma based on online affinity solid phase extraction-high performance liquid chromatography and ultra performance liquid chromatography-mass spectrometry. Mol Biosyst 6(10):1947-1955.

Wang Y, Bollard ME, Keun H, Antti H, Beckonert O, Ebbels TM, Lindon JC, Holmes E, Tang H, Nicholson JK. 2003. Spectral editing and pattern recognition methods applied to high-resolution magic-angle spinning

1H nuclear magnetic resonance spectroscopy of liver tissues. Anal Biochem 323(1):26-32.

Wang Y, Cloarec O, Tang H, Lindon JC, Holmes E, Kochhar S, Nicholson JK. 2008. Magic angle spinning NMR and 1H-31P heteronuclear statistical total correlation spectroscopy of intact human gut biopsies. Anal Chem 80:1058-1066.

Wang Y, Holmes E, Comelli EM, Fotopoulos G, Dorta G, Tang H, Rantalainen MJ, Lindon JC, Corthesy-Theulaz IE, Fay LB, Kochhar S, Nicholson JK. 2007. Topographical variation in metabolic signatures of human gastrointestinal biopsies revealed by high-resolution magic-angle spinning 1H NMR spectroscopy. J Proteome Res 6:3944-3951.

Wang Y, Tang H, Holmes E, Lindon JC, Turini ME, Sprenger N, Bergonzelli G, Fay LB, Kochhar S, Nicholson JK. 2005. Biochemical characterization of rat intestine development using high-resolution magic-angle-spinning 1H NMR spectroscopy and multivariate data analysis. J Proteome Res 4:1324-1329.

Warburg O. 1956. On the origin of cancer cells. Science 123(3191):309-314.

Want EJ, Coen M, Masson P, Keun HC, Pearce JT, Reily MD, Robertson DG, Rohde CM, Holmes E, Lindon JC, Plumb RS, Nicholson JK. 2010. Ultra performance liquid chromatography-mass spectrometry profiling of bile acid metabolites in biofluids: application to experimental toxicology studies. Anal Chem 82(12):5282-5289.

Weiss L. 2000. The morphologic documentation of clinical progression, invasion metastasis - staging. Cancer Metast Rev 19:303-313.

Welthagen W, Shellie RA, Spranger J, Ristow M, Zimmermann R. 2005. Comprehensive two dimensional gas chromatography - time of flight mass spectrometry (GCxGC-TOF) for high resolution metabolomics: Biomarker discovery on spleen tissue extracts of obese NZO compared to lean C57BL/6 mice. Metabolomics 1:57-65.

Westerhuis J, Hoefsloot H, Smit S, Vis D, Smilde A, van Velzen E, van Duijnhoven J, van Dorsten F. 2008. Assessment of PLSDA cross validation. Metabolomics 4, 81-89.

Wiklund S, Nilsson D, Eriksson L, Sjostrom M, Wold S, Faber K. A randomization test for PLS component selection. 2007. J of Chemometrics 21, 427-439.

Wilson ID, Plumb R, Granger J, Major H, Williams R, Lenz EM. 2005. HPLC-MS-based methods for the study of metabonomics. J Chromatogr B Analyt Technol Biomed Life Sci 817(1):67-76.

Wishart DS, Knox C, Guo AC, Eisner R, Young N, Gautam B, Hau DD, Psychogios N, Dong E, Bouatra S, Mandal R, Sinelnikov I, Xia J, Jia L, Cruz JA, Lim E, Sobsey CA, Shrivastava S, Huang P, Liu P, Fang L, Peng J, Fradette R, Cheng D, Tzur D, Clements M, Lewis A, De Souza A, Zuniga A, Dawe M, Xiong Y, Clive D, Greiner R, Nazyrova A, Shaykhutdinov R, Li L, Vogel HJ, Forsythe I. 2009. HMDB: a knowledgebase for the human metabolome. Nucleic Acids Res 37(Database issue):D603-610.

Wold S, Ruhe A, Wold H, Dunn WJ. 1984. The collinearity problem in linear regression. The partial least squares approach to generalized inverses. SIAM J. Sci Stat Comput 5(3):735-743.

Wolmark N, Wieand HS, Rockette HE, Fisher B, Glass A, Lawrence W, Lerner H, Cruz AB, Volk H, Shibata H, et al. 1983. The prognostic significance of tumor location and bowel obstruction in Dukes B and C colorectal cancer. Findings from the NSABP clinical trials. Ann Surg 198(6):743-752.

Xin H, Yi-Fei G, Ke Y, Yi-Yu C. 2006. Gas chromatography-mass spectrometry based on metabonomic study of carbon tetrachloride-induced acute liver injury in mice. Chinese J Anal Chem 27:1736-1740.

Yan M, Rerko RM, Platzer P, Dawson D, Willis J, Tong M, Lawrence E, Lutterbaugh J, Lu S, Willson JK, Luo G, Hensold J, Tai HH, Wilson K, Markowitz SD. 2004. 15-Hydroxyprostaglandin dehydrogenase, a COX-2 oncogene antagonist, is a TGF-beta-induced suppressor of human gastrointestinal cancers. Proc Natl Acad Sci USA 101(50):17468-17473.

Yang J, Xu G, Zheng Y, Kong H, Pang T, Lv S, Yang Q. 2004. Diagnosis of liver cancer using HPLC-based metabonomics avoiding false-positive result from hepatitis and hepatocirrhosis diseases. J Chromatogr B Analyt Technol Biomed Life Sci 813(1-2):59-65.

Yang P, Chan D, Felix E, Madden T, Klein RD, Shureiqi I, Chen X, Dannenberg AJ, Newman RA. 2006. Determination of endogenous tissue inflammation profiles by LC/MS/MS: COX- and LOX-derived bioactive lipids. Prostaglandins Leukot Essent Fatty Acids 75(6):385-395.

Yang VW, Shields JM, Hamilton SR, Spannhake EW, Hubbard WC, Hylind LM, Robinson CR, Giardiello FM. 1998. Size-dependent increase in prostanoid levels in adenomas of patients with familial adenomatous polyposis. Cancer Res 58(8):1750-1753.

Yoshimatsu K, Golijanin D, Paty PB, Soslow RA, Jakobsson PJ, DeLellis RA, Subbaramaiah K, Dannenberg AJ. 2001. Inducible microsomal prostaglandin E synthase is overexpressed in colorectal adenomas and cancer. Clin Cancer Res 7(12):3971-3976.

Yue H, Jansen SA, Strauss KI, Borenstein MR, Barbe MF, Rossi LJ, Murphy E. 2007. A liquid chromatography/mass spectrometric method for simultaneous analysis of arachidonic acid and its endogenous eicosanoid metabolites prostaglandins, dihydroxyeicosatrienoic acids, hydroxyeicosatetraenoic acids, and epoxyeicosatrienoic acids in rat brain tissue. J Pharm Biomed Anal 43(3):1122-1134.

Yue H, Strauss KI, Borenstein MR, Barbe MF, Rossi LJ, Jansen SA. 2004. Determination of bioactive eicosanoids in brain tissue by a sensitive reversed-phase liquid chromatographic method with fluorescence detection. J Chromatogr B Analyt Technol Biomed Life Sci 803(2):267-277.

Zhang GQ, Hirasaki GJ. CPMG relaxation by diffusion with constant magnetic field gradient in a restricted geometry: numerical simulation and application. 2003.J Mag Resonance 163, 81-91.

Zomer S, Guillo C, Brereton RG, Hanna-Brown M. 2004. Toxicological classification of urine samples using pattern recognition techniques and capillary electrophoresis. Anal Bioanal Chem 378(8):2008-2020.

Zurek G, Schneider B, Zey T, Shockcor J, Spraul M, Baessmann C. 2005. Hyphenated LC-NMR/MS for the characterization of complex metabolic profiles and biomarker discovery in biofluids. 8th Conference of the Israel Analytical Chemistry Society, Jan 11-12.

APPENDIX I: List of Publications

1. **Mal M**, Koh PK, Cheah PY, Chan EC. 2009. Development and validation of a gas chromatography/mass spectrometry method for the metabolic profiling of human colon tissue. Rapid Commun Mass Spectrom 23(4):487-494.

2. Chan EC, Koh PK, **Mal M**, Cheah PY, Eu KW, Backshall A, Cavill R, Nicholson JK, Keun HC. 2009. Metabolic profiling of human colorectal cancer using high-resolution magic angle spinning nuclear magnetic resonance (HR-MAS NMR) spectroscopy and gas chromatography mass spectrometry (GC/MS). J Proteome Res 8(1):352-361.

3. **Mal M**, Koh PK, Cheah PY, Chan EC. 2011. Ultra-pressure liquid chromatography/tandem mass spectrometry targeted profiling of arachidonic acid and eicosanoids in human colorectal cancer. Rapid Commun Mass Spectrom 25(6):755-764.

4. Chan EC, **Mal M**, Pasikanti KK. Book chapter: Metabonomics. In: Handbooks of Separation Science: Gas Chromatography. Editor: CF Poole. (To be published by Elsevier in 2012).